FACTORS AFFECTING CARBOHYDRATE PRODUCTION AND THE FORMATION OF TRANSPARENT EXOPOLYMER PARTICLES (TEP) BY DIATOMS

A Dissertation

by

JIE CHEN

Submitted to the Office of Graduate and Professional Studies of
Texas A&M University
in partial fulfillment of the requirements for the degree of

DOCTOR OF PHILOSOPHY

Chair of Committee,	Daniel C. O. Thornton
Co-Chair of Committee,	Guanpin Yang
Committee Members,	Mike M. Tice
	Antonietta Quigg
Head of Department,	Debbie J. Thomas

May 2014

Major Subject: Oceanography

Copyright 2014 Jie Chen

ABSTRACT

Diatoms exude large amounts of exopolymers (EPS), which are predominantly composed of carbohydrates. EPS may coagulate into transparent exopolymer particles (TEP). Sticky TEP affects the formation of aggregates and marine snow, and consequently, the efficiency of the biological carbon pump. The objective of this research was to determine how different factors affect carbohydrate production and the formation of TEP by diatoms, and their role in aggregation. Diatoms were grown in laboratory cultures to test the hypothesis that stress increases the cell membrane permeability and subsequently enhances TEP formation. In addition, an experiment was conducted to compare the effect of oxidative stress on both a diatom (*Thalassiosira weissflogii*) and a cyanobacterium (*Synechococcus elongates*).

For some diatoms (*Thalassiosira weissflogii* and *Skeletonema marinoi*) and the cyanobacterium *Synechococcus elongatus*, TEP formation was associated with permeable cells. Greater TEP production was observed in cultures under stress conditions (higher temperature, nutrient limitation, and oxidative stress), and more dissolved extracellular carbohydrate was released by dying cells. In the contrast, TEP formation by *Cylindrotheca closterium* was associated with healthy cells. More dissolved extracellular carbohydrate produced by healthy cells, rather than permeable cells. Therefore, my results indicate that carbohydrate production is important for TEP formation. Stress causes cell leakage, but TEP formation is a complex process. Cell leakage does not always result in the release of dissolved extracellular carbohydrate and

enhanced TEP production. In addition, this study investigated the relationship between TEP and aggregate formation. Higher temperature increased TEP production, which was associated with greater aggregation in cultures of *S. marinoi*, but not in *T. weissflogii*. Therefore, enhanced TEP production by diatoms does not always affect aggregate formation. This research indicates that environmental factors affect carbohydrate and TEP production by diatoms, and consequently influences aggregate formation. These influences have a profound impact on biogeochemical cycling of carbon.

ACKNOWLEDGEMENTS

I would like to thank my committee members, my friends and my family members. Only because of their guidance, their help and their support, did I finish my dissertation. I would like to express my sincerely grateful to my advisor, Dr. Daniel. C. O. Thornton, who trained me to be a researcher, encouraged me and supported me in my research, and patiently corrected my writing. I would like to thank my co-chair, Dr. Guanpin Yang, who was always willing to help me and supply excellent advice. I cannot thank my committee member, Dr. Mike Tice enough for his guidance in research and laboratory assistance. I appreciate Dr. Antonietta Quigg, for her guidance in analysis of chlorophyll. I would like to thank Dr. Thomas Bianchi, Dr. Lisa Campbell and Dr. Shari Yvon- Lewis for their provision of laboratory facilities. I would like to thank Dr. Yina Liu and Lauren Railey for their assistance in the laboratory. I would like to thank Charles Rzadkowolski for guidance me in the analysis of particle size by LISST.

I am grateful for Ocean University of China and China scholarship council to support my live expense during my Ph. D study.

I would like to thank the National Science Foundation (USA) for financial to support under Grant No. OCE 0726369 from the Division of Ocean Sciences. Any opinions, findings, and conclusions or recommendations expressed in this material are those of the authors and do not necessarily reflect the views of the National Science Foundation.

I would like to thank my husband, Jinchang Zhang for his love and encouragement and his patience in helping me correct my writing.

I would like to thank my family members, especially my daughter, for suffering the great distance between us.

Finally, I would like to thank my friends for their companionship, making my life at Texas A&M University so wonderful.

NOMENCLATURE

ANOVA	Analysis of variance
ASW	Artificial sea water
C. closterium	*Cylindrotheca closterium*
Chlorophyll *a*	Chl. *a*
CSP	Coomassie Staining Particles
DEC	Dissolved extracellular carbohydrate
DOC	Dissolved organic carbon
DOM	Dissolved organic matter
EPS	Extracellular polymeric substances
LISST	laser *in situ* scattering and transmissometry
PCD	Programmed cell death
POC	Particular organic carbon
POM	Particular organic matter
PSD	Particular size distribution
S. elongatus	*Synechococcus elongatus*
S. marinoi	*Skeletonema marinoi*
TCHO	Total carbohydrate
TEP	Transparent exopolymer particle
T. weissflogii	*Thalassiosira weissflogii*
UHP	Ultra high purity

TABLE OF CONTENTS

Page

LIST OF FIGURES

Page

LIST OF TABLES

Page

CHAPTER I

INTRODUCTION AND LITERATURE REVIEW

1.1 Role of diatoms in primary production and carbon cycling

Phytoplankton are important primary producers and are responsible for almost 50 % of global annual primary productivity (40 ~ 45Pg C yr^{-1}) (Field et al. 1998, Falkowski et al. 1998). Dissolved organic carbon (DOC) and particulate organic carbon (POC) produced by phytoplankton make a significant contribution to the global carbon cycle. Organic matter sinks into the ocean interior, where it is aggregated or respired (Passow 2012). Hansell et al. (2009) estimated that the oceans contain 662 Pg C (1 Pg = 1 gigaton = 10^{15} g) as DOC, which is close to the CO_2 content contained in the atmosphere. The atmosphere contained an estimated 784 Pg C in 2000 (Thornton 2012). Thus, marine DOC production plays an important role in affecting global carbon cycling through acting as a major reservoir of carbon. Phytoplankton in the ocean have a small total biomass, estimated to be between 0.25 and 0.65 Pg C, accounting for < 1% of global primary production (Falkowski and Raven 2007). However, phytoplankton has high primary productivity, and the biomass of phytoplankton can be replaced every 2 to 6 days (Falkowski and Raven 2007). Because of their high productivity, significant amounts of particulate organic matter (POM) and dissolved organic matter (DOM) are contributed by phytoplankton to the global carbon cycle.

Diatoms are a major group of phytoplankton and are widely distributed in the ocean, sometimes forming fast-growing blooms. Large numbers of aggregates frequently form when seasonal diatoms blooms terminate, which strongly affects the particle flux of carbon from the surface of the ocean to deep sea (Honjo 1982, Alldredge and Gotschalk 1988, Thornton 2002). More importantly, diatoms excrete large amounts of exopolymers (EPS) (Staats et al. 2000, Smith and Underwood 1998), which can coagulate into transparent exopolymer particles (TEP) (Passow 2002a). TEP are sticky gel-like particles, which promote aggregate formation by adhering cells and other POC together into marine snow aggregates (Passow 2002b, Thornton 2002, Verdugo et al. 2004). Aggregations of diatoms and their subsequent sinking as marine snow influence the biological carbon pump, which exports a rapid flux of POM from the surface to the ocean interior (Billett et al. 1983, Passow 1995, 2002c). In addition, some metals could accumulate in biopolymers and be transported to higher trophic levels, influencing oceanic biogeochemical cycle (Huang & Santschi 2001). Hence, understanding the amount of the extracellular products released by diatoms would be of great value for better understanding microbial food webs and carbon cycling in global biogeochemistry.

1.2 Introduction to EPS production by diatoms

An important contribution to the biological carbon pump is production of EPS by diatoms. EPS in the ocean are formed of DOC and colloidal precursors that are excreted by the cell external to the plasmalemma (Hoagland et al. 1993). DOC is an essential

substrate for microorganisms; refractory biopolymers contribute a source of DOC and might play an important role in the carbon cycle (Verdugo and Santschi 2010). Some EPS exuded by diatoms are rich in acid polysaccharides and proteoglycans (Hoagland et al. 1993, Underwood et al. 2003, Borchard and Engel 2012). Polysaccharides are a major component of the high-molecular weight DOM in the surface ocean (Benner et al. 1992). The production and composition of EPS vary in different species and environmental conditions (Hoalang et al 1993, Underwood et al. 1995; Smith and Underwood 1998; Khandeparker and Bhosle 2001, Abdullahi et al. 2006, Ding et al. 2009). From studies of microalgae, diatoms exude significant portion of carbohydrate as EPS under nutrient stress (Staats et al. 2000, Passow 2002a). Under nutrient limitation, carbon is often fixed in excess of requirements and cells release fixed carbon into the surrounding medium as extracellular carbohydrates (Myklestad and Haug 1972, Fogg et al. 1983, Staats et al. 2000). These polymers have many different functions for the cells including: motility, mediation of extracellular exchange, a photosynthetic overflow, and desiccation resistance (Hoagland et al. 1993). EPS plays a significant role in many ecosystems, in the bio-stabilization of sediments (Underwood et al. 2003), as a carbon source for heterotrophic species (Decho 1990), and in stimulatory or inhibitory interactions between diatoms and bacteria (Hoagland et al. 1993). EPS includes TEP and Coomassie Staining Particles (CSP), which will be introduced in detail below.

Alldredge et al. (1993) first time described TEP as transparent gel particles, which are formed from acid polysaccharides. TEP are a type of particulate EPS, which can be retained on a filter with a pore size of 0.4 μm (Alldredge et al. 1993). They are

individual particles rather than cell coatings (Passow and Alldredge 1994). TEP was largely ignored for a long time because its transparency meant that TEP could not be seen by light microscopy. Since the development of techniques for the visualization of TEP by staining it using Alcian Blue (Alldredge et al. 1993), high concentrations of TEP and their significant role in the biogeochemical cycling of elements were revealed (Engel and Passow 2001, Ramaiah et al. 2001, Passow 2002c). Many observations have recorded high concentration of TEP ($> 10^6$ L^{-1}) *in situ* during phytoplankton blooms (Alldredge et al. 1993, Kiørboe and Hansen 1993, Kiørboe et al. 1998). The size of TEP ranges from 1 to 100 μm or more in diameter (Passow and Alldredge 1994). TEP are formed from colloidal TEP precursors, which consist of fibrils 1 to 3 nanometers long and belong to the dissolved pool (Passow 2002b). These TEP precursors form submicron gels abiotically by spontaneous assembly (Chin et al. 1998), bubble adsorption (Zhou et al. 1998, Mari 1999), or shear coagulation (Engel and Passow 2001, Passow 2002c). Considerable amounts of TEP may also be formed biotically by fibrils exuded by algae and cyanobacteria (Grossart et al. 1997, Berman et al. 2007). Eventually, these submicron particles coagulate to form TEP, which are large particles and belong to the particulate carbon pool. Thus, TEP become a bridge linking the DOM and POM pools (Verdugo et al. 2004).

Another type of particulate EPS is of proteinaceous origin and was found by Long and Azam (1996). These protein particles can be stained by Coomassie Brilliant Blue, and as such are named Coomassie Staining Particles (CSP). CSP can be produced by algae and bacteria from DOM precursors (Long and Azam 1996). CSP are sticky

organic particles which could affect the adhesive properties of bacteria and have important role in the ecology of pelagic bacteria (Long and Azam 1996). These particles can be present in high concentrations in seawater during phytoplankton blooms (Long and Azam 1996). Concentrations of CSP were reported on the order of 10^6 to 10^8 L^{-1} in coastal water (Long and Azam 1996).

The chemical compositions of TEP and CSP are different, and are polysaccharide and protein-rich, respectively. The sedimentation of TEP may represent selective enrichment of carbon into deep water, whereas sedimentation of CSP may constitute a selective contribution to fluxes to the deep sea not only of carbon but also of nitrogen.

1.3 Ecological role of TEP

1.3.1 Role of TEP in food web

TEP and TEP precursors are food for heterotrophs and grazers (Tranvik 1993, Shimeta 1993, Kepkay 2000). Some studies have indicated that feeding on diatom cells by copepods was reduced in the presence of high molecular weight (HMW) exudates in the environment (Malej and Harris 1993), so TEP as HMW exudates may also inhabit the grazing of diatoms. Consumption of TEP microaggregates by macro or megazooplankton may shortcut the traditional food web and efficiently the transport of energy to higher trophic levels (Passow 2002a). It is not clear whether TEP can be utilized by bacteria (Stoderegger and Herndl 1998, Aluwihare and Repeta 1999, Ogawa

et al. 2001). Some experiments have proposed that decomposition of TEP by bacteria is an important way of decreasing the pool of TEP (Stoderegger and Herndl 1998, Ogawa et al. 2001). TEP is degraded by bacteria into DOM and is recycled in the upper ocean (Kepkay 2000). However, this finding has been challenged. Analysis of TEP composition suggests that TEP are rich in fucose, which increases the resistance of TEP to bacteria degradation (Zhou et al. 1998). Thus, this topic requires further investigation.

1.3.2 TEP influence biological carbon pump efficiency

The biological carbon pump is a biologically-mediated process that transports particulate and dissolved organic matter from the euphotic zone into the deep ocean (Passow 2012). The efficiency of the biological pump is affected by nutrient availability for phytoplankton in the euphotic zone and the exportation rate of organic matter (Christina et al. 2007, Passow 2012). TEP precursors are dissolved organic matter (DOM). TEP coagulation supplies a pathway for sequestration of originally dissolved organic carbon to the deep ocean (Mari 1999). High fluxes of POM co-occurred with a disappearance of TEP at the end of phytoplankton bloom in California coastal surface water (Logan et al. 1995), suggesting TEP concentration has close relation with high sedimentation rates. Thus, TEP strongly influences the efficiency of the biological carbon pump by significantly affecting aggregate formation and increasing the rapid sedimentation of POM.

1.3.3 Ecological stoichiometry of TEP

Redfield stoichiometry indicates that ratio of C: N: P in the organic matter is approximately 106: 16: 1 (Redfield et al. 1963). Studies of stoichiometry indicate that the Redfield ratio is an average; there is flexibility in ratios and different taxa have C: N ratios that are slightly different from Redfield stoichiometry (Quigg et al. 2003). Variations between taxa and with physiological status may lead to different compositions of exudates and therefore variation in the C: N ratio of TEP (Engel and Passow 2001). As TEP are carbon rich particles, their C: N ratio should differ from Redfield stoichiometry. Studies of the stoichiometry of TEP show that the C: N ratio of TEP differs with species, growth condition, and composition of the TEP (Mari 1999). The C: N ratio of TEP collected from the Baltic Sea was higher than the Redfield ratio, with a ratio of 26: 1 (Engel and Passow 2001). Thus, sedimentation of TEP may selectively export carbon into the ocean interior (Engel and Passow 2001). However, it isn‟t known how much carbon may be contributed by TEP to the carbon flux. Thus, understanding the carbon and nitrogen content of TEP and its relation to subsequent POM sedimentation is important for knowing the fate of carbon in the global carbon cycle.

1.4 Aggregation

Diatom aggregation occurs when cells collide and stick together (Jackson et al. 1995). According to coagulation theory, particle numbers and size, collision mechanisms, and coagulation efficiency (or stickiness, α) all control aggregation rate (Jackson 1990, Engel 2000). Stickiness is the probability that the particles stick together once they collide. In diatom aggregation observations, variation in stickiness has been recorded during blooms in the field (Dam and Drapeau 1995, Kiørboe et al. 1998, Engel 2000). Phytoplankton blooms are frequently terminated by aggregation (Alldredge and Gotchalk 1988). Several observations of diatom aggregates *in situ* are documented. For example, Kranck and Milligan (1988) reported diatom aggregation in the Bedford Basin. Riebesell (1991) found that diatom aggregates occurred in the North Sea. The sinking of diatom aggregates and marine snow leads to the removal of primary production from the euphotic zone to depth. The downward flux of energy and nutrients serves as an important food source for bacteria and zooplankton (Decho 1990). Because larger particles sink faster than the smaller ones, aggregation accelerates the speed of sinking flux. The sinking of marine snow aggregates affects the rapid vertical fluxes of POM, at rates up to 100 m day^{-1} (Billett et al. 1983, Smetacek 1985). In addition, diatom aggregate serve as microhabitats for heterotrophic organisms in which diffusion and advection of flow are strongly reduced (Alldredge and Sliver 1988, Alldredge and Gotschalk 1988, Grossart and Simon 1993, Azam and Long 2001). Bacterial

productivity associated with aggregates is greater than that of free living bacteria in the water column (Smith et al. 1992, Grossart and Simon 1998).

Many observations of aggregation *in situ* have confirmed that the presence of TEP enhances aggregation. TEP is very sticky, almost 2 to 4 orders of magnitude more sticky than phytoplankton cells (Mari & Adrian 1998, Engel 2000, Passow 2002c). More aggregates are formed from adhesion cells and particles by TEP than by cells sticking directly to one another (Kiørboe et al. 1993, Logan et al. 1994, Passow & Alldredge 1994, Jackson et al. 1998). *In situ*, peak values of TEP were observed during the decline of diatom blooms (Logan 1995, Passow and Alldredge 1995). TEP abundance is similar to the range of phytoplankton concentrations *in situ*. Thus, TEP facilitates the formation of aggregates and marine snow. However, there are few studies that have examined environmental factors, such as temperature or nutrient availability, on the aggregation of diatoms. Thus, understanding the aggregation mechanisms of diatoms and their response to environmental change is very important.

1.5 Carbohydrate metabolism in diatoms

Carbohydrates have an important role in the metabolism of diatoms. They serve as storage components and structural supports in organisms (Aspinall 1970, 1983). In phytoplankton, carbohydrates account for approximately 40 % of cell biomass (Parsons et al. 1984). The keystone of carbohydrates is the simple sugar. Carbohydrates can be divided into monosaccharide, oligosaccharide and polysaccharide. Monosaccharide is

composed of simple sugars; oligosaccharide is made of a few monosaccharides, and polysaccharides are polymers of a chain of many mono and disaccharides. There are different fractions of carbohydrates associated with different carbon pools in microalgae cultures, including total carbohydrates, the extracellular carbon pool, and the intracellular carbon pool (Underwood et al. 1995, Smith and Underwood 1998). Total carbohydrate is the total amount of carbohydrate in a volume of culture and includes both the particulate (e.g. cells) and dissolved components of the carbohydrate. Carbohydrates inside of diatom cells include cell wall-associated carbohydrate, storage-associated carbohydrate, and residual carbohydrate. Storage carbohydrate is a molecular reserve of energy for the metabolism of the organism, such as glucan. Cell wall carbohydrate is carbohydrate in the form of the cell wall. Carbohydrates outside of diatom cells include colloidal carbohydrate and EPS fractions. Colloidal carbohydrate is the pool of dissolved extracellular carbohydrate in the culture medium. EPS is the high molecular weight component of the colloidal carbohydrate. EPS are rich in acid polysaccharides, which is an important component of organic matter in the form of marine snow (Alldredge et al. 1993). Chemical composition analysis of EPS indicates that it contains of seven carbohydrate components: glucose, uronic acid, galactose, rhamnose, fucose, xylose and mannose (Underwood et al. 2004, Abdullahi et al. 2006). Different growth conditions can produce EPS with different components. For example, EPS generated from nutrient-deplete cultures showed more uronic acid than from nutrient-replete cultures (Underwood et al. 2004). Some studies on carbohydrate composition of EPS have indicated that carbohydrate components can be allocated

between inside and outside cell carbon pools under different environment conditions (Underwood et al. 2004, Bellinger et al. 2005).

1.6 Oxidative stress effect on phytoplankton

The process of respiration and photosynthesis can cause oxidative stress (Apel and Hirt, 2004). Oxidative stress is a physiological status where oxidant production exceeds the antioxidant defense mechanisms in cells (Latifi et al. 2009). Under oxidative stress, many organisms release reactive oxygen species (ROS), including superoxide anion (O_2^-); hydrogen peroxide (H_2O_2); singlet oxygen ($^1O_2$) and hydroxylradical ($HO^\cdot$) (Apel and Hirt, 2004). ROS is toxic to most cyanobacteria and microalgae (Kay 1982, Apel and Hirt 2004) and can trigger them to release caspase-like enzymes and cause programmed cell death (PCD) (Bouchard and Purdie 2011). Berman-Frank et al. (2007) reported a positive coupling between PCD and TEP production in cyanobacteria grown under oxidative stress. This study provided insight into oxidative stress induced cell death and the subsequent influence on TEP production, which may have important implications for the carbon cycle.

1.7 Outline of thesis

TEP affects the formation of aggregates and marine snow and consequently influences the biological carbon pump and global carbon cycle. Therefore,

understanding the production and formation of TEP by diatoms is necessary for the study of the carbon cycle in global biogeochemistry. However, there are still many unanswered questions about TEP production by diatoms. **The objective of my proposed research is to determine the factors affecting carbohydrate production and the formation of TEP by diatoms and their role in aggregation.**

This research addresses potential feedbacks between environmental factors in the surface oceans and diatom physiology. The value of this research is that it contributes to our understanding of the dynamics of TEP production by diatoms and it improves our understanding of the fate of primary production and carbon cycling in the ocean. Four studies were designed to investigate different factors which could influence TEP production and aggregate formation by diatoms. Specific aims and hypotheses of these studies are detailed below.

Specific aim:

Aim 1: Investigate effect of temperature on TEP production

Aim 1 proposes to understand exopolymer production by diatoms and the aggregation of diatoms in response to temperature change. In my lab experiment, *Thalassiosira weissflogii* and *Skeletonema marinoi* were grown in semi-continuous cultures at a sequence of different temperatures. The experiments were designed to test the following hypotheses:

H1: Diatoms produced more EPS with increasing temperature.

Previous experiments have shown that increased temperature affects DOC release (Zlotnik and Dubinsky 1989) and the proportion of carbon excreted as TEP by

diatoms (Claquin et al. 2008). EPS is a fraction of DOC, which may be enhanced when temperature increases. If diatoms release more EPS with rising temperature, then this may result in greater TEP production.

H2: As temperature increase, greater amounts of intracellular carbohydrate were exported out of cell.

EPS are a component of extracellular carbohydrate. The increase of EPS and TEP may be related to increasing extracellular and decreasing intracellular carbohydrate fractions. The allocation of carbon into carbohydrate fractions may change with temperature.

H3: Aggregation of diatoms increased with increasing temperature.

If EPS production elevated with increasing temperature, this may facilitate increased aggregation of diatoms in cultures grown at higher temperatures.

H4: The permeability of cells increased with increasing temperature.

At high temperature, cultures should be more stressed. Thus, cell membranes may become more permeable with increasing temperature.

Aim 2: Investigate the effect of growth rate on TEP production.

I propose to investigate how growth rate affects the productivity of TEP by diatoms and its subsequent influence on diatom aggregation. The growth rate of microalgae is a physiological factor that could influence biomass, cell quota, and cell size (Droop 1983, Martens et al. 1993). Cells in different phases of growth have different properties related to morphology, metabolic production, photosynthesis and respiration rate, and shear sensitivity (Fogg and Thake 1987, Martens et al. 1993). However, how

growth rate affects the production of TEP by diatoms and its subsequent influence on diatom aggregation is not clear. In this experiment, diatom *Thalassiosira weissflogii* was grown at a series of growth rates under nitrogen limitation to determine the effects of growth rate on TEP production and aggregate formation by *T. weissflogii*. This experiment was designed to test the following hypotheses:

H1: Diatoms produced more TEP with decreasing growth rate.

Slow-growing cells would be severely nitrogen-limited, so they would produce more extracellular products, including TEP and TEP precursors.

H2: Diatom aggregation increased with decreasing growth rate.

Diatoms exuded more TEP or TEP precursors at relatively low growth rate, thereby increasing the stickiness of the cultures and resulting in increased aggregate formation.

H3: The proportion of the population with compromised cell membranes increased with decreasing growth rate.

At a slow growth rate, cultures are more nutrient-limited and therefore stressed. Therefore, more TEP and TEP precursors may leak at this lower growth rate.

Aim 3: Investigate the effect of growth and death on TEP production.

I propose to investigate how TEP production and formation are influenced by the growth and death of diatoms. Previous studies have shown that TEP production and composition were different in cultures grown at different growth phases (Fukao et al. 2010). In my lab experiment, three diatom species, *Thalassiosira weissflogii*, *Skeletonema marinoi* and *Cylindrotheca closterium,* were grown in batch culture to

determine TEP production and formation during different phases of growth and cell death. The experiment was designed to test the following hypotheses:

H1: EPS production increased through the growth and death phases.

In the death phase, cells were more stressed and could exude more EPS production to the external environment than those cells in growth phase. As TEP are a form of EPS, their production might increase at the same time.

H2: The allocation of carbon into different carbohydrate pools within the cell changes during different phases of growth and death of the diatoms.

EPS are a part of extracellular carbohydrate. The change of EPS concentration during different phases of growth and death might result in a change in the proportions of extracellular and intracellular carbohydrate. In addition, the allocation of different fractions of carbohydrate inside the cells, including storage carbohydrate, cell wall carbohydrate, and residual carbohydrate, all might change at different growth phases.

H3: The proportion of the population with compromised cell membranes increased in the death phase.

In the death phase, cultures are dying and cell membranes lose membrane integrity. Therefore the cells might leak more TEP and TEP precursors.

Aim 4: Determine the effect of oxidative stress on cell death mechanism and TEP production.

Aim 4 proposes to investigate how TEP production and formation are influenced by oxidative stress. In a study of oxidative stress effects on TEP production by cyanobacteria, results showed that cell permeability increased and photosynthesis

efficiency increased under oxidative stress (Bouchard and Purdie 2011). In addition, Berman-Frank et al. (2007) indicated a positive coupling between PCD and TEP production in cyanobacteria grown under oxidative stress. However, no study has proven that oxidative stress enhances TEP production by diatoms. Thus, I conducted a lab experiment using the diatom *Thalassiosira weissflogii* and the cyanobacterium *Synechococcus elongatus*, which were grown in batch culture with oxidative stress, to test hypotheses below.

H1: Caspase activity increased in cultures under oxidative stress.

Many studies have indicated that organisms release caspase and activate programmed cell death (PCD) in response to oxidative stress (Berman-Frank et al. 2007, Qian et al. 2010, Bouchard and Purdie 2011). Caspase is used as an indicator of PCD. Thus, caspase activity would increase when diatom and cyanobacteria are exposed to oxidative stress.

H2: Mortality increased as cultures were grown in oxidative stress.

Oxidative stress triggers cell death. Therefore, a greater proportion of permeable cells would exist in cultures under oxidative stress.

H3: Cell abundance decreased as oxidative stress increased.

If oxidative stress causes higher mortality in the cultures, cell abundance would decrease at the same time.

H4: Photosynthetic efficiency declined in cultures grown under oxidative stress.

Photosynthetic efficiency is an indication of physiological status. If more unhealthy cells are present in cultures under oxidative stress, photosynthetic efficiency would decline.

H5: More TEP production occurred in cultures exposed to oxidative stress.

Increasing cell degradation under oxidative stress would release more TEP precursors, such as DOM, into the external environment. Thus, TEP production would be enhanced by oxidative stress.

CHAPTER II

METHODS AND DATA ANALYSIS

2.1 Experiments

2.1.1 Cultures for experiments

Diatom and cyanobacteria species used in experiments were obtained from the National Center for Culture of Marine Algae and Microbiota (NCMA). Diatom species were *Thalassiosira weissflogii* (strain CCMP 1051), *Skeletonema marinoi* (CCMP 2092) and *Cylindrotheca closterium* (strain CCMP 339). The cyanobacterium was *Synechococcus elongatus _cf* (strain CCMP 1379). *T. weissflogii* is a dominant planktonic species in euryhaline, warm water in the North Pacific. The optimal growth temperature range for *T. weissflogii* is between 11 °C to 16 °C. *S. marinoi* is another dominant planktonic species in the North Atlantic. The optimal growth temperature range for *S. marinoi* is between 11 to 16 °C. *C. closterium* is a benthic species in the North Atlantic. The optimal growth temperature range for *C. closterium* is between 22 to 26 °C (information from NCMA website). *S. elongatus* is a dominant green strain of cyanobacterium in the South Pacific. The optimal growth temperature range for *S. elongatus* is between 18 to 26 °C. Because these species are widespread in the ocean, these species are used as lab model species in many microalgae studies (Crocker and Passow 1995, Smith and Underwood 1998, Claquin et al. 2008, Fukao et al. 2009).

Many previous studies have demonstrated that these three species have different shapes and different aggregation properties. *Thalassiosira weissflogii* is a centric solitary cell and are relatively not sticky. Their aggregation is facilitated by TEP adhering to cells to become TEP-cell aggregates (Crocker and Passow 1995). *Skeletonema marinoi* is a centric, chain-forming cell. They are sticky and can adhere to one another to form of cell-cell aggregates (Kiørboe and Hansen 1993, Crocker and Passow 1995). *Cylindrotheca closterium* is a lanceolate cell with two thin ends. They are sticky cells as well and can form cell-cell aggregates (Passow& Alldredge 1994, Smith and Underwood et al. 1998). *Synechococcus elongatus* are sticky cells and always form cell-cell aggregates. Because of the specific aggregation patterns and wide temperature range of these species, they were selected as lab models species to test how factors affect EPS production and aggregation.

2.1.2 Medium for culturing species

2.1.2.1 Artificial seawater media

The formulation of artificial seawater media was based on the ion concentrations found in natural seawater. The salt base of artificial seawater (ASW) followed the recipe in Table 2 (Berges et al. 2001). All salts used in the preparation of ASW conformed to ACS specifications. Anhydrous salts were first dissolved in ultra pure water (UHP) in 20 liter acid-cleaned polypropylene bottles (VWR Science). After anhydrous salts were

mixed well by stir bar on a stir plate for one day, hydrated salts were added into the bottle and allowed to dissolve in 20 liters UHP water. The pH value of ASW was adjusted to 8.1 before autoclaving and use of the media.

2.1.2.2 Nutrients media

I used L1 nutrient medium (Guillard and Hargraves 1993) for subculturing the cultures on arrival in the laboratory. As cultures biomass intense, subculturing of the cells were grown in adapted nutrients media with $NaNO_3$ concentration of 8.82×10^{-4}M, $NaH_2PO_4 \bullet H_2O$ concentration of 3.62×10^{-5} M and $Na_2SiO_3 \bullet 9H_2O$ concentration of 1.06×10^{-4} M. Trace metals and Vitamins concentration, which was following the recipe in Table 2 (Guillard and Hargraves 1993). In different experiments, trace metals and Vitamins concentration in the cultures were kept constant in all cultures, which were following the recipe in Table 2 (Guillard and Hargraves 1993). However, concentration of nitrogen, phosphate and silicate were manipulated relate to each experiment. The detail concentrations of them see text.

Table 1. Salt base of artificial seawater (ASW) (Berges et al. 2001).

Salt base for ASW	
Anhydrous salts	Final Conc.
NaCl	363 mM
Na_2SO_4	25.0 mM
KCl	8.04 mM
$NaHCO_3$	2.07 mM
KBr	725 µM
NaF	323 µM
Hydrated salts	
$MgCl_2•6H_2O$	41.2 mM
$CaCl_2•2H_2O$	9.14 mM
$SrCl_2•6H_2O$	82 µM

2.1.3 Batch culture and semi-continuous culture

2.1.3.1 Batch culture

Batch culture is a closed culture system. Microorganisms are grown in medium with a certain amount of nutrients, which is only enough to support the growth of organisms to arrive at a given population. In batch cultures, organisms proceed through lag phase, exponential phase, stationary phases, and death phase. In lag phase, cell growth is very slow. In the exponential phase, cell abundance logarithmically increases. When the cell population arrives at a certain density, a stationary phase follows where cultures maintain a constant number of cells and stop growth. Finally, the remaining

nutrients are not enough to support the growth of organisms, and cultures shift into death phase. The growth rate of the organisms can be controlled in batch culture.

Table 2. Nutrient medium for batch culture. Chemical composition and concentrations adapted from (Guillard and Hargraves 1993).

Nutrient, trace metals, vitamins for adapted nutrients medium	
Major nutrient I-nitrate	Final Conc.
$NaNO_3$	see text
Major nutrient II-phosphate	
$NaH_2PO_4 \cdot H_2O$	see text
Major nutrient III-silicate	
$Na_2SiO_3 \cdot 9H_2O$	see text
Metals stock I-iron	
$Na_2EDTA \cdot 2H_2O$	6.56 µM
$FeCl_3 \cdot 6H_2O$	6.56 µM
Metals stock II-trace metals	
$ZnSO_4 \cdot 7H_2O$	254 nM
$CoSO_4 \cdot 7H_2O$	5.69 nM
$MnSO_4 \cdot 4H_2O$	2.42 µM
$Na_2MoO_4 \cdot 2H_2O$	6.1 nM
Na_2SeO_3	1 nM
$NiCl_2 \cdot 6H_2O$	6.3 nM
$Na_2EDTA \cdot 2H_2O$	8.29 µM
Vitamin	
Thiamine-HCl	297 nM
Biotin	4.09 nM
B_{12}	1.47 nM

On arrival of the cultures from NCMA, 5 ml of culture from each 15 ml tube was immediately subcultured into three 50 ml autoclaved culture tubes, each of which was filled with 20 ml of autoclaved artificial sea water (ASW) salt base according to Berges et al. (2001) (Table 1). L1 nutrients (Guillard and Hargraves 1993) were added to cultures, which is consistent with nutrient supplements for growing species from NCMA. Cultures were grown at 20 °C in an incubator (Precision Company) with a day/night cycle of 14h: 10 h, and with a photon flux density of 42 μmol m^{-2} s^{-1} to keep stock cultures. Afterward, all subsequent subcultures were grown in autoclaved ASW salt base medium (Table 1) in sterile bottles or tubes (Berges et al. 2001). Adapted nutrient media (Guillard and Hargraves 1993) were filtered through 0.2 μm pore sized syringe filters (Nalgene, Thermo Scientific) to remove bacteria and were added into cultures. Trace metals and vitamins concentrations were kept constant in all cultures. However, nitrogen, phosphate and silicate concentrations were manipulated for each experiment.

The maximum specific growth rate of each taxon under the same growth conditions in the experiment was measured in batch culture based on the Equation 1:

$$\mu_{max} = ln\ (N_2\text{-}N_1) / (t_2\text{-}t_1) \qquad \text{(Equation 1)}$$

Where N is cell abundance and t is the culture time. The maximum growth rate of each species was used to determine the maximum dilution rate, which could be used in the semi-continuous cultures.

2.1.3.2 Continuous culture

Continuous cultures differ from batch culture in that they are continuously supplemented with fresh nutrients to support growth of the microorganisms and remove an equal volume of culture simultaneously. Chemostat is an apparatus which is used for continuous cultivation of microorganisms through automatically adding fresh medium at a given rate and removing culture liquid at the same rate. The volume of cultures in continuous culture is constant. The input nutrient rate controls the cell growth rate. When continuous cultures arrive at a steady state, cell abundance is constant, and the growth rate can be controlled by dilution rate under limitation, which can be useful for studying the physiology or EPS production of microorganisms (Fogg and Thake 1987). Continuous cultures allow organisms to be grown in constant physiological status. Because a pretest of Chemostat did not work to keep cultures bacteria-free, we selected semi-continuous culture for my nitrogen limitation experiment. Semi-continuous cultures were grown in closed bottles diluted with culture medium once to supply fresh nutrients and to remove the same volume of culture.

In the semi-continuous culturing, cultures were maintained on stirrer plates and mixed by stirrer bars at 120 revolutions min^{-1}. When cultures were grown at a new condition, samples were taken for five days from each replicate culture to calculate average cell abundance. A culture was defined to be in steady state when the cell abundance deviated by less than 10 % of the mean cell abundance taken over the previous 5 consecutive days. At steady state biomass is constant, and the growth rate (μ)

equals to the dilution rate (D) based on Equation 2 (James 1961); therefore, dilution rate determines growth rate.

$$\frac{dX}{dt} = \text{growth} - \text{output} = \mu X - DX = 0 \qquad \text{(Equation 2)}$$

Where X is cell abundance; t is time; μ is growth rate of the culture and D is dilution rate. Four replicate cultures were grown in 2000 ml or 1000 ml borosilicate medium bottles (VWR Scientific). Cultures were grown in autoclaved ASW salt base (Berges et al. 2001). In order to obtain nitrogen limitation in the cultures, adapted macronutrient concentrations were modified from the original recipe (Guillard and Hargraves 1993) with different N concentrations added to each species cultures to induce nitrogen limitation and still keep the cultures alive. Macronutrients with nitrogen added to a final concentration of 60 µM or 100 µM of $NaNO_3$, with100 µM of $NaH_2PO_4 \bullet H_2O$ and 100 µM of $Na_2SiO_3 \bullet 9H_2O$, in order to affect nitrogen limitation in the cultures. Cultures in the bottles were located in a glass water bath filled with water. The temperature of the cultures was controlled through manipulating water in a glass water bath by a thermocirculator (VWR model 1196D). Light was provided by four fluorescent tubes (40 watt 122 cm Daylight Deluxe, Philips) that were placed on either side of the water bath in pairs. The light cycle was 14 h light: 10 h dark, providing a photon flux density of 150 µmol m^{-2} s^{-1} on the surface of the culture containers. The semi-continuous cultures were diluted at same time every day to control the specific growth rate of the cultures. For example, to get a steady-state growth rate of 0.5 day^{-1}, 50 % of the culture volume (500 ml) was removed from the culture and replaced with 500 ml of fresh medium to maintain a constant total culture volume. Dilutions were

made with sterile medium using sterile technique in a clean hood. Artificial seawater was sterilized by autoclaving after pre-filtration through 0.2 μm pore sized syringe filters. Nutrient stock solutions were also filtered through 0.2 μm pore sized syringe filters (Nalgene, Thermo Scientific). Cell concentrations in the cultures were determined each day and samples were only taken from the cultures when it was established that they were in steady-state. All samples were taken at the time of daily dilution from the volume of culture that was discarded each day. Consequently, all samples were taken from the cultures at the end of the 24 hour period between dilutions.

2.1.4 Preparation of axenic cultures

To prepare axenic cultures for semi-continuous growth, we followed the McCracken method (McCracken 1989) by the addition of antibiotics to the batch cultures to kill bacteria. One ml of culture and Penicillin G (final concentration 400 μg ml^{-1}), Ampicillin (200 μg ml^{-1}), Streptomycin (200 μg ml^{-1}) and Neocillin (200 μg ml^{-1}) were added to 40 ml of autoclaved artificial seawater supplemented with L1 nutrients in culture tubes. After cultures were grown in the antibiotic treatments for 5 days, cultures were washed using the following steps. First, cells were pelleted by centrifugation in 50 ml sterile centrifuge tubes at 1000 × *g* (10 min, 20 °C). Second, the supernatant was removed and the cells were resuspended in 40 ml of autoclaved artificial seawater. Then, antibiotics were added to the cultures once more and the cultures were washed again after a further 5 days exposure to antibiotics. One ml of cell pellet was transferred to 1

liter autoclaved artificial seawater supplemented with macronutrients according to Guillard and Hargraves (1993). When the biomass of cultures arrived at a high concentration (10^5 cells ml^{-1}), cultures were checked to determine if axenic through staining bacteria with DAPI and microscopically checking bacteria concentration in cultures. Axenic cultures were used to test hypotheses in experiments.

2.2 Materials and methods

2.2.1 Cell counts and cell size

Samples (1 ml) were transferred to a small glass vial and a drop of Lugol"s iodine was added to fix the cells. For diatom cells, 400 cells were counted by light microscopy at 10 × magnification using a hemacytometer (Fuchs-Rosenthal ruling, Hauser Scientific) (Guillard and Sieracki 2005). Because *Synechococcus* cells are small and form aggregates in the cultures, cells were counted by light microscopy at 100 × magnification and a pipettor was used to break up aggregates into individual cells before cell counting. Samples were flushed in and out of a 1 ml pipette tip 20 times to ensure that the aggregates were broken apart. In addition, cell turbidity in the cultures was measured (absorbance at 750 nm) to indirectly indicate changes in cell abundance. Cells collected from each treatment were observed using light microscopy at 100 × magnification.

After samples were taken, the lengths and widths of 25 individual diatom cells from an unpreserved sample from each replicate culture were measured by a microscope (Axioplan 2, Carl Zeiss MicroImaging) under 400 × magnification (Menden- Duer & Lessard 2000). These dimensions were used to calculate cell volume based on the assumption that *T. weissflogii* and *S. marinoi* are cylinder shaped and *C. closterium* are shaped as two cones adhered together. Cyanobacterium was not measured cell size in my research.

2.2.2 Bacteria abundance

Bacteria in the cultures were stained with 4'6-diamidino- 2-phenylindole dihydrochloride (DAPI). Samples of 5.0 ml of culture were placed into 15 ml sterile centrifuge tubes and 100 µl of formalin was added to fix samples. Sub-samples (1.0 ml) of the preserved culture were placed into 1.5 ml sterile microcentrifuge tubes and 50 µl of working DAPI stock solution (5 µg ml^{-1}) was added to the samples for one hour in the dark at 4 ºC. The stained sample (0.5 ml) was diluted with 1.5 ml of sterile (0.2 µm filtered and autoclaved) artificial seawater and mixture was filtered onto a 0.2 µm pore-size black polycarbonate filter (Whatman), which was rinsed twice with 1 ml aliquots of sterile artificial seawater. Filters were mounted on glass slides using immersion oil and stored in the dark at -20 °C. Bacteria (400 cells) were counted using a fluorescence microscope (Axioplan 2, Carl Zeiss MicroImaging) according to Porter and Feig (1980).

2.2.3 Chlorophyll *a* analysis

Five ml from each replicate culture was filtered onto 25 mm GF/C filters. Chlorophyll *a* was extracted from the filters in 15 ml sterile polypropylene centrifuge tubes (VWR Scientific) containing 5 ml of cold (4 ºC) 90 % acetone. A pretest proved that acetone did not dissolve these tubes. Cells were broken on the filters using a sonicator (Qsonica, 125 Watts, 20 kHz) for 10 minutes with the amplitude at 40 % in 5 second pulses with 5 second pauses between pulses to prevent heat buildup. The tubes were kept on ice during sonication. After sonication, the filters were extracted in the dark overnight at 4 °C. The extractions were centrifuged at 1000 *g* at 4 °C for 20 minutes, and the chlorophyll *a* concentration in the supernatant was measured using a Turner Designs 700 fluorometer (Arar & Collins 1997), which had been calibrated using chlorophyll *a* standards (Sigma company).

2.2.4 Bioassay experiment

A bioassay experiment was used to check that nitrogen was the source of nutrient limitation in the semi-continuous cultures several times during the growth rate and temperature experiments. At each temperature or growth rate, 40 ml samples were taken from each replicate culture and placed in a sterile polystyrene tissue culture flask (Corning). The following nutrient additions were made: no additions (control), nitrate addition (at twice the initial concentration in the semi-continuous cultures), and a

treatment to which all nutrients were added at the same concentration as in the semi-continuous cultures with the exception of nitrate, which was not added. After 48 hours, the abundance of diatoms in each treatment was determined by cell counts. It was hypothesized that if the cultures were nitrogen limited, then the addition of nitrate would stimulate the growth of the cultures more than in the controls or in the cultures to which all nutrients were added with the exception of nitrate.

2.2.5 Transparent exopolymer particle (TEP) staining and analysis

TEP were stained using a modification of the method from Alldredge & Logan (1993) and Passow et al. (1994, 1995a) and the microscope analysis of TEP proceeded according to Logan et al. (1994). One ml sample of each replicate was diluted with 1 ml of 0.2 μm filtered artificial seawater and then filtered onto a 0.4 μm pore size polycarbonate filter (Whatman) under low pressure (< 150 mm of Hg). Samples were diluted to 2 ml to produce a random distribution of particles on the filters (Hobbie et al. 1977). TEP particles on the membrane were stained with 1 ml of Alcian Blue (0.02 % in 0.06 % acetic acid at pH 2.5). After filtration, the membrane was washed with twice with 1 ml of 0.2 μm filtered UHP water (ultra pure water) and mounted on a Cytoclear slide (GE Water & Process Technologies) using immersion oil. These slides enable TEP to be observed on top of the filters using a light microscope with illumination from below the slide. Ten images of TEP on each slide were taken using a microscope (Axioplan 2, Carl Zeiss MicroImaging) at 100 × magnification. The TEP concentration and area were

analyzed from light micrographs using either Axio Vision 4.8 software (Carl Zeiss MicroImaging) or, later in the project, a method using Image J software (National Institutes of Health) (Engel 2009). Image analysis of TEP using Axio vision 4.8 required each TEP particle to be manually drawn around to determine TEP size and TEP abundance. Image analysis using Image J method followed the method of Engel (2009). Ten images of TEP were taken using a microscope as described above and color JPEG images were edited in Image J. If there were any non-blue particles (such as cells) in the images, they were removed using the dropper icon in Image J to select background color and then using „pencil" or „brush" tool in Image J to paint over these cells. Only blue particles were left in the images for subsequent image analysis. The images were split into the three color channels (red, blue and green) that form the color image and analysis was done only on the red channel, where the contrast between background and blue gel particles was most clear. The 256 step grayscale threshold was adjusted to determine which pixels were to be included in the analysis and which pixels were too pale to be included. Pale pixels below the threshold were defined as „background". Any pixels as darker than the threshold (above the threshold) were included in the analysis. Using the drop down menu, „triangle" was selected as the thresholding method, using a method originally developed by Zack et al. (1977). Thresholded images were compared with original images to check if the triangle method showed the exact area of the gel particles, and then the scale was set in „set scale" in the „ANALYZE" drop down menu. For an image taken at 100 × magnification, the length of one pixel was equivalent to 0.642 µm, with an aspect ratio of 1 as the pixels were square. A minimum cut-off size was set in

„analyze particles" in the „ANALYZE" drop- down menu. The minimum cut-off size is the size below which particles will not be count. We determined 30 μm^2 as the minimum size because of significant differences in total particle numbers or total area of particles when setting smaller number as minimum size. The image analysis produced a set of data that included total number of particles, total area, and mean individual particle area. TEP concentration and area in the cultures were calculated using these data.

2.2.6 Coomassie staining particles (CSP) staining and analysis

Coomassie staining particles (CSP) were stained by Coomassie Brilliant Blue (a protein stain) according to Long and Azam (1996) and were observed using a light microscope (Axioplan 2, Carl Zeiss MicroImaging). Ten pictures of CSP images from cultures grown at every treatment were taken under 100 × magnification and then CSP concentration and CSP size were analyzed using the Image J analysis method described above.

2.2.7 Aggregation

The particle size distribution (PSD) and volume concentration of particles in the cultures was measured using laser scattering following the method of Rzadkowolski and Thornton (2012). The Laser *in situ* scattering and transmissometry instrument (LISST-100X, Type C; Sequoia Scientific, Bellevue, WA, USA) was used to measure the

volume concentration of particles in 32 logarithmically placed size bins over the size range 2.5 to 500 µm. In each size bin, the largest particle diameter was 1.18 × the smallest diameter (LISST-100X User‟s Manual, Sequoia Scientific). Particle size was not referred to an absolute size, rather the median size in a size range (Rzadkowolski and Thornton 2012).

Samples of culture (approximately 150 ml) were added to the LISST chamber. Particles in the light path attenuated and diffracted the laser light and the scattered light struck a detector. The detector included 32 concentric rings which indicated a series of size ranges from small to large. The sizes of particles were determine based on which rings the diffracted light hit. The PSD and volume concentration of particles in the samples were estimated by LISST SOP software (Sequoia Scientific, Bellevue, WA, USA). PSDs were blank corrected by subtracting the PSD of 0.2 µm filtered artificial seawater.

2.2.8 C: N ratio of particulate matter

Samples of culture (30 ml) were filtered through pre-combusted (500 °C, 4 h) GF/F filters (Whatman), which were stored frozen (-20 ºC) until analysis. Prior to elemental analysis, the filters were acidified with HCl (12 M) vapor in a desiccator overnight to remove inorganic carbon. Analysis for particulate C: N ratio was carried out in the Stable Isotope Geosciences Facility (Texas A&M University) using a Carlo Erba

NA1500 Elemental Analyzer for analysis (Verardo et al. 1990). Standards were Acetanilide, Methionine, USGS 24, USGS 40, USGS 41 (Verardo et al. 1990).

2.2.9 Cell permeability

SYTOX Green (Invitrogen S7020) is a plasma membrane impermeable nucleic acid stain that is used to test the permeability of cells (Veldhuis et al. 2001, Franklin et al. 2012). In cells with a compromised plasma membrane, the nucleus inside the cells becomes stained with SYTOX Green and fluoresces with an emission peak of 523 nm when excited by a 450 to 490 nm source.

Culture samples were stained by SYTOX Green method, which is adapted from (Veldhuis et al. 2001). One ml of culture was stained with 40 µl of working SYTOX Green stock solution (50 µM solution) for one hour in the dark (Franklin et al. 2012). Stained sample (0.5 ml) was mixed with 1.5 ml of filtered (0.2 µm) artificial seawater and was filtered onto a 0.4 µm polycarbonate filter. Filters were rinsed twice using artificial seawater and mounted on glass slides using immersion oil. Slides were stored in the dark at -20 °C. The proportion of SYTOX Green labeled cells was counted by examining 400 cells from each slide at 400 × magnification using a fluorescence microscope (Axioplan 2, Carl Zeiss MicroImaging).

2.2.10 Carbohydrate measurement

Different fractions of carbohydrate isolated from the diatom cultures were determined using two spectrophotometric methods, TPTZ (2, 4, 6-tripyridyl-s-triazine) and PSA (Phenol sulphuric acid) method. Many samples from open oceans were measured by TPTZ method and many studies on lab cultures were measured with the PSA method. In here, hydrolysis efficiency, precision of method, factor effects measurements of two methods were investigated. These investigations of the two methods help to understand their advantages and disadvantages and therefore better utilize these methods in real measurements.

2.2.10.1 Phenol-sulfuric acid (PSA) method

The PSA method is based on the hydrolysis of sugars in concentrated H_2SO_4 (11.2 M), and yields monomers, such as furfurals and hydroxyfurfurals, with reducing groups, which react with phenol and give an orange yellow color that is proportional to the concentration of carbohydrate (Dubois et al. 1956, Liu et al. 1973). Little is yet known about the nature of the color product in this reaction.

The procedure of PSA method was as follows:

Sample (0.8 ml) was pipetted into a 20 ml glass boiling tube, and 0.4 ml phenol was added to the sample. Samples were mixed well and 2 ml concentrated sulfuric acid were added into samples rapidly using a dispenser bottle. Tubes were shaken gently and

placed in the dark at room temperature for 30 minutes to enable the reaction to complete and enable the tubes to cool. Absorbance was measured at 485 nm in a 10 mm Polystyrene cuvette (VWR Science). The concentration of carbohydrate was expressed as D-glucose equivalents.

Standard curves

A typical standard curve of the PSA method is shown in Figure 1. Triplicate data points are on top of one another in this Figure. The PSA method measures the concentration of carbohydrate, in a range of 0 to 50 μg glucose ml^{-1} ($r^2 = 0.9996$). The precision of the PSA method in absorbance of 66.7μM C (n = 4) was about 5.7 %, and the detection limit was calculated as three times the standard deviation of absorbance of the blank at 2.67 μM C.

Hydrolysis efficiency

For the PSA method, carbohydrate was hydrolyzed in 11.3 M H_2SO_4. The recovery of carbohydrate was in the range 70 ~ 100 % (Dubois 1956, Liu et al. 1973, Burney & Sieburth 1977, Underwood et al. 1995).

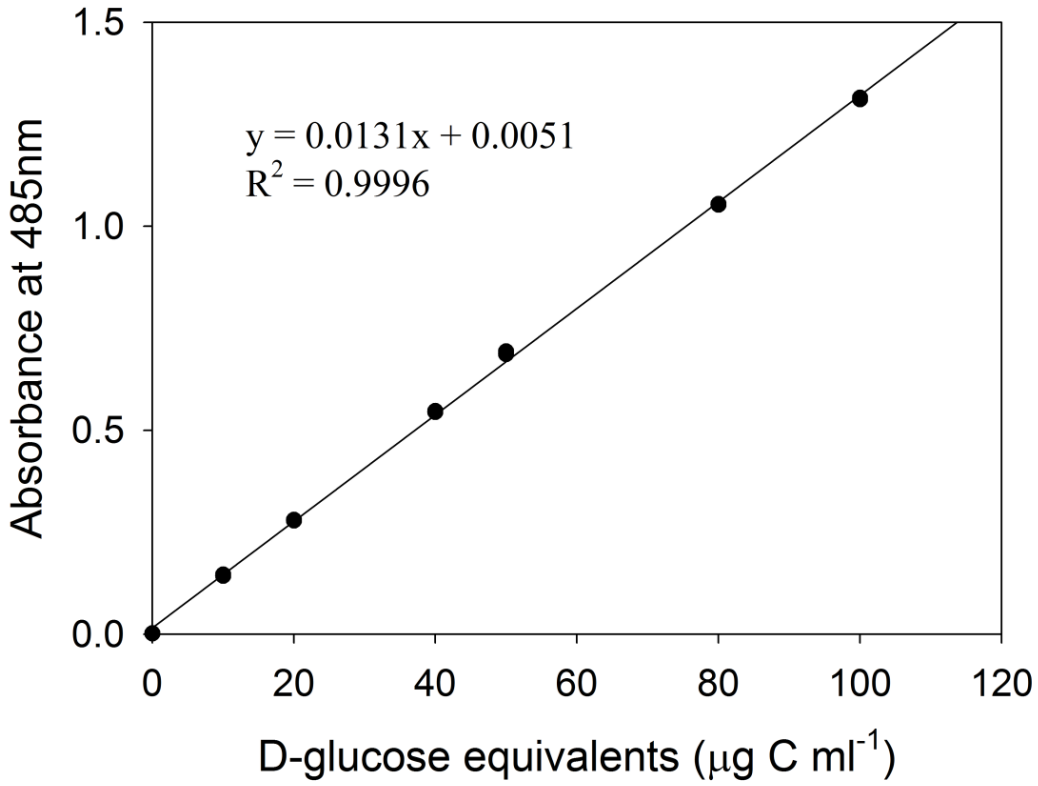

Figure 1. Standard curve for D-glucose measured using the Phenol sulfuric acid (PSA) method (n = 3). The absorbance was measured at 485 nm. n = 3, $r^2 = 0.9996$. Black cycles represent absorbance measured in PSA method.

Salt interference

The regression lines of absorbance of D-glucose standard measured by PSA in ultrapure water (UHP) and artificial seawater (ASW) were showed in Figure 2. Data points are on top of one another in the figure. The slope of the calibration curves in salt water was similar to slope in no salt water. The calibration curve in no salt water is y = 0.0131x + 0.0051($R^2 = 0.9996$). The calibration curve in salt water is y = 0.014x +

0.0038 ($R^2 = 0.9992$). This result indicated that effect of salt (salinity ≈ 35) on absorbance was low.

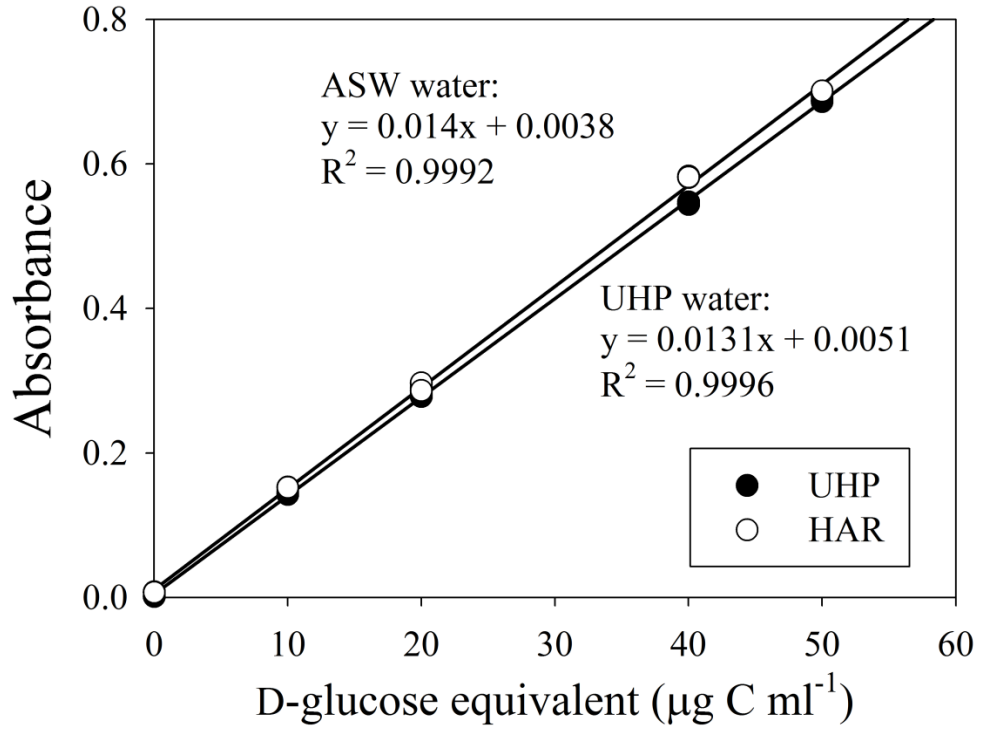

Figure 2. Standard curve of D- glucose in ultra pure water (UHP) and artificial sea water (ASW) measured by PSA method. Solid cycles represent glucose standard in UHP water. Open cycles represent glucose standard in HAR water (n = 4).

Carbohydrate fractions were determined by PSA method

There are different fractions of carbohydrates in microalgae cultures, including total carbohydrate, colloidal and EPS, carbohydrate associated with storage and carbohydrate associated with cell wall (refer to 1.5). The concentrations of different fraction of carbohydrate were extracted followed the method by Underwood (Underwood et al. 1995, 2004) and were measured using the phenol-sulfuric acid (PSA) method (Dubois et al. 1956).

Total carbohydrate. Total carbohydrate is the total amount of carbohydrate in a volume of culture and includes both the particulate (e.g. cells) and dissolved components of the carbohydrate. Total carbohydrate concentrations were determined in unfiltered liquid samples from the cultures using the PSA method (Dubois et al. 1956) calibrated with D-glucose. A 1 ml sample from each replicate was stored in an autoclaved 1.5 ml microcentrifuge tube, and the samples were kept frozen (-20 ºC) until analysis. Phenol (0.4 ml) was mixed with 0.8 ml of sample in a glass boiling tube. Concentrated sulfuric acid (2 ml) was added rapidly with a dispensing bottle. Tubes were shaken gently and left to react for 30 minutes. The concentration of total carbohydrate was analyzed spectrophotometrically and was expressed as glucose equivalents.

Colloidal carbohydrate. Colloidal carbohydrate is the pool of dissolved extracellular carbohydrate in the culture medium. Colloidal carbohydrate can be obtained by centrifugation of culture medium to remove the particulate carbohydrate and the supernatant contains the colloidal (Underwood et al. 1995). After centrifuging 50 ml of the culture at 5000 *g* (30 minutes, 4 °C), 1 ml of supernatant was placed in a sterile

1.5 ml microcentrifuge tube and stored frozen (-20 ºC) until analysis. Colloidal carbohydrate concentration was determined by analyzing 0.8 ml of the sample using the PSA method (Dubois et al. 1956).

EPS. EPS is the high molecular weight component of the colloidal, which can be separated from low molecular weight carbohydrate in the colloidal by precipitation using cold alcohol. After centrifuging, as described above, 15 ml of supernatant was placed in 35 ml of cold (-20 ºC) reagent alcohol in a 50 ml sterile centrifuge tube to precipitate the EPS overnight (Underwood et al. 2004). The EPS precipitate was separated by centrifugation at 4500 *g* for 20 minutes. After removing the alcohol, the precipitate was dried in an oven (5 min, 60 °C). The precipitate was resuspended in 1 ml of 0.2 µm filtered UHP water and stored frozen (-20 ºC) in a 1.5 ml sterile microcentrifuge tube. EPS carbohydrate was measured by analyzing 0.8 ml of sample using the PSA method (Dubois et al. 1956).

Intracellular carbohydrate. Intracellular carbohydrate includes carbohydrate associated with storage and carbohydrate associated with the cell wall. Intracellular carbohydrate is the carbohydrate in the cells and can be extracted by centrifugation of the cell pellet down to separate the cells from the colloidal carbohydrate. The cell pellets were used for analyzing intracellular storage carbohydrates by hot water (HW) extraction (Underwood et al. 2004). First, the rest of the supernatant in the centrifuge tube was removed, leaving only the cell pellet in the bottom of centrifuge tube. The cell pellets were washed by resuspension in 4 ml of 70 % alcohol. After being centrifuged at 4500 *g* for 20 minutes, the supernatant was discarded, and 4 ml of 70 % alcohol was

added again to wash the cell pellets. Pigment and fat were removed from the pellets. Afterward, 4 ml of 0.2 µm filtered UHP water was added and cell pellets were incubated at 95 ºC for 1 hour. After being centrifuged at 4500 *g* for 20 minutes, 1 ml of supernatant was placed in a sterile 1.5 ml microcentrifuge tube and frozen (-20 ºC). The concentration of HW carbohydrate was determined by analyzing 0.8 ml of HW extraction by the PSA method (Dubois et al. 1956).

Cell wall associated carbohydrate. Cell wall associated carbohydrate is carbohydrate in the form of the cell wall and can be obtained by hot bicarbonate (HB) extraction. After HW extraction, the rest of supernatant was discarded. The pellet was extracted with 4 ml of 0.5 M $NaHCO_3$ at 95 ºC for 1 hour. The mixture was centrifuged at 4500 *g* for 20 minutes. The supernatant contained the hot bicarbonate (HB) extract, which is composed of carbohydrates associated with the cell wall (Smith and Underwood 1998). One ml of supernatant (HB extract) was stored in a sterile 1.5 ml microcentrifuge tube and frozen (-20 ºC). The concentration of HB carbohydrate was determined by analyzing 0.8 ml of the HB extraction by the PSA method (Dubois et al. 1956). The rest of the supernatant of the HB extraction was discarded. The remaining carbohydrate in the pellet after HB extraction was defined as residual carbohydrate. The pellet was resuspended in 1 ml of 0.2 µm filtered UHP water and was stored in a sterile 1.5 ml microcentrifuge tube and frozen (-20 ºC). The concentration of residual carbohydrate was determined by analyzing 0.8 ml of residual carbohydrate using the PSA method (Dubois et al. 1956).

2.2.10.2 TPTZ (2, 4, 6-tripyridyl-s-triazine) method

The 2, 4, 6-tripyridyl-s-triazine (TPTZ) method is based on an oxidation reaction between monosaccharide and ferricyanide which causes ferricyanide reduction and gives a violet color of the Fe $(TPTZ)_2^{2+}$ that is proportional to the concentration of carbohydrate (Myklestad et al. 1997). Monosaccharide concentration was measured directly by the TPTZ method calibrated with D-glucose. For polysaccharides, sugars were hydrolyzed by HCl and yielded monomers that were measured by the TPTZ method. In polysaccharide analysis, 4 ml of cultures and 0.4 ml 1 M HCl were added together into 10 ml glass ampoule (VWR Trace Clean). The sealed ampoules were placed in an oven at 85 °C for 24 hours to hydrolyze the polysaccharide. After hydrolysis, the samples were neutralized with 1 M NaOH. The samples were analyzed using the same procedure as the monosaccharide analysis. The concentration of polysaccharide was calculated by subtracting the monosaccharide content.

Standard curve

Figure 3 shows TPTZ standard curve. Carbohydrate concentration measured using TPTZ method is not linear at higher concentrations (≥ 20 μg C ml^{-1}, glucose as equivalents). Thus, TPTZ method was suitable for measuring relatively low concentrations of carbohydrate. The calibration curve of D-glucose measured by TPTZ method was in the range of 0 to15 μg C ml^{-1}(glucose as equivalents) is $y = 0.0804x + 0.2082$ ($r^2 = 0.992$). The precision of the TPTZ method was 1.3 % at a concentration of 66.67μM C as in D-glucose equivalents (n = 3) with a detection limit of 3.22 μM C.

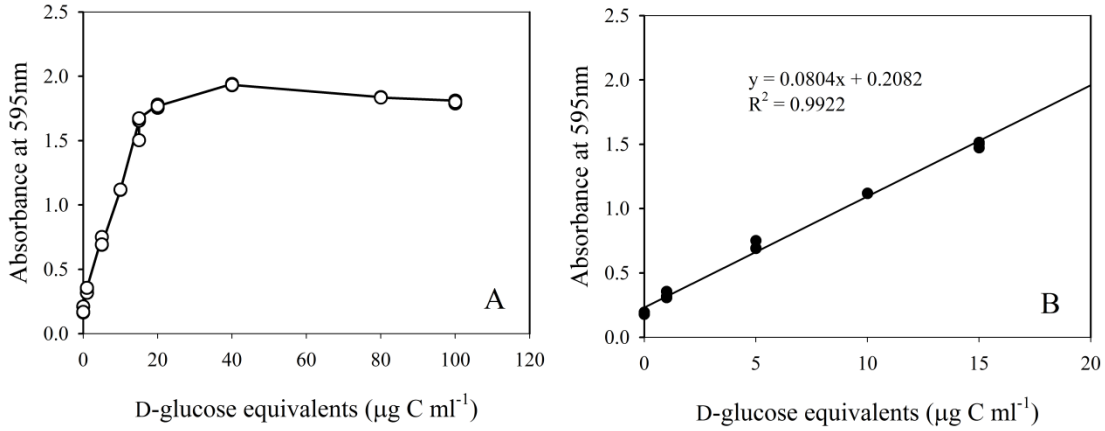

Figure 3. Standard curve for D-glucose measured using the 2, 4, 6-tripyridyl-s-triazine (TPTZ) method. (A) D-glucose in the range of 0 to 100 µg C ml^{-1} were measured by Fe $(TPTZ)_2^{2+}$ as absorbance at 595 nm (B) calibration curve of D-glucose in the range of 0 to15 µg C ml^{-1} were measured by Fe $(TPTZ)_2^{2+}$ as absorbance at 595 nm. Solid lines represent regression lines of absorbance of the D-glucose standard. (r^2 = 0.992). Three replicate samples were measured at each glucose concentration.

Salt interference

The effect of salt on the TPTZ assay was determined by comparing measurements of D-glucose concentrations in standards (n = 3) dissolved in UHP water and artificial seawater (Figure 4). The regression equation in UHP water is y = 0.0807x + 0.254 (R^2 = 0.991), and the regression equation in artificial seawater is y = 0.0804x + 0.2082 (R^2 = 0.992). The slope of the calibration curve in artificial seawater (ASW) was similar to slope of the calibration curve for standards dissolved in UHP water. Thus, the effect of salt on absorbance was low.

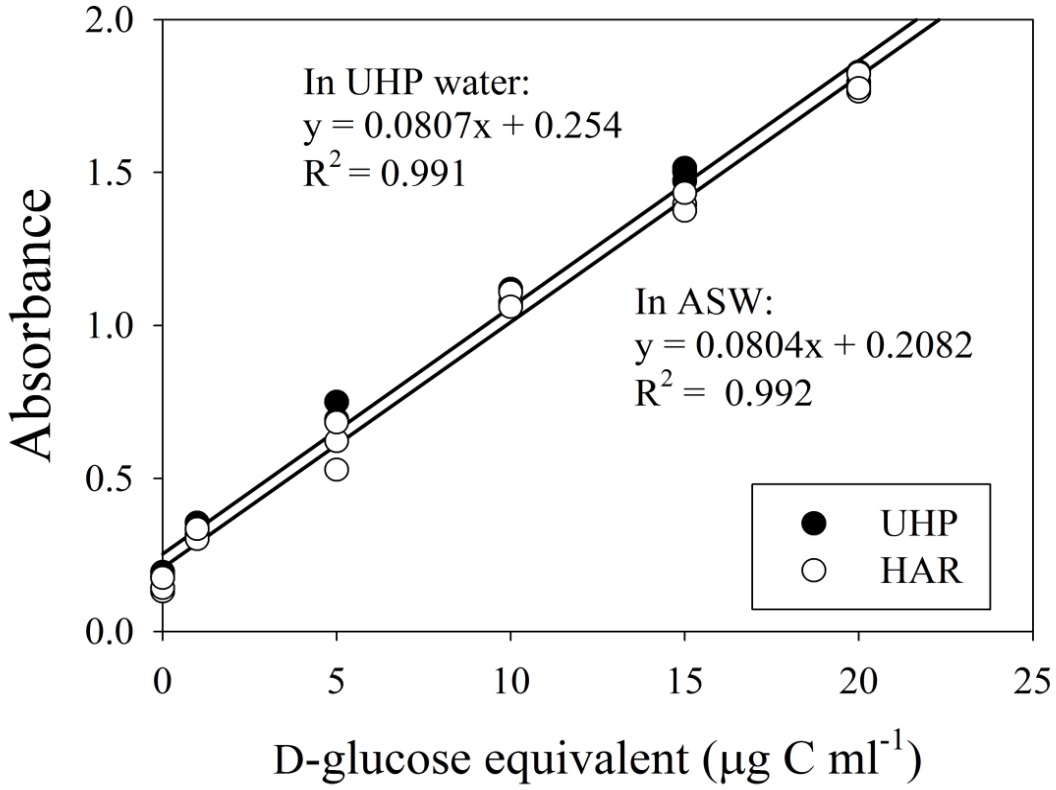

Figure 4. Standard curve of D-glucose in ultra pure water (UHP) and artificial seawater (ASW) measured by TPTZ method (n = 3). Solid cycles represent glucose standard in UHP water. Open cycles represent glucose standard in HAR water.

Hydrolysis efficiency

Polysaccharides must be hydrolyzed by HCl to become monosaccharides to be measured by TPTZ method. Thus, an appropriate operation procedure was determined to find the highest hydrolysis efficiency possible for this experiment. We selected starch as the model polysaccharide because it is a common storage polymer and constructed of a chain of glucose. To test the hydrolysis efficiency of polysaccharide by 1M HCl, four

replicates of 4 ml of starch (Sigma company) 10 μg ml^{-1} were hydrolyzed by 0.4 ml 1M HCl in sealed 10 ml ampoules for different time periods (0, 2, 4, 8, 24, 48 hours) and at different temperatures (75, 85, 90 and 100 °C). Ampoules including samples were weighed before and after hydrolysis in the oven to measure the loss of the samples. Results indicated that hydrolysis efficiency increased with temperature (results not shown in here). However, sealed ampoules (10 ml) exploded at temperatures higher than 90 °C. Hydrolysis efficiency increased with time. The results showed that hydrolysis efficiency at 85 °C increased with time. The recoveries of polysaccharide increased from 1.34 % ± 0.47 % at time 0 up to the 76.7 % ± 1.69 % at 24 hours. After 24 hours, recovery decreased to 56.23 % ± 6.85 % at 48 hours (Figure 5). Thus, the maximum hydrolysis efficiency was at 85 °C for 24 hours with recovery of about 78 %.

Degradation of monosaccharides during hydrolysis

Carbohydrates may be composed of both mono- and polysaccharides. We wanted to check whether hydrolysis processes cause monosaccharides to significantly decompose. Four replicates of 4 ml monosaccharide (D-glucose) with a concentration of 10 μg ml^{-1} were hydrolyzed in 0.4 ml 1M HCl in sealed 10 ml ampoules. The sealed ampoules were placed in an oven at 85 °C for hydrolysis for different lengths of time. The results showed that recoveries of glucose decreased with hydrolysis time, indicating that longer hydrolysis (more than 24 hours) cause monosaccharides to decompose (Figure 6). When three replicates of 4 ml monosaccharide (D-glucose) 10 μg ml^{-1} were hydrolyzed with 0.4 ml 1M HCl and 0.4 ml UHP water as a control at high temperature, the recovery of D-glucose decreased with time both in the acid treatment and the

controls (Figure 5). These results indicate that high temperature was the main factor resulting in the decomposition of the monosaccharides.

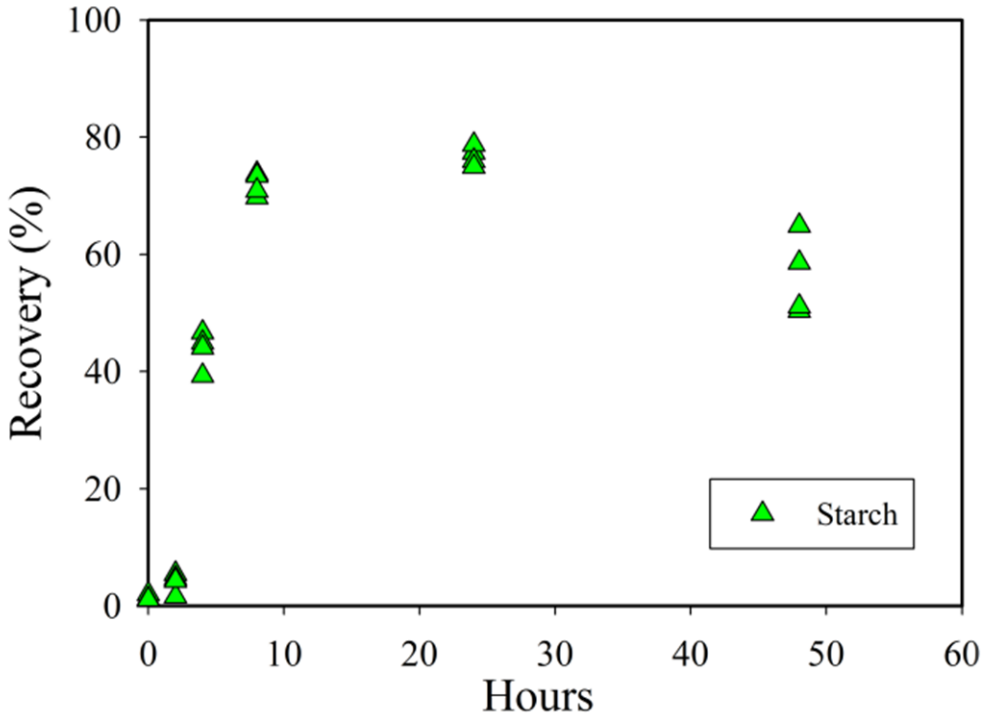

Figure 5. The change of hydrolysis efficiency of starch with time. The solid triangles represent recoveries of starch with hydrolysis time (n = 4).

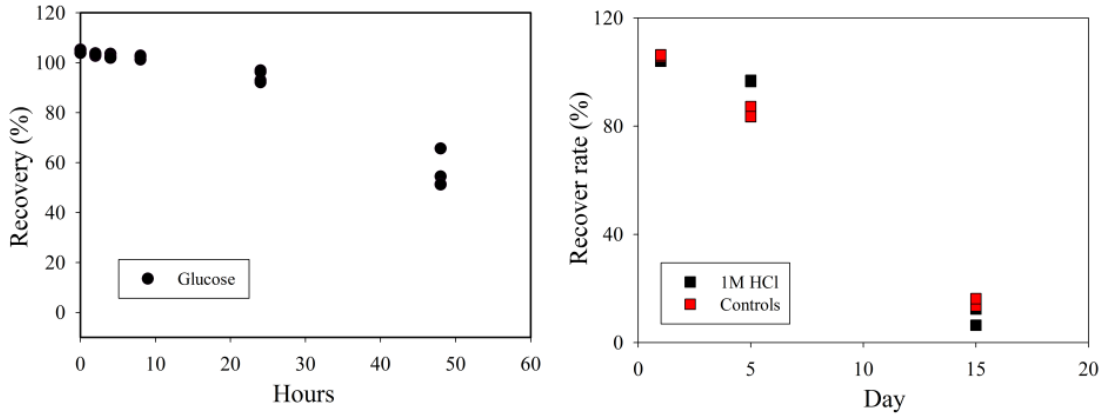

Figure 6. Glucose decomposed with time in 1M HCl acid treatment and a UHP water control (n = 3) A) Glucose decomposed with time in 1M HCl. The solid cycles represent recoveries of glucose with hydrolysis time (n = 4). B) Glucose decomposed with time in 1M HCl and in UHP control. The black rectangles represent glucose in 1M HCl acid treatment (n = 3). Red rectangles represent glucose in controls (n = 3).

2.3 Statistical analysis

Data were analyzed using SigmaPlot 10.0 and SYSTAT 11 (Systat software). One way analysis of variance (ANOVA) was conducted on all data except cell volume data and TEP data. The data were checked to ensure that they met the assumptions of normality and equality of variance. If data did not meet assumptions, data were log (x + 1) transformed before analysis or a non-parametric ANOVA was carried out on ranks (Kruskal-Wallis ANOVA). Correlation analysis was conducted using the Pearson product moment correlation.

CHAPTER III

EFFECT OF TEMPERATURE ON TEP PRODUCTION

3.1 Introduction

Diatoms in the ocean have important ecological role, not only because of their high productivity, but also because they can excrete large amounts of extracellular polymeric substances (EPS) (Hoagland et al. 1993, Thornton 2002, Underwood and Paterson 2003). EPS constitute 10 % of carbon in the oceanic DOC pool (Chin et al. 1998, Verdugo 2004). Most EPS are acid polysaccharides, which can coagulate into transparent exopolymer particles (TEP) (Passow 2002c). TEP are sticky gel-like particles (Alldredge et al. 1993, Engel 2000, Passow 2002a), which affect the formation of aggregates, as they collide with diatoms and other particulate organic carbon (POC) to form larger particles that sink rapidly in the water column (Kiørboe et al.1998, Thornton 2002, Verdugo et al. 2004). Aggregates of diatoms sink as marine snow, exporting a rapid flux of particulate organic matter from the surface to the ocean interior (Billett et al. 1983, Passow 1995, 2002b). This process strongly affects the biological carbon pump and biogeochemical cycling of carbon in the ocean (Jackson and Burd 1998, Thornton and Thake 1998, Passow 2002a, 2012).

Since the industrial revolution, the Earth‟s temperature has increased faster than any other time in the past 420,000 years (IPCC 2013). Global warming leads to a rising temperature in the surface ocean. Models project a warming of ocean surface

temperature by 1 to 1.5 °C by the end of the 21st century (IPCC 2013). Increasing water temperature of the surface ocean affects planktonic community structure (Sarmento et al. 2010, Lassen et al. 2010, Lewandowska and Sommer 2010). As Kirby et al. (2007) noted, warming the ocean affects the early onset of spring phytoplankton blooms. Increasing temperature in the North Sea has changed plankton community composition and seasonality (Kirby et al. 2007). Metabolic processes, such as phytoplankton growth and microbial respiration, generally increase with elevated temperatures (Sarmento et al. 2010). Zlotnik and Dubinsk (1989) reported that increased temperature triggers of DOC excretion by phytoplankton. Thornton and Thake (1998) reported that more aggregates of *Skeletonema costatum* formed in laboratory cultures grown at higher temperature. In the open ocean, where nutrient supply generally limits growth, temperature is a factor that influences the growth of organisms and may influence EPS and TEP production by phytoplankton (Wolfstein and Stal 2002, Engel et al. 2011). Laboratory studies indicated that temperature can affect cellular metabolic imbalances and lead to increased excretion of primary photosynthetic products (Claquin et al. 2008). The aim of this experiment was to test the hypothesis that temperature increases induce increased TEP production and aggregation in diatoms.

3.2 Experimental approach

The temperature experiment was designed to determine the effect of temperature on the release of TEP and aggregation by diatoms. Four replicate cultures of

Thalassiosira weissflogii and Skeletonema marinoi (500 ml) were grown in semi-continuous cultures (refer to 2.1.3.2) with autoclaved artificial seawater (refer to 2.1.2.1) at three temperature treatments (20, 24 and 28 °C). The initial temperature was the natural temperature in the ocean where species were grown. In order to obtain nitrogen limitation in the cultures, macronutrient concentrations were modified from the original recipe (Table 2 in 2.1.2.2). Different N concentrations were added to each species‟ cultures to induce nitrogen limitation and still keep cultures alive. Macronutrients with a final concentration of 60 µM of $NaNO_3$, 100 µM of $NaH_2PO_4 \cdot H_2O$, and 100 µM of $Na_2SiO_3 \cdot 9H_2O$ were added to the cultures of *T. weissflogii*, whereas macronutrient with a final concentration of 100 µM of $NaNO_3$ and 100 µM of $NaH_2PO_4 \cdot H_2O$ and 100 µM of $Na_2SiO_3 \cdot 9H_2O$ were added to the cultures of *S. marinoi*. Cultures in bottles were placed in a glass water bath filled with water. The temperature of cultures was controlled through the manipulation of water in glass water bath by a thermocirculator (VWR model 1196D). A photon flux density of 150 µmol m^{-2} s^{-1} on the surface of cultures with a 14 h light: 10 h dark cycle was provided for the cultures. The maximum growth rate is 1.10 day^{-1} in *T. weissflogii* and 0.93 day^{-1} in *S. marinoi* in batch culture with modified nutrients (refer to Table 2 in 2.1.2.2) under same light conditions. Considering that cultures needed to be kept alive under temperature stress and nitrogen limitation during the whole experiment, *T. weissflogii* were grown with growth rate of 0.7 day^{-1} (~ 70 % of maximum growth rate); *S. marinoi* were grown with growth rate of 0.65 day^{-1} (70 % of maximum growth) at 10:00 am in each day of experiment. Cell concentrations in the cultures were determined every day (refer to 2.2.1) and other samples were taken from

the cultures only when it was established that they were in steady state. All samples were taken at the time of daily dilution from the volume of culture that was discarded each day. After arriving at steady state, cultures were left to acclimate to the new temperature for at least four generations before sampling. Cultures were sampled three times at each temperature and were maintained for more than 3 days between sampling times. Samples were used to measure cell concentration (refer to 2.2.1); chlorophyll *a* concentration (refer to 2.2.3); EPS concentrations (refer to 2. 2.10.1); TEP (refer to 2.2.5) and CSP (refer to 2.2.6) concentration and size by Image J method (referred to 2.2.5); C: N ratio in the particulate (refer to 2.2.2.8); the allocation of carbon into different carbohydrate pools (refer to 2.2.10); aggregation of diatoms (according to 2.2.7); and cell permeability (according to 2.2.9). In addition, a bacteria check (2.2.2) and bioassay (2.2.4) were conducted in the cultures to prove that cultures were grown with low bacteria concentration and that the whole experiment was proceeding correctly under nitrogen limitation.

3.3 Results

3.3.1 Cell concentration

Cultures arrived at steady states after four or more generations during the acclimation period. Cell concentrations in the steady states were less than 10 % of deviation of average cell abundance. Cell concentrations in the steady state cultures were

not significantly different in the cultures of *T. weissflogii* grown at different temperatures, with average cell abundance of $6.67 \times 10^4 \pm 0.36 \times 10^4$ cells ml^{-1} (mean ± SD) (Figure 7). However, there was a significant negative correlation between cells concentration and temperature ($r = -0.973$, $p < 0.05$, $n = 36$) in the cultures of *S. marinoi*, decreasing from $1.82 \times 10^5 \pm 0.08 \times 10^5$ cells ml^{-1} (mean ± SD) at 20 °C to $0.70 \times 10^5 \pm 0.04 \times 10^5$ cells ml^{-1} (mean ± SD) at 28 °C (Figure 7). Therefore, temperature caused a decrease of cell abundance in the cultures of *S. marinoi*, but not in the cultures of *T. weissflogii*.

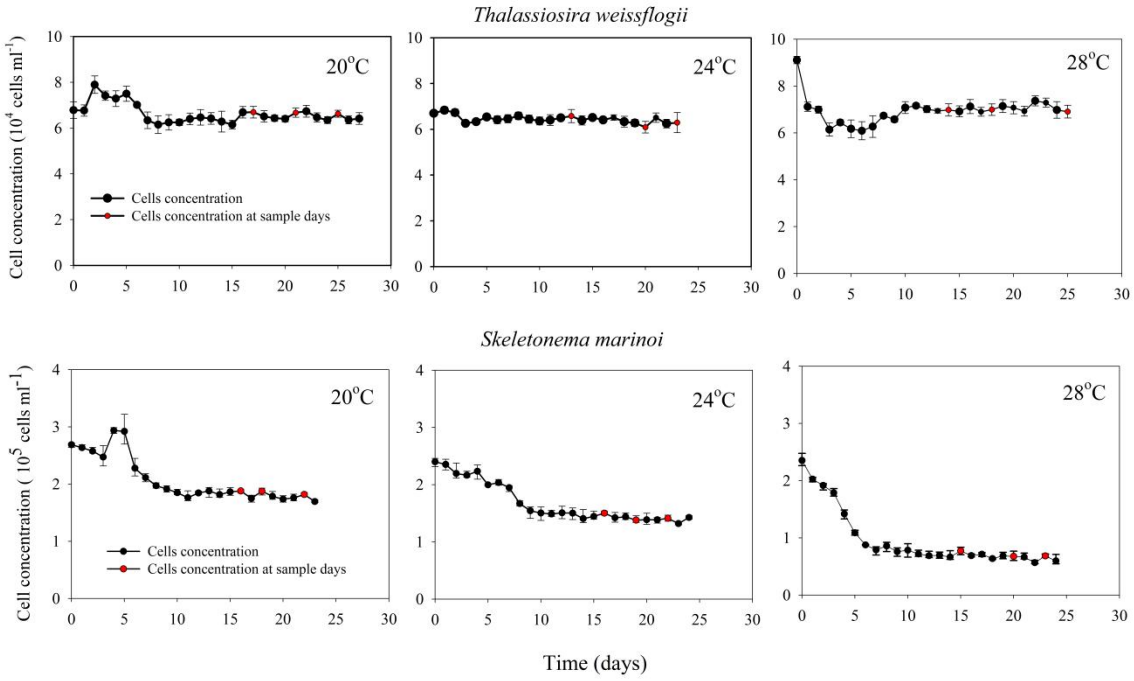

Figure 7. Cell abundances with time of *Thalassiosira weissflogii* and *Skeletonema marinoi* grown in semi-continuous cultures at 20 °C, 24 °C, and 28 °C. Black circles (●) represent mean cell abundances. Red circles (●) represent mean cell abundances on sample days. Error bars ± SD (n = 4 replicate cultures).

3.3.2 Chlorophyll *a*

The chlorophyll *a* concentration was determined at each temperature (Figure 8). There was no relationship between chlorophyll *a* content and temperature in *T. weissflogii*. Chl. *a* concentration decreased as temperature increased from 20 to 24 °C and then increased to concentration of 74.67 ± 6.62 µg L^{-1}at higher temperature of 28 °C (Figure 8). Unlike *T. weissflogii*, there was a negative relationship between chlorophyll *a* concentration and temperature ($r = -0.883$, $p < 0.05$, $n = 36$) in the cultures of *S. marinoi* (Figure 8). Their chl. *a* concentrations decreased at 20 °C to 13.77 ± 1.37 µg l^{-1} (mean ± SD) at 28 °C. Chlorophyll *a* concentrations were significantly different at different temperatures in both species (*T. weissflogii*: $F_{2, 35} = 34.085$, $p < 0.05$; *S. marinoi*: $F_{2, 35} = 214.473$, $p < 0.05$).

Chlorophyll *a* content per cell presented the same trend of chlorophyll *a* concentrations with temperature in two species. The greatest chlorophyll *a* per cell in the cultures of *T. weissflogii* was 1.06 ± 0.11 pg $cell^{-1}$ (mean ± SD), which was ten times higher than that in the *S. marinoi* cultures. The maximum chlorophyll *a* per cell was only 0.19 ± 0.02 (mean ± SD) pg $cell^{-1}$ in the cultures of *S. marinoi*.

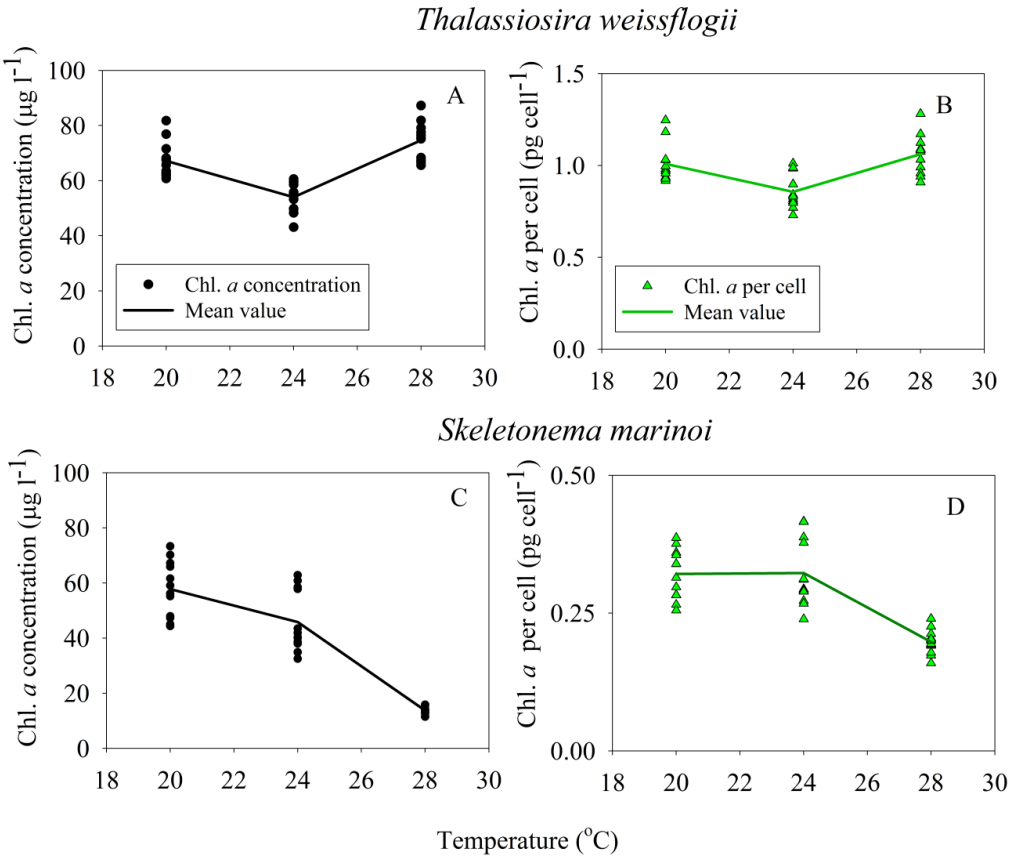

Figure 8. Chlorophyll *a* concentration and chlorophyll *a* content per cell in semi-continuous cultures of *Thalassiosira weissflogii* and *Skeletonema marinoi* grown at 20, 24, and 28 °C. A.C) Chl. *a* concentration. B.D) Chl. *a* concentration per cell. Black circles (●) represent the chl. *a* concentrations (n = 12). Green triangles (▲) represent chl. *a* per cell (n = 12). Solid lines represent the mean value of chl. *a* content in cultures at 20, 24 and 28 °C (n = 36).

3.3.3 Carbohydrates

3.3.3.1 Carbohydrate allocation

In the cultures of *T. weissflogii*, total carbohydrate concentration per cell had a positive correlation with temperature, increasing from 0.31 ± 0.05 (mean ± SD) ng cell^{-1} at 20 °C to 0.45 ± 0.08 (mean ± SD) ng cell^{-1} at 28 °C (Figure 9 A). There was a significant difference in total carbohydrate per cell at different temperatures ($F_{2, 35}$ = 41.399, $p < 0.05$). However, there was no relationship between dissolved extracellular carbohydrate concentrations per cell or cell associated carbohydrate concentration per cell and temperature.

In cultures of *S. marinoi*, there were significant positive correlations between total carbohydrate per cell ($r = 0.391$, $p < 0.01$, $n = 36$), dissolved extracellular carbohydrate per cell ($r = 0.336$, $p < 0.01$, $n = 36$), cell-associated carbohydrate per cell ($r = 0.792$, $p < 0.01$, $n = 36$) and temperature (Figure 9 B). There was a significant difference in cell-associated carbohydrate at different temperatures in the cultures of *S. marinoi* ($F_{2, 35}$ = 28.366, $p < 0.05$). The increase of total carbohydrate was associated with more extracellular carbohydrate and more carbohydrate stored in the cells.

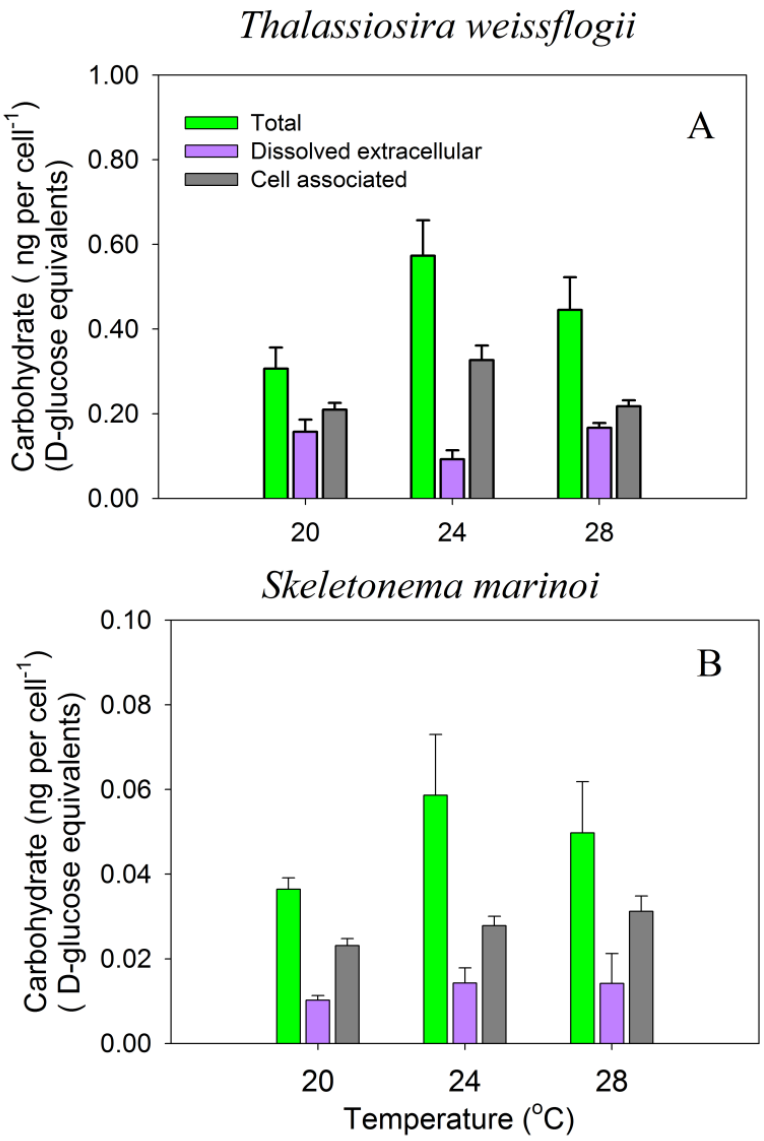

Figure 9. Carbohydrate allocation in semi-continuous cultures grown at 20 °C, 24 °C and 28 °C. Error bars show mean + SE (n = 12). A) In the cultures of *Thalassiosira weissflogii.* B) In the cultures of *Skeletonema marinoi.* Green bars represent total carbohydrate concentration per cell. Purple bars represent dissolved extracellular carbohydrate per cell. Grey bars represents associated with cell carbohydrate per cell.

The relationship between extracellular and cell-associated carbohydrate pools in cultures at different temperatures is shown in three pie charts (Figure 10). The cell associated carbohydrate included carbohydrate associated with storage, carbohydrate associated with the cell wall and residual carbohydrates. The dissolved extracellular carbohydrate is carbohydrate exported from or lost from the cells. For the cultures of *T. weissflogii*, the proportion of cell-associated carbohydrate to total carbohydrate increased with a decrease in the proportion of dissolved extracellular carbohydrate as temperature was elevated to 24 °C (Figure 10 A). When temperature continued to increase, there was an opposite trend in carbohydrate allocation into different pools within cells. Unlike to *T. weissflogii*, there was no significant statistical difference ($P > 0.05$) in proportions of cell-associated carbohydrate and extracellular carbohydrate in total carbohydrate with temperature in the cultures of *S. marinoi* (Figure 10 B).

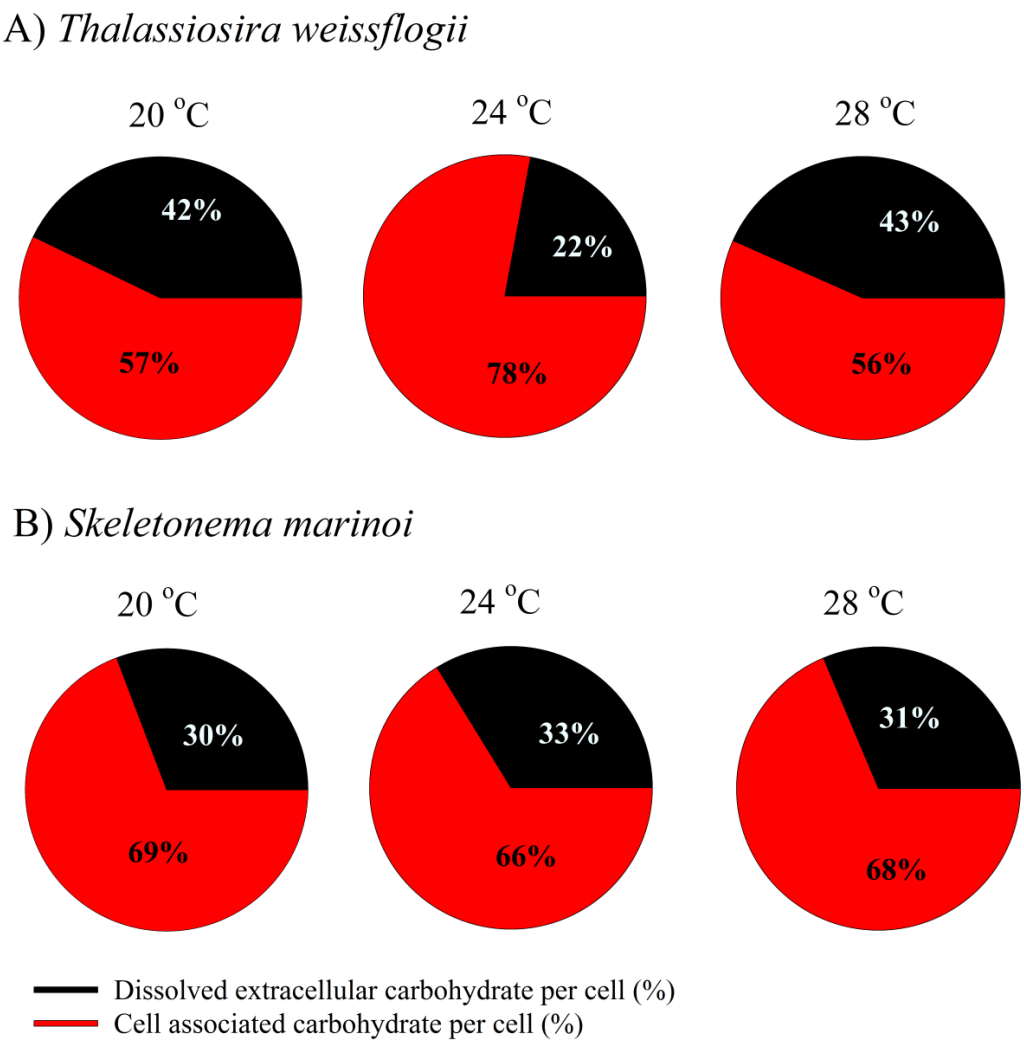

Figure 10. Relationship between two carbohydrate pools (cell associated carbohydrate and extracellular carbohydrate) in cultures grown at 20 °C, 24 °C and 28 °C**.** A) In the cultures of *Thalassiosira weissflogii*. B) In the cultures of *Skeletonema marinoi.* Black color represents the proportion of dissolved extracellular carbohydrate per cell out of total carbohydrate per cell. Red color represents proportional of cell-associated carbohydrate per cell out of total carbohydrate per cell.

3.3.3.2 EPS

EPS concentration was greater in the higher temperature cultures of *T. weissflogii*. As temperature increased from 20 to 28 °C, the abundance of EPS increased from a mean concentration of 3.2 to 6.7 μg ml^{-1} (Figure 11). When normalized to cells, EPS per cell was positively correlated with temperature ($r = 0.828$, $p < 0.05$, $n = 36$). There were significant differences in EPS concentration ($F_{2, 35} = 58.259$, $p < 0.05$) and EPS per cell ($F_{2, 35} = 43.024$, $p < 0.05$) at different temperatures. Thus, hypothesis of EPS concentration increasing with temperature was accepted in the cultures of *T. weissflogii*.

On the contrary, there was a negative relationship between EPS concentration and temperature ($r = -0.565$, $p < 0.05$, $n = 36$) in the cultures of *S. marinoi*. EPS concentration decreased from mean concentration of 0.9 μg ml^{-1} at 20 °C to 0.6 μg ml^{-1} at 28 °C (Figure 11). However, EPS per cell was greater at the higher temperature because lower cell abundance was lower at higher temperature.

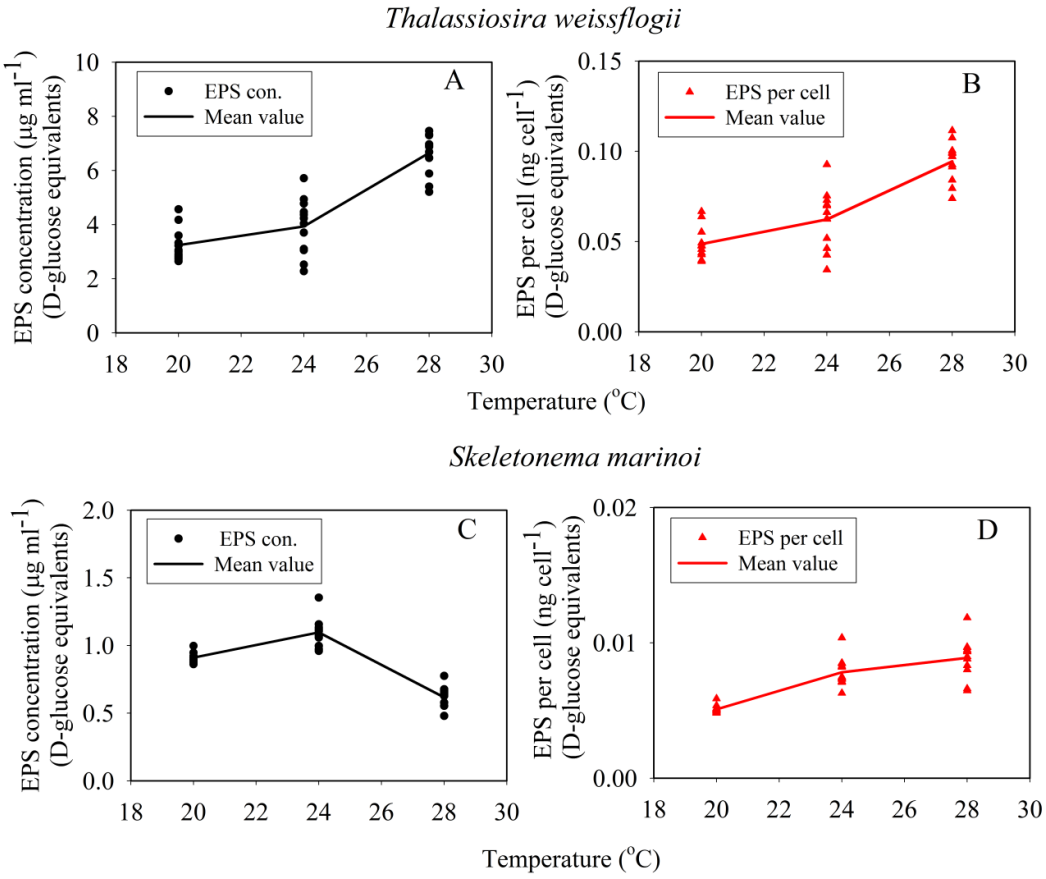

Figure 11. EPS concentration and EPS concentration per cell in semi-continuous cultures of *Thalassiosira weissflogii* and *Skeletonema marinoi* when they grown at 20, 24, and 28 °C. A.C) EPS concentration. B.D) EPS concentration per cell. Black circles (●) represent EPS concentration (n = 12). Red triangles (▲) represent EPS per cell (n = 12). Solid lines represent the mean value of EPS content (n = 36).

3.3.4 TEP formation

TEP concentration and TEP area were analyzed in Image J. The production of TEP responded to increasing temperature differently in two species. The images of TEP associated with the two species are shown below (Figure 12).

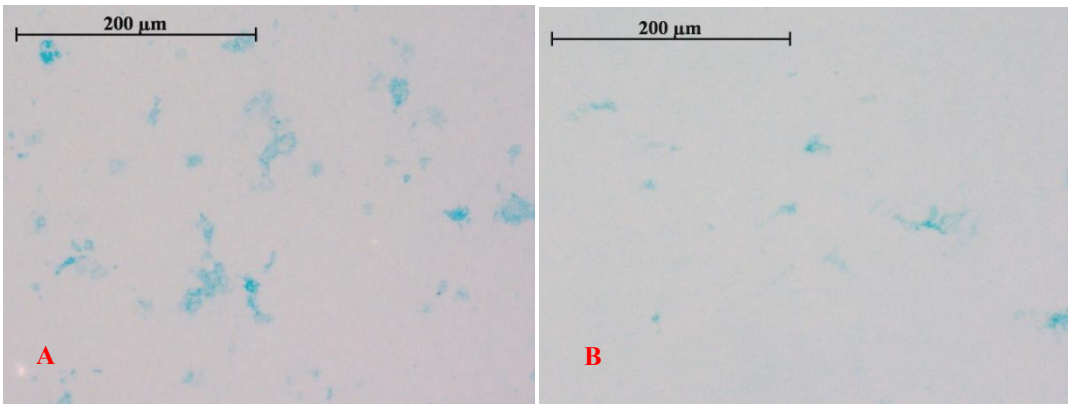

Figure 12. Image of TEP in semi-continuous cultures of *Thalassiosira weissflogii* (A) and *Skeletonema marinoi* (B). TEP were stained by Alcian Blue and shown as blue particles.

Several measures of TEP dynamics are shown in Figure 13. There was an increase of TEP abundance in the cultures of *T. weissflogii* as temperature increased (Figure 13 A). On the contrary, TEP abundance in the cultures of *S. marinoi* decreased with rising temperature (Figure 13 A). There were significant differences between TEP abundance and temperature in both cultures (*T. weissflogii*: $F_{2, 35} = 19.482$, $p < 0.05$; *S. marinoi*: $F_{2, 35} = 19.482$, $p < 0.05$). The mean size of individual TEP did not significantly

change with temperature in the cultures of *T. weissflogii*, whereas TEP size became larger in higher temperature cultures of *S. marinoi* (Figure 13 B). Because TEP particles with different sizes occurred in the cultures, TEP production was determined by total TEP area (TEP concentration × mean TEP size). The total area of TEP in the cultures of *T. weissflogii* was larger at higher temperature (Figure 13 C). However, in cultures of *S. marinoi*, total area of TEP did not have any correlation with temperature (Figure 13 C). When total TEP area was normalized to cell numbers, total TEP area per cell increased with temperature in both cultures (*T. weissflogii*: $r = 0.683$, $p < 0.01$, $n = 36$; *S. marinoi*: $r = 0.530$, $p < 0.01$, $n = 36$), (Figure 13 D) indicating more TEP production occurred cultures growing at higher temperatures.

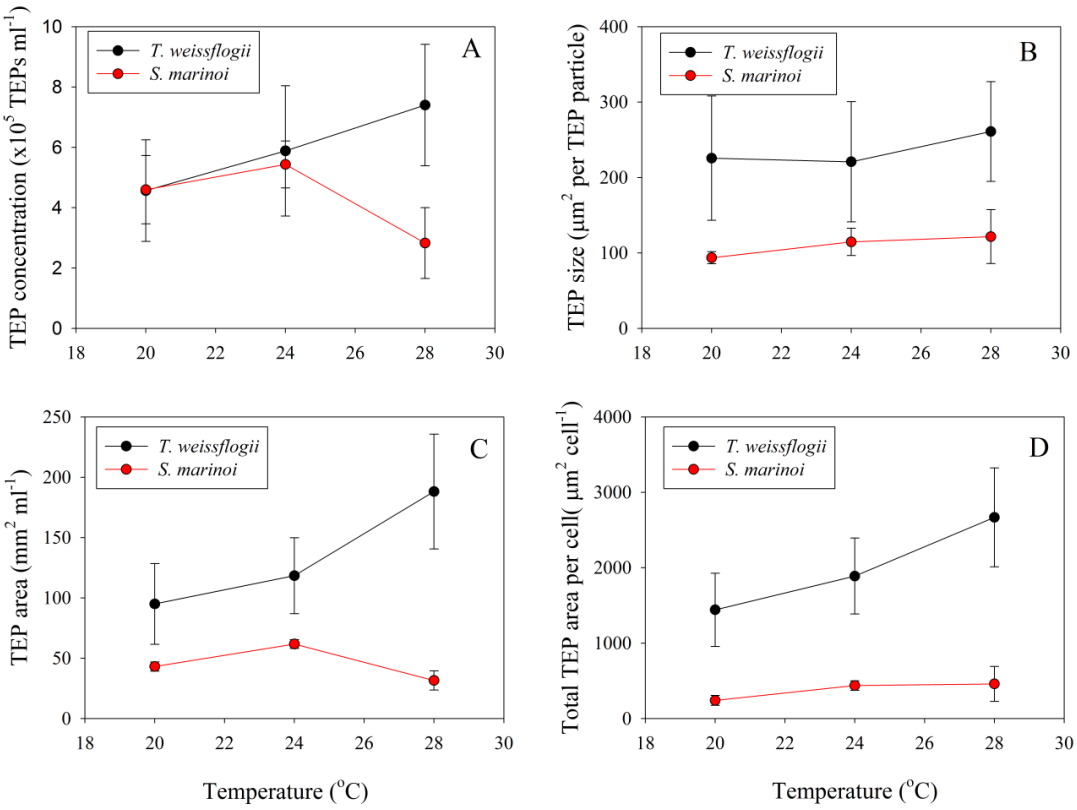

Figure 13. The relationship between TEP content with temperature in semi-continuous cultures of *Thalassiosira weissflogii* and *Skeletonema marinoi* under nitrogen limitation. Error bars show mean ± SD (n = 120). A) TEP concentration. B) Mean TEP size. C) Total TEP area. D) Total TEP area per cell. Black circles (●) represent TEP content in the cultures of *T. weissflogii*. Red circles (●) represent TEP content in the cultures of *S. marinoi*.

3.3.5 CSP formation

CSP concentration and particle size at different temperatures were determined from both diatom species by image analysis using Image J. Typical images of CSP in two species are shown in the images below (Figure 14).

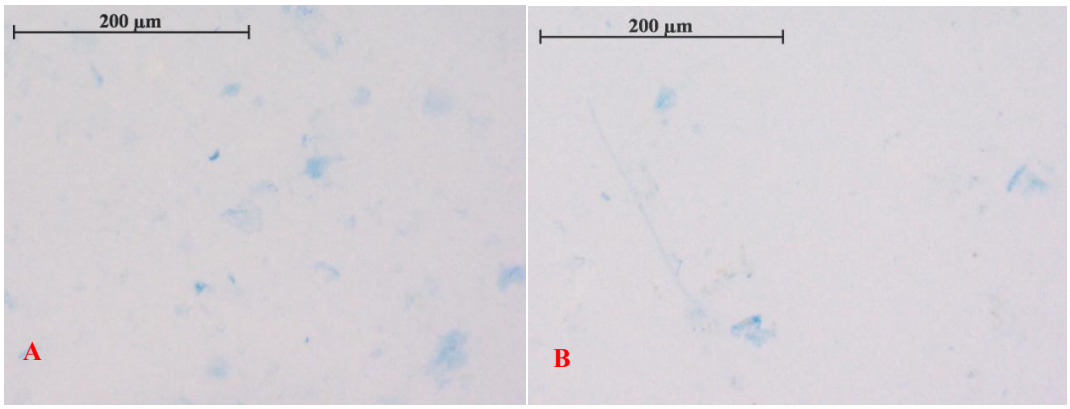

Figure 14. Image of CSP in semi-continuous cultures of *Thalassiosira weissflogii* (image A) and *Skeletonema marinoi* (image B). CSP were stained by Coomassie Brilliant Blue and show as blue particles.

The variation of CSP concentrations in the cultures of *S. marinoi* and *T. weissflogii* was showed in Figure 15. There was no significant correlation between CSP abundance and temperature in both cultures (Figure 15 A). The mean size of each CSP particle and total area of CSP in the cultures of *T. weissflogii* also had no correlation with temperature (Figures 15 B & C). However, the mean size of each CSP particle had a positive correlation with temperature in the cultures of *S. marinoi* ($r = 0.374$, $p < 0.05$,

n = 36) (Figure 15 B). The greatest total area concentration of CSP associated with *T. weissflogii* occurred at a temperature of 24 °C, and the greatest in *S. marinoi* occurred at 20 °C (Figure 15 C). When total CSP area was normalized to cell abundance, there was no correlation between total CSP area per cell and temperature in both species (Figure 15 D).

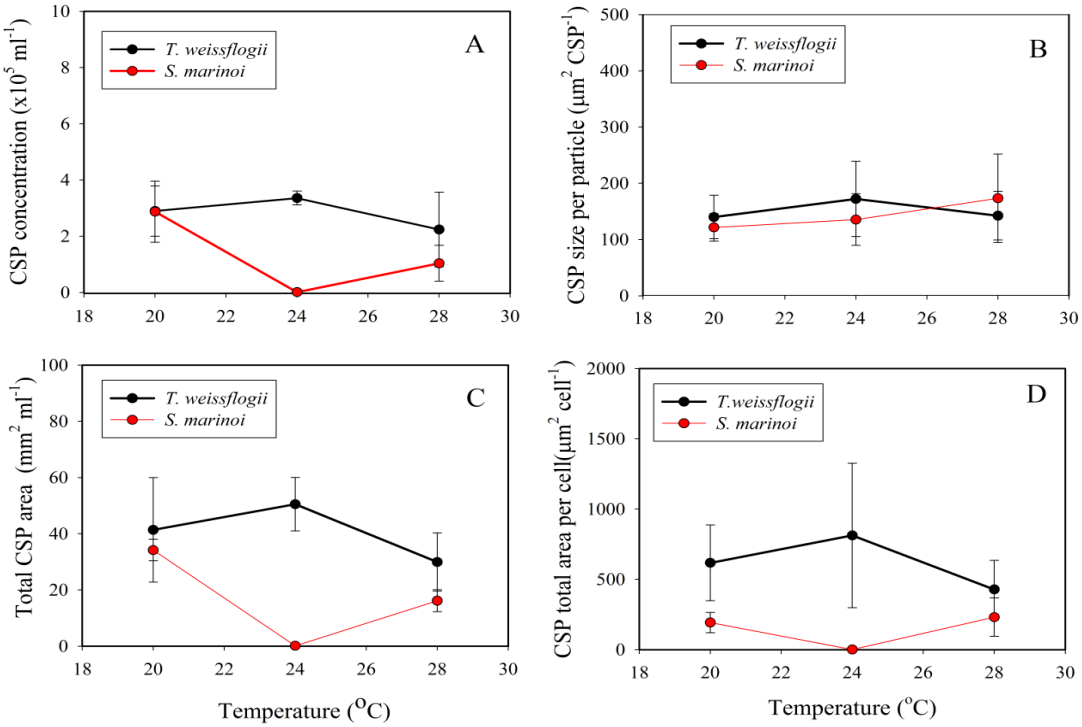

Figure 15. The relationship between CSP content with temperature in semi-continuous cultures of *Thalassiosira weissflogii* and *Skeletonema marinoi* under nitrogen limitation. Bars show mean ± SD (n = 120). A) CSP concentration. B) Mean CSP size. C) Total CSP area. D) CSP concentration per cell. Black circles (●) represent CSP content in the cultures of *T. weissflogii*. Red circles (●) represent CSP content in the cultures of *S. marinoi*.

3.3.6 Particle size distribution and aggregation

Particle size distributions (PSD) for two species grown at different temperatures are shown below (Figure 16). All particles with an ESD ≥ 63 μm, which was bigger than individual cell size were designated as aggregates. The ratio of volume concentration of aggregates to the volume concentration of unaggregated cells in the cultures of *T. weissflogii* decreased with elevated temperature, from 2.36 at 20 °C to 1.59 at 28 °C (Figure 16), indicating aggregation was greater at lower temperatures. In the contrast, the ratio of total volume of aggregates to total volume of unaggregated particles in the cultures of *S. marinoi* increased with temperature, from 1.37 at 20 °C to 3.91 at 28 °C (mean ± SD) (Figure 16). *Thus,* aggregation increased with rising temperature in the cultures of *S. marinoi* and decreased with temperature in cultures of *T. weissflogii*. There were significant differences in the ratio of aggregate to un-aggregate at different temperatures (*T. weissflogii*: $F_{2, 35} = 4.377$, $p < 0.05$; *S. marinoi*: $F_{2, 35} = 27.689$, $p < 0.05$).

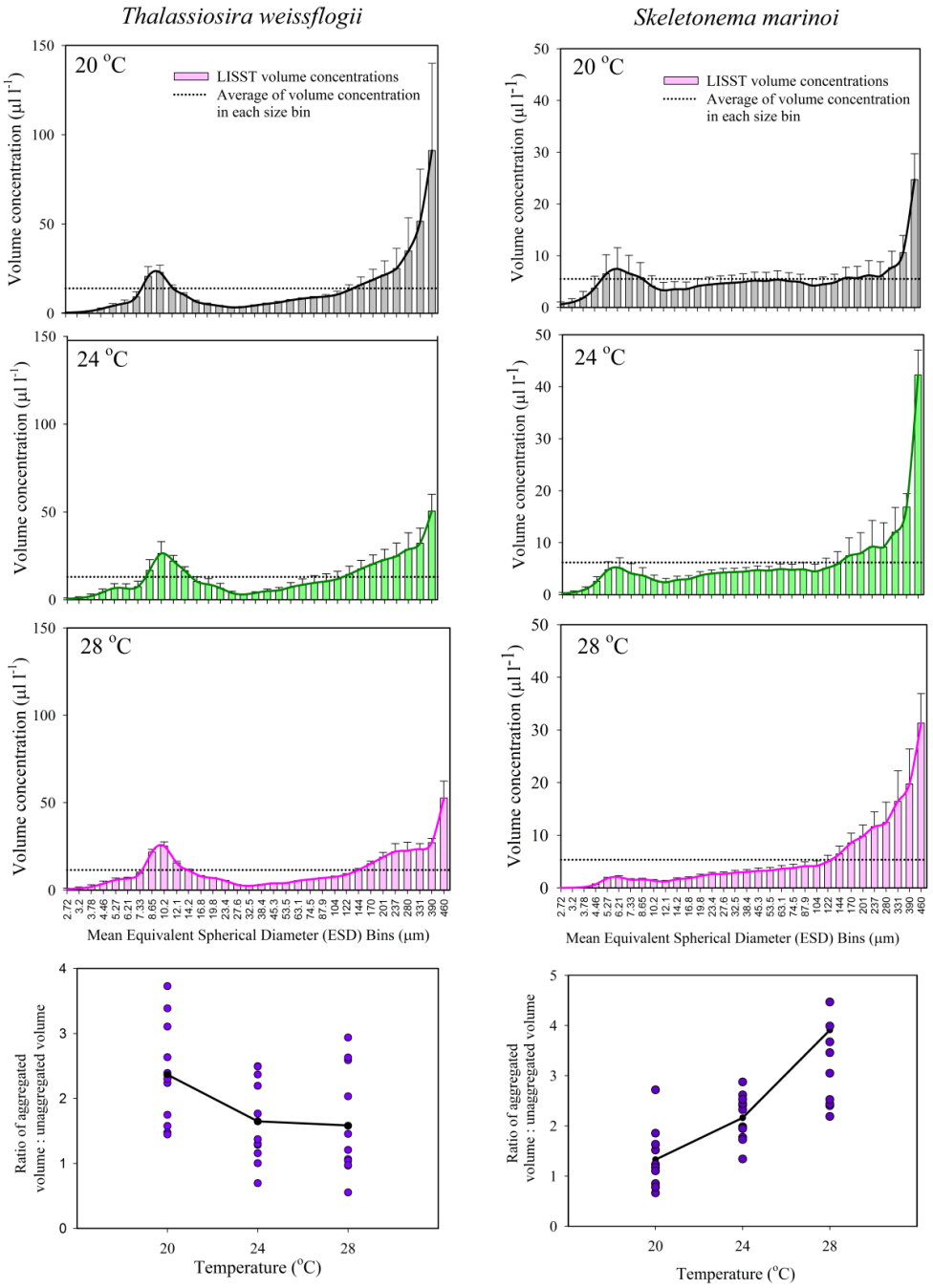

Figure 16. Particles size distributions (PSD) and ratio of aggregated to unaggregated culture in semi-continuous cultures grown at 20, 24 and 28 °C. Bars represent volume concentration in each size bin in the cultures grown at different temperatures. Bar shows mean + SD (n = 1200). Solid circles represent ratio of aggregates to unaggregated volume in cultures at different temperatures. Dash lines represent the mean value of total volume concentration. Solid lines represent the mean value of the ratio.

3.3.7 Cell permeability

The permeable cells of *T. weissflogii* and *S. marinoi* are shown in the images below (Figure 17). There were positive relationships between proportion of SYTOX Green labeled cells and temperatures in both species (*T. weissflogii*: $r = 0.636$, $p < 0.05$, $n = 36$; *S. marinoi*: $r = 0.827$, $p < 0.05$, $n = 36$) (Figure 18), indicating cells grown at higher temperature were more permeable. The proportion of SYTOX Green labeled cells increased from 2.6 % (mean) at 20 °C to 4.1 % (mean) at 28 °C in the cultures of *T. weissflogii* and elevated from 2.6 % at 20 °C to 5.5 % at 28 °C in the cultures of *S. marinoi*. There were significant differences in SYTOX Green stained cell numbers at different temperatures in both cultures (*T. weissflogii*: $F_{2, 35} = 11.49$, $p < 0.001$; *S. marinoi*: $F_{2, 35} = 46.733$, $p < 0.001$). Hence, the hypothesis of a greater proportion of the population with compromised cell membranes at higher temperatures was accepted for both species.

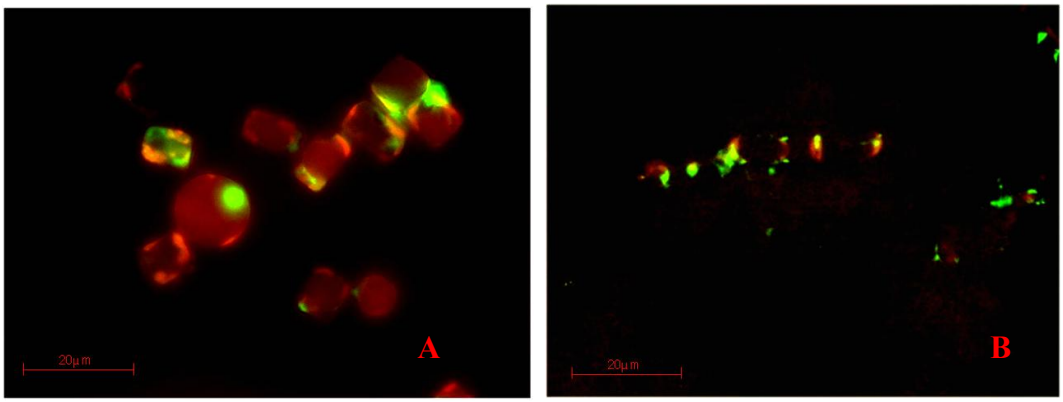

Figure 17. Images of permeable *Thalassiosira weissflogii* and *Skeletonema marinoi* cells. Damaged cells fluoresce green and chlorophyll *a* fluorescence is shown in red. A) *T. weissflogii*. B) *S. marinoi*.

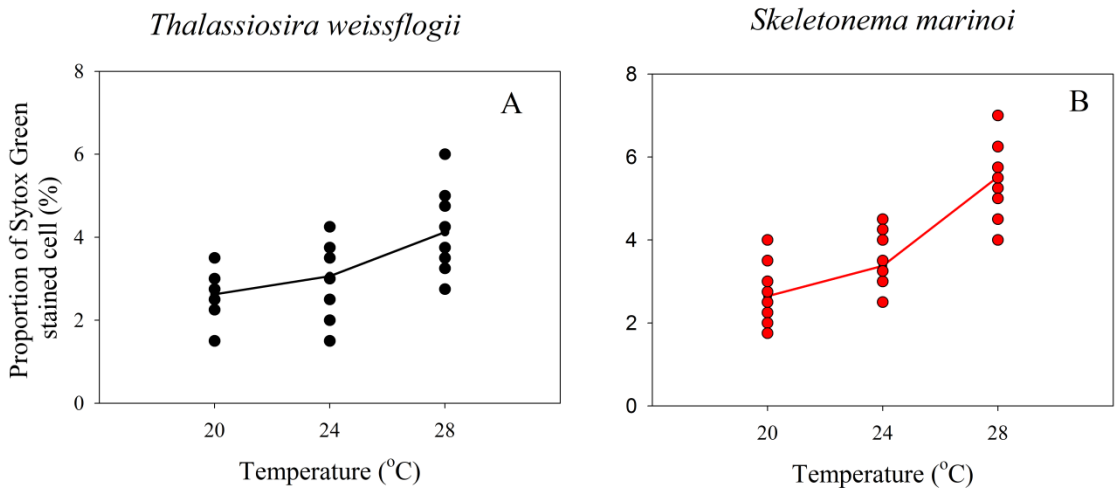

Figure 18. Relationship between proportions of SYTOX Green stained cell in 400 cells in the different cultures and temperatures. n = 12. A) In the cultures of *Thalassiosira weissflogii*. B) In the cultures of *Skeletonema marinoi*.

3.3.8 Bacteria

There was no significant correlation between bacteria concentration and temperature. Initial bacteria concentrations in the cultures were very low (less than 1.0 $\times 10^4$ cells ml^{-1}) and increased over time. Bacteria concentration was greatest in the cultures of *S. marinoi* grown at 24 °C, with a concentration of $1.52 \times 10^5 \pm 1.64 \times 10^5$ cells ml^{-1} (mean ± SD) The greatest concentration of bacteria in the cultures of *T. weissflogii* occurred at 28 °C, with a concentration of $1.85 \times 10^5 \pm 2.01 \times 10^5$ cells ml^{-1} (mean ± SD).

3.4 Discussion

3.4.1 Temperature affects cell growth

Cell growth was followed in the cultures of *T. weissflogii* and *S. marinoi* when they were grown at temperatures between 20 and 28 °C. Our results showed that cell abundances in the cultures of *T. weissflogii* were consistent irrespective of temperature (Figure 7). The chlorophyll *a* concentration per cell also showed no significant difference in the cultures of *T. weissflogii* grown at different temperatures (Figure 8), indicating that the thermal range between 20 °C and 28 °C did not affect growth of *T. weissflogii*. Unlike the *T. weissflogii*, a decrease in cell abundance of *S. marinoi* with rising temperature was observed (Figure 7). The cell concentration of *S. marinoi* at the

higher temperature of 28 °C was one of third of that at the lower temperature of 20 °C. In addition, lower chlorophyll *a* concentration per cell occurred at higher temperature in the cultures of *S. marinoi* (Figure 8). Thus, these two organisms could have different widths of thermal tolerance and/or different temperature ranges. In the field, *T. weissflogii* is distributed worldwide in the oceans and contributes to spring blooms in coastal surface water with temperatures between 3 and 24 °C; for example, in the Atlantic Ocean, Pacific Ocean, Hawaiian seas and Indonesian seas during spring and autumn at temperatures of 15 to 24 °C (Armbrust and Galindo 2001, Sorhannus et al. 2010). Compared to *T. weissflogii*, many observations of blooms *in situ* have confirmed that the *S. marinoi* dominates in coastal waters with a cooler temperature range between 2 and17 ℃ . For instance, a *S. marinoi* bloom occurred in the surface of the Baltic Sea where the temperature was around 4 °C (Kaeriyama et al. 2011). Barofsky et al. (2010) reported a *S. marinoi* bloom in the Raunefjord, Western Norway, at temperatures of 7 to 8 °C. In the North Atlantic, *S. marinoi* is most abundant during the spring bloom with a temperature of 2 to7 °C (Sarno et al. 2005). Kent et al. (1995) reported that mix blooms of *Thalassiosira spp*. and *Skeletonema spp*. occurred in the coastal ocean in the British Columbia, Canada, indicating these two diatoms have overlapping distributions. From these observations, I propose that the range of thermal tolerance for *T. weissflogii* is wider than *S. marinoi*, indicating that *T. weissflogii* may have an advantage in competing with *S. marinoi* as ocean surface temperature increases in next several decades.

In addition, the climate change will also influence the physiology of cells, such as inorganic carbon concentration mechanisms (CCMs). CCMs increase the supply of

CO_2 to RUBISCO in most photosynthetic organisms, including cyanobacteria, algae, aquatic plants and C_4 plants (Raven et al. 2008). CCMs in cyanobacteria and algae catalyze movement of CO_2, HCO_3 and/or H^+ across membranes, and directly associated with biochemistry of cell growth. CCMs increase CO_2 concentration and the rate of C assimilation in Rubisco (Badger et al. 2002; Price et al. 2007). The atomospheric CO_2 concentration has important influence in evolution of CCMs. Some data suggested that CCM have been influenced by the glacial–interglacial cycles of atmospheric CO_2 (Raven et al. 2008). Increasing CO_2 in the atmosphere will result in more CO_2 dissolving in the ocean. This will not only decrease the pH of the ocean (ocean acidification), but it will also change the equilibrium of the different components of the DIC system. The relative concentration of dissolved CO_2 will increase. These environmental changes have significant effects on CCMs expression in algae and aquatic plants (Giordano et al. 2005, Raven et al. 2005, Raven 2010). Results from laboratory experiments suggested that a decreased affinity for inorganic carbon from cells grown at higher inorganic carbon concentrations (Giordano et al. 2005, Falkowski and Raven 2007, Raven 2010). Raven et al. (2005, 2010) suggested that climate change may alter the phytoplankton community structure associated with species with or without CCMs. In addition, almost all cyanobacteria have CCMs and prefer grow in warmer water (Paerl and Huisman 2008). So, global warming may lead to a greater prevalence of cyanobacteria. Decreased combined nitrogen supply (Giordano et al. 2003) and iron availability (Young and Beardall 2005) generally increases CO_2 affinity, which has varying effects on the different organisms. Thus, climate change will have implications for the kinetics of C

fixation by Rubisco and therefore the competitive ability and productivity of different phytoplankton groups.

3.4.2 Temperature affects TEP production

Many studies have indicated that temperature is an important factor that influences photosynthesis in microalgae and could also indirectly influence TEP production. The effect of temperature on TEP production might be associated with carbohydrate allocation. Wolfstein and Stal (2002) found that temperature affected cellular metabolic imbalances, leading to increased excretion of primary photosynthetic products. My results indicated that elevated temperature caused more EPS production by the two species (Figure 11), which is consistent with Zotnik and Dubinsy (1989), who found that more dissolved primary production, was excreted at higher temperatures. EPS is a fraction of that dissolved primary production that would likewise increase with temperature. As a subgroup of EPS, TEP production per cell fitted the temperature model of EPS in two species (Figure 13). In the studies of relationship between TEP production and temperature in microalgae, Fukao et al. (2012) indicated that TEP production decreased with increasing temperature in the diatoms *Coscinodiscus granii*. Nevertheless, Claquin et al. (2008) showed an increase of TEP production as temperature increased to an optimal temperature for the diatoms of *Thalassiosira pseudonana*, *Skeletonema marinoi*, and *Pseudo-nitzschia fraudulenta*. Our results here are in agreement with the observations of Claquin et al. (2008). My results might be the

result of elevated enzyme activity at higher temperatures, which is related to TEP production mechanisms (Claquin et al. 2008). Bhaskar and Bhosle (2005) proposed that TEP precursors could be attributed to cell exudation or cell lysis. My results showed that cell permeability increased with temperature (Figure 18). However, more permeable cells did not directly lead to more dissolved carbohydrate outside the cells because dissolved extracellular carbohydrate did not increase with temperature. Thus, whether cell permeability contributed to TEP precursors needs to be verified in future.

Composition of carbohydrates varied in the different carbohydrate fractions associated with the cell wall, cell storage, and extracellular carbohydrates. For example, carbohydrate associated with storage is rich in glucan, whereas cellulose is a major component of carbohydrate associated with the cell wall. The variation of carbohydrate allocation in the cells at different temperatures may be associated with different quantities or compositions of cell surface carbohydrates. In addition, the different compositions may be attributed to diverse chemical and /or physical properties. Thus, TEP with different compositions might have different characteristics, such as variable stickiness. Some studies have reported that different compositions of organic matter and different types of EPS were formed at different growing conditions (Underwood et al. 2004, Engel et al. 2011). Therefore, further studies are necessary to investigate TEP and EPS compositions related to distinct characteristics of TEP, such as stickiness and structure.

3.4.3 Temperature affects aggregation

My results indicated that aggregation in *S. marinoi* was enhanced with elevated temperature, whereas aggregation in *T. weissflogii* decreased at lower temperature (Figure 16). In the study of the effect of temperature on aggregation, Thornton and Thake (1998) found a positive correlation between aggregate concentration and temperature in the cultures of *Skeletonema costatum*, which was consistent with what I found in the cultures of *S. marinoi*. The difference in aggregate formation with elevated temperature between the two species is probably due to their distinct stickiness. Previous experiments suggested that cells have different aggregation patterns based on their stickiness. Cell - TEP aggregation occurred in the cells that have low stickiness, and cell – cell aggregates formed when cells were very sticky (Kiørboe and Hansen 1993, Crocker and Passow 1995). Several studies have shown that *T. weissflogii* are not sticky and aggregation must be facilitated by TEP in the form of cell-TEP aggregate TEP (Kiørboe and Hansen 1993, Crocker and Passow 1995). However, *Skeletonema costatum* are sticky cells, and their aggregation proceeds because of their high stickiness (Kiørboe and Hansen 1993). In diatom aggregation observations, variation in stickiness has been recorded (Kiørboe et al. 1998). Many studies have shown that stickiness of cells can vary with temperature (Kiørboe and Hansen 1993, Thornton and Thake 1998). Thus, I propose that the *S. marinoi* cells became stickier and produced more aggregation at high temperature, whereas *T. weissflogii* had lower stickiness and produced less aggregation at higher temperature. Aggregation is a source of marine snow; therefore, the response of

aggregation formation to temperature also influences the vertical flux of carbon in the ocean. Sticky cells, such as *S. costatum*, will tend to aggregate during blooms and result in a fast-sinking flux of organic carbon. On the contrary, if the cells have low stickiness, such as *T. weissflogii*, they will remain in surface waters for a long time during the bloom. Many observations of aggregates of *S. costatum* in the coastal ocean and their subsequent sedimentation have been documented (Crocker 1993). The sinking of diatom aggregates and marine snow plays a critical role in the rapid transfer of primary production from the euphotic zone to depth. EPS production and aggregation have a significant impact on the biogeochemistry of organic matter and the ecology of marine snow. However, there have been few studies of the effect of temperature on EPS production and the attendant effect on marine biogeochemistry. Hence, the effect of temperature on the stickiness of different species and their distinct aggregation mechanisms are a potential avenue for further investigation.

3.5 Conclusions

In conclusion, I showed that temperature affects TEP production and aggregation in the diatom species *T. weissflogii* and *S. marinoi*. However, the response to temperature change by different species was not same. As temperature increased, cell abundance decreased in the cultures of *S. marinoi* but not in the cultures of *T. weissflogii*, indicating that these two organisms could have different widths of thermal tolerance and/or different temperature ranges. My results suggest that TEP production can be

enhanced at higher temperature, which was associated with more EPS production and greater permeability in the cultures. However, there was not sufficient evidence to demonstrate the relationship between TEP formation and cell lysis. It remains unclear if TEP precursors were created by leakage from permeable cells or exudation by cells. Such a question would be an interesting topic for future study. In my results, increase in temperature did not enhance aggregation in both species. More aggregates of *S. marinoi* occurred in higher temperature cultures, indicating *S. marinoi* cells become stickier at higher temperatures. On the contrary, fewer aggregates occurred in the cultures of *T. weissflogii* at higher temperatures even though TEP production was enhanced. This indicates that temperature may affect TEP composition and consequently influence their chemical or physical properties and aggregate formation. TEP production and aggregate formation have important role in the transport of carbon in the ocean. Therefore, accumulation of *S. marinoi* in the form of marine snow in response to elevated temperatures will enhance the transportation of carbon to the deep ocean.

CHAPTER IV

EFFECT OF GROWTH RATE ON TEP PRODUCTION BY DIATOMS

4.1 Introduction

Growth rate of microalgae is a physiological factor on the growth mechanisms of cells, such as changes of biomass, cell quota and cell size with time (Droop 1983, Martens et al. 1993). In the study of cell quota conducted in chemostat experiment, Droop found that there is a relationship between growth rate and cell quota under Vitamin B_{12} limitation (Droop 1970). Cell quota is quantity of uptake substrate for producing a given biomass. Thus, the biomass of cells directly affect by the factor of growth rate. Growth rate is a distinguish expression of a species in adapting to the environmental conditions that it are experienced (Conway et al. 1977, Fogg and Thake 1987). Organisms have specific responds in the growth to present the experimental change imposed on it, such as nutrients limitation (Conway et al. 1977). Cells perform a physiological adaption strategy of nutrients uptake system during nutrient limited growth, such as increase nutrient uptake rate (Droop 1983) and carbon fixation rate (Lancelot & Mathot 1985). Cells in different phases of growth have different properties related to morphology, metabolic production, photosynthesis and respiration rate, and shear sensitivity (Fogg and Thake 1987, Martens et al. 1993). However, how growth rate affects the production of TEP by diatoms and its subsequent influence on diatom aggregation is not clear. During this work, we grew *T. weissflogii* at a range of growth

rates under nitrogen limitation to determine the effects of growth rate on TEP production and aggregate formation by *T. weissflogii.*

4.2 Experimental approach

The growth rate experiment was designed to determine how growth rate affects TEP production and aggregation by a diatom (Aim 2). Four replicate cultures (1 liter) of *Thalassiosira weissflogii* were grown in semi-continuous cultures (refer to 2.1.3.2) at a series of dilution rates (0.3, 0.5, 0.7, and 0.9 day^{-1}), below the maximum specific growth rate of 1.1 day^{-1}, that was measured in nutrient replete batch culture under the same conditions of light and temperature. In order to obtain nitrogen limitation in the cultures, macronutrient concentrations were modified from the original recipe (Table 2 in 2.1.2.2). Macronutrients (N, P, and Si) were added to a final concentration of 60 μM of $NaNO_3$, 100 μM of $NaH_2PO_4 \cdot H_2O$, and 100 μM of $Na_2SiO_3 \cdot 9H_2O$. Cultures in 2 liter bottles were located in a glass water bath which filled of water. The temperature of cultures was controlled through manipulation water in glass water bath by a thermocirculator (VWR model 1196D). Cultures were grown in a glass water bath at 20 °C with a photon flux density of 150 μmol m^{-2} s^{-1} on the surface of the culture bottles. The light cycle was 14 h light: 10 h dark. Cultures were diluted at 10:00 am in everyday of experiment.

Cell concentrations in the cultures were determined every day (refer to 2.2.1) and other samples were only taken from the cultures when it was established that they were in steady state (i.e. dilution rate = growth rate). After arriving at steady state,

cultures were left to acclimate to the new growth rate at least for four generations before sampling. Cultures were sampled to test hypotheses at each dilution rate. Cultures were sampled three times at each growth rate and maintained cultures for 3 days between sampling.

Sample were used to measure cell count and cell size (2.2.1); chlorophyll *a* concentration (2.2.3); TEP concentrations and area by Axio Vision 4.8 software (refer to 2.2.5); carbohydrate allocation (refer to 2.2.10); aggregation (refer to 2.2.7); the proportion of permeable cells in total cell abundance (refer to 2.2.9). In addition, bacteria check (2.2.2) and bioassay (2.2.4) were conducted in the cultures grown at different growth rate to prove that cultures are grown with low bacteria concentration and whole experiment is working under nitrogen limit.

4.3 Results

4.3.1 Diatom abundance and biomass

Figure 19 shows changes in the concentration of *Thalassiosira weissflogii* cells over the 123 days of the experiment. Steady state cell concentrations were greatest in cultures growing at low dilution rates (Table 3). At steady state, cell concentration had a significant negative correlation with dilution rate (r = -0.980, $p < 0.001$, n = 60), decreasing from a mean cell concentration of 1.4×10^5 cells ml^{-1}, at a dilution rate of 0.3 day^{-1}, to 2.5×10^3 cells ml^{-1} at 0.9 day^{-1} (Table 3). There was a significant difference ($F_{4,}$

$_{59}$ = 818.6, $p < 0.001$) between steady state cell concentrations in cultures grown at different dilution rates. Increasing the dilution rate resulted in a rapid decline in cell concentration over the next 2 to 3 days (Figure 19). Conversely, decreasing the dilution rate from 0.9 to 0.3 day $^{-1}$ resulted in a rapid increase in cell concentration over the next 4 days (Figure 19). During steady- state, mean cell division rates were 0.43, 0.72, 1.01, and 1.30 divisions day^{-1} at dilution rates of 0.3, 0.5, 0.7, and 0.9 day^{-1}, respectively.

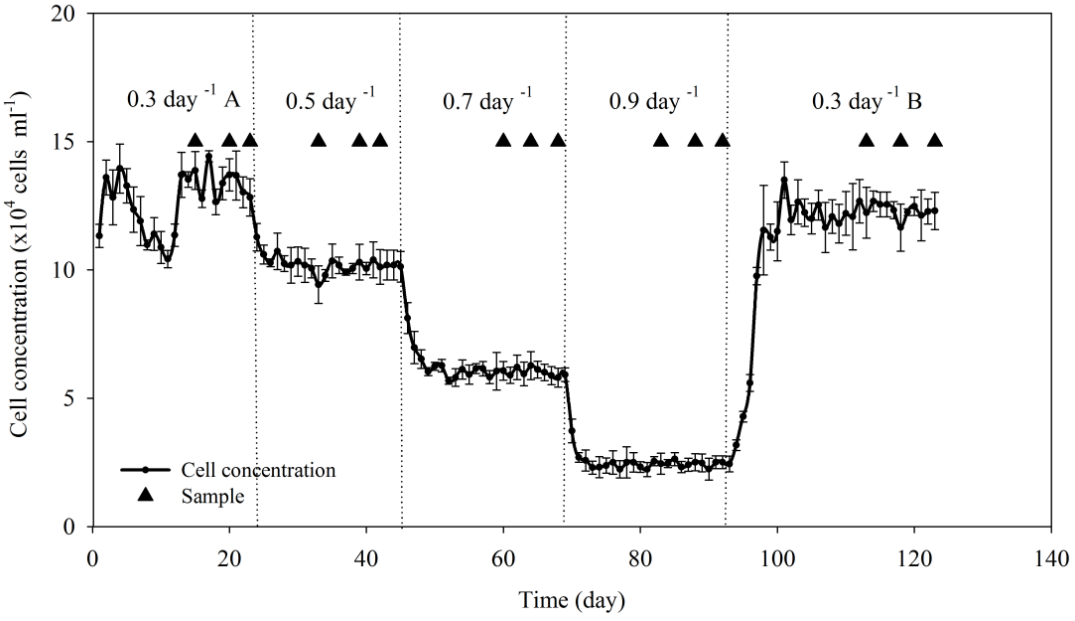

Figure 19. Cell concentration of *Thalassiosira weissflogii* with time in semi-continuous cultures grown in a sequence of dilution rates (0.3, 0.5, 0.7, 0.9, and 0.3 day $^{-1}$) under nitrogen limitation. Filled circles (●) show the mean ± SD (n = 4). Black triangles (▲) indicate days on which a full set of samples were taken.

Chlorophyll *a* is commonly used as a proxy for biomass in field and culture studies (Thornton 2012). Chl. *a* concentration in the cultures decreased as dilution rate increased, following the same pattern as cell abundance (Table 3) (Figure 20). A Kruskall-Wallis ANOVA showed that there were significant differences in chl. *a* concentrations between the different dilution rates ($H = 44.578$, $p < 0.001$). There was a negative correlation between chl. *a* concentration and dilution rate ($r = -0.847$, $p < 0.001$, $n = 60$) and a positive correlation between chl. *a* concentration and cell abundance ($r = 0.855$, $p < 0.001$, $n = 60$).

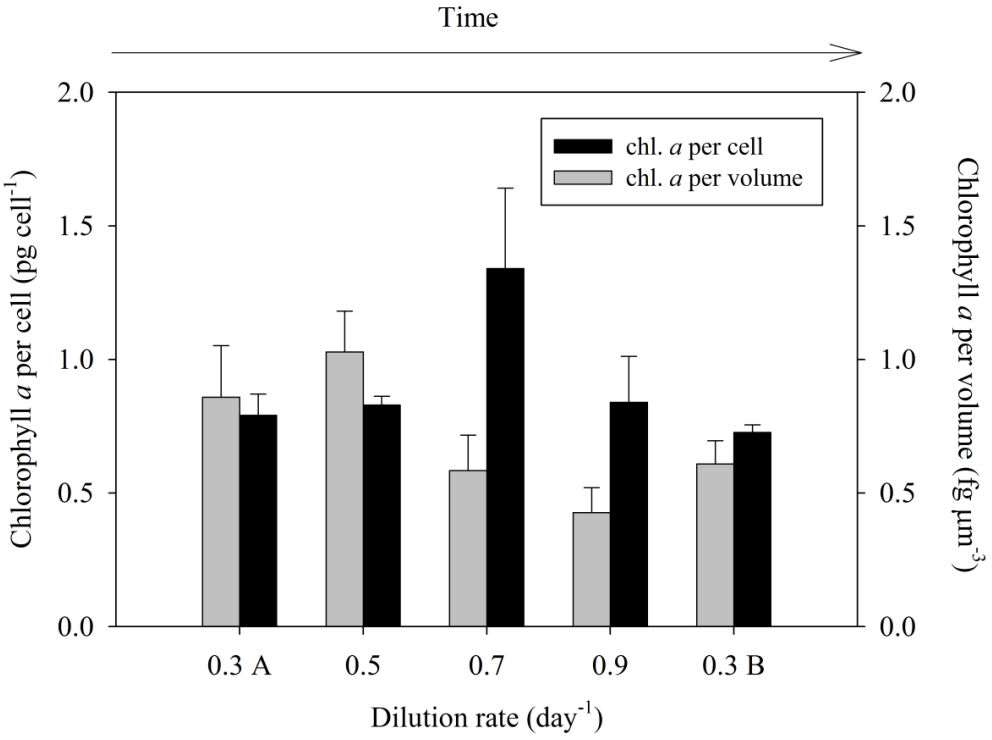

Figure 20. Chlorophyll *a* content of *Thalassiosira weissflogii*. Steady-state chlorophyll a concentrations per cell per cell (black bars) and per cell volume (grey bars) in semi-continuous cultures grown at different dilution rates. Bars show mean + SD (n = 12).

Cell volume of the diatoms also changed with changes in the steady-state growth rate (Figure 21). Cell volume was twice as large in the cultures grown at higher dilution rates (0.7 day^{-1} and 0.9 day^{-1}) compared with lower dilution rates (0.3 day^{-1} and 0.5 day^{-1}) (Figure 21). There was a significant difference in cell volume ($F_{4, 59} = 53.880$, $p < 0.001$) at the different dilution rates and a positive correlation between dilution rate and cell volume ($r = 0.683$, $p < 0.05$, $n = 60$). Therefore, as the dilution rate of the cultures increased, there was an increase in steady-state mean cell volume and a decrease in cell concentration.

As cell volume changed with dilution rate, the total cell volume concentration in the cultures may have been a better indicator of biomass that cell concentration. Two methods were used to estimate the volume concentration of diatoms in the cultures over time. Firstly, data obtained using the light microscope was used to calculate the volume concentration of diatoms (cell abundance × mean cell volume) per volume of culture (Table 3). Secondly, laser *in situ* scattering and transmissometry (LISST) was used to measure the volume concentration of particles in the cultures (Table 3). Using the LISST, the mean (± SD) volume concentrations of particles at a dilution rate of 0.3 day^{-1} were 242 ± 42 µl l^{-1} (0.3A) and 319 ± 48 µl l^{-1} (0.3B), compared with 95 ± 41 µl l^{-1} at a dilution rate of 0.9 day^{-1} (Figure 21). Estimates of volume concentration derived from direct observations with the light microscope were 3.5 ± 1.3 (mean ± SD) times lower than the volume concentrations derived from the LISST. However, the pattern in volume concentrations was in general agreement and there was a positive correlation between the volume concentrations produced by the two methods ($r = 0.717$, $p < 0.001$, $n = 60$).

Moreover, volume concentration in the cultures followed the same general pattern as cell abundance and chl. *a* concentrations with dilution rate. There were significant differences in volume concentrations with dilution rate derived from both the microscope observations ($F_{4, 59} = 80.823$, $p < 0.001$) and the LISST measurements ($F_{4, 59} = 57.364$, $p < 0.001$).

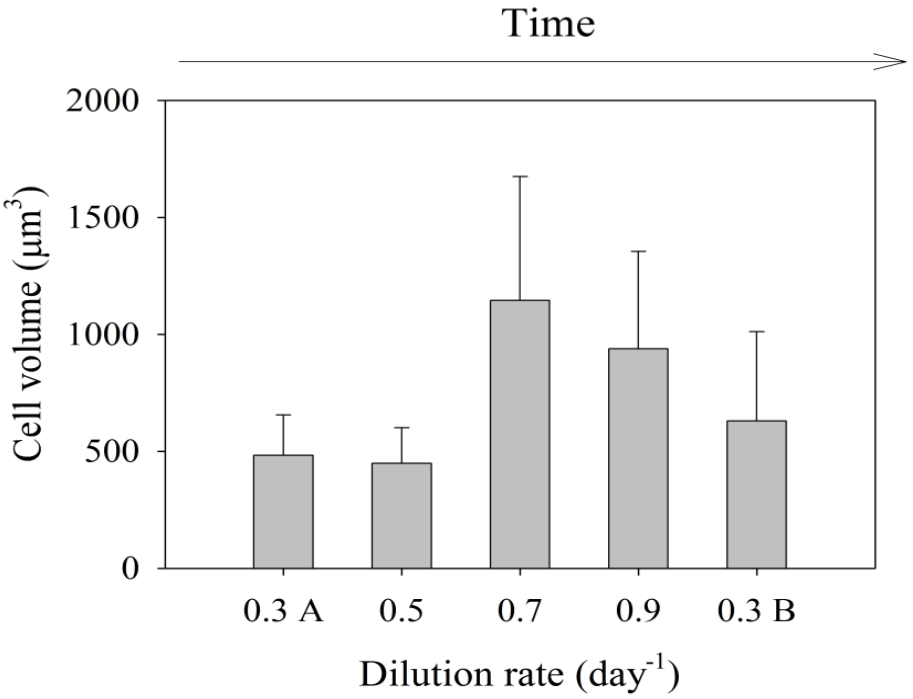

Figure 21. Cell volume of *Thalassiosira weissflogii* grown at different dilution rates. Bars show mean + SD (n = 300).

Total carbohydrate includes both the carbohydrate associated with particulate matter in the cultures (i.e. cells) and extracellular dissolved carbohydrate. There was a significant difference in total carbohydrate concentration at steady state as the different dilution rates ($H = 45.281$, $p < 0.001$, $n = 60$). Mean total carbohydrate concentrations were greater in cultures growing at low dilution rates compared with cultures growing at high dilution rates (Table 3). Total carbohydrate concentration followed the same pattern as cell abundance and chl. *a* concentration (Table 3); for example, there was a significant positive correlation between cell abundance and carbohydrate concentration ($r = 0.795$, $p < 0.001$, $n = 60$).

Steady state conditions were determined based on counts of diatom cell concentrations in the cultures. During steady state, there should not be any significant change in diatom concentration over time. While there were significant differences in diatom concentration between different dilution rates, there was no significant difference in cell concentration between sampling days during steady-state (Table 4). There was no significant difference in steady state chl. *a* concentrations, with the exception of during the steady state period diluted at 0.7 day^{-1} (Table 4). Total carbohydrate showed significant differences between days during steady state at 0.5 and 0.9 day^{-1}. However, total carbohydrate was composed of both cell associated and extracellular carbohydrate and therefore may not be as useful as a proxy for biomass as diatom cell and chl. *a* concentrations.

Table 3. Abundance and measures of biomass for *Thalassiosira weissflogii* grown in nitrate-limited steady-state cultures grown at a range of dilution rates. Values are mean ± SD (n = 4 replicate cultures).

Dilution rate (day^{-1})	**0.3A**	**0.5**	**0.7**	**0.9**	**0.3B**
C: N ratio (mol: mol)	12.40 ± 1.39	11.06 ± 1.38	12.05 ± 2.31	13.17 ± 2.28	12.03 ± 1.28
Diatom concentration (cells mL^{-1}) (x 10^3)	135 ± 8	99 ± 7	60 ± 4	25 ± 3	121 ± 9
Chl. a (µg L^{-1})	109 ± 11	90 ± 4	80 ± 18	20 ± 4	91 ± 4
Total carbohydrate (mg L^{-1})	10.50 ± 2.14	6.19 ± 1.11	6.13 ± 1.60	3.26 ± 0.53	8.78 ± 1.63
Diatom volume (microscope) (µL L^{-1})	65 ±10	45 ± 7	69 ± 10	23 ± 4	76 ± 10
Diatom volume (LISST) (µL L^{-1})	242 ± 42	122 ± 27	167 ± 47	95 ± 41	319 ± 48

Table 4. Results from ANOVA to determine whether there were significant changes in indicators of biomass between sampling days during the five steady state periods grown at different dilution rates. For each analysis, four replicates cultures were sampled on three different days (n = 9). N.S. means there was no significant difference between the mean measure of biomass on different sampling days.

Dilution rate (day^{-1})	Diatom concentration ($cells\ mL^{-1}$)	Chl. a ($\mu g\ L^{-1}$)	Total carbohydrate ($mg\ L^{-1}$)
0.3A	N.S.	N.S.	N.S.
0.5	N.S.	N.S.	**$p < 0.05$**
0.7	N.S.	**$p < 0.01$**	N.S.
0.9	N.S.	N.S.	**$p < 0.05$**
0.3B	N.S.	N.S.	N.S.

4.3.2 Evidence for nitrogen limitation

The addition of nitrogen (as nitrate) to samples of culture from all dilution rates resulted in an approximate doubling of cell abundance over 48 hours compared with the control bioassay to which no nutrient additions were made (Table 5). Moreover, the addition of all nutrients except nitrogen (i.e. silicate, phosphate, vitamins and trace metals) resulted in no increase in cell abundance. These results indicate that nitrogen supply limited growth in the semi-continuous cultures. This conclusion is supported by the C: N ratio of particulate matter from the cultures. If the cultures were nutrient replete, then the C: N ratio would be expected to approximate to the Redfield ratio of 6.6. The mean observed C: N ratio of the POM in the cultures was 12.38 ± 0.98 (mean ± SD, n = 60), with no significant difference between steady-state cultures growing at different growth rates (Table 3). A C: N ratio of almost twice Redfield indicates that the carbon was in excess compared to nitrogen and the cultures were nitrogen limited.

Table 5. Cell concentrations after 48 hours in bioassays to determine the source of nutrient limitation in steady-state semi-continuous cultures of *Thalassiosira weissflogii*. Treatments were control (no additions), + nitrate (120 μM added), and – nitrate (all nutrient added except nitrate. Numbers in the table are means ± SD (n = 4 replicate cultures).

Dilution rate (day^{-1})	Cell concentration ($\times 10^4$ cells ml^{-1})		
	+ Nitrate	**Control**	**- Nitrate**
0.3A	22.60 ± 1.25	11.24 ± 1.13	12.65 ± 0.56
0.5	19.56 ± 3.14	11.52 ± 0.72	11.55 ± 0.64
0.7	11.43 ± 1.65	7.22 ± 0.75	7.05 ± 0.52
0.9	5.24 ± 1.43	2.94 ± 0.72	2.34 ± 0.39
0.3B	21.09 ± 1.48	12.65 ± 0.85	12.50 ± 0.44

4.3.3 TEP

Several measures of TEP dynamics are shown in Figure 22. Differences between TEP abundances at the different steady state dilution rates were significant ($H = 54.444$, $p < 0.001$, $n = 60$). TEP abundance in the cultures were generally greater than cell abundances (Figure 22 A), with a maximum mean TEP abundance at a dilution rate of 0.3 day^{-1} of 473,000 ± 23,000 (± SD) particles ml^{-1} (0.3A) and the lowest mean concentration of 163,000 ± 5,000 particles ml^{-1} at a dilution rate of 0.9 day^{-1}. There was a decrease in TEP abundance as the dilution rate of the cultures was increased (Figure 22 A). When the dilution rate was stepped down from 0.9 to 0.3 day^{-1} (0.3B), there was an increase in steady state TEP abundance (Figure 22 A). There was a significant difference in TEP abundances between 0.3A and 0.3B (Tukey test, $p < 0.05$). The size of the TEP particles also changed with dilution rate ($F_{4, 59} = 108.452$, $p < 0.001$, $n = 60$); individual

TEP particles were generally larger in surface area at higher dilution rates (0.7 and 0.9 day^{-1}). There was no significant difference in the size of the TEP particles during the two steady state periods with a dilution rate 0.3 day^{-1} (0.3A and 0.3B).

TEP concentration (i.e. total TEP area) was a better measure of the amount of TEP in the cultures (Figure 22 C) as it accounted for the variability in both the area of individual particles and their abundance. There were significant differences in TEP concentration at the different dilution rates ($F_{4, 59} = 13.095$, $p < 0.001$, $n = 60$), but there was no obvious pattern. There were significant differences in TEP concentration between the two steady state periods of dilution at 0.3 day^{-1} ($p < 0.05$). TEP production rate at steady state (Figure 22 D) correlated with dilution rate ($r = 0.922$, $p < 0.001$, $n = 60$) and there was a significant difference in TEP production rates with dilution ($F_{4, 59} = 174.888$, $p < 0.001$, $n = 60$). *Post hoc* comparisons showed that there was no difference in TEP production rate between the two highest dilution rates (0.7 and 0.9 day^{-1}) and the two periods of dilution at 0.3 day^{-1} (0.3A and 0.3B). These data show that TEP production rates were greater in faster growing cultures of nitrogen-limited *T. weissflogii.*

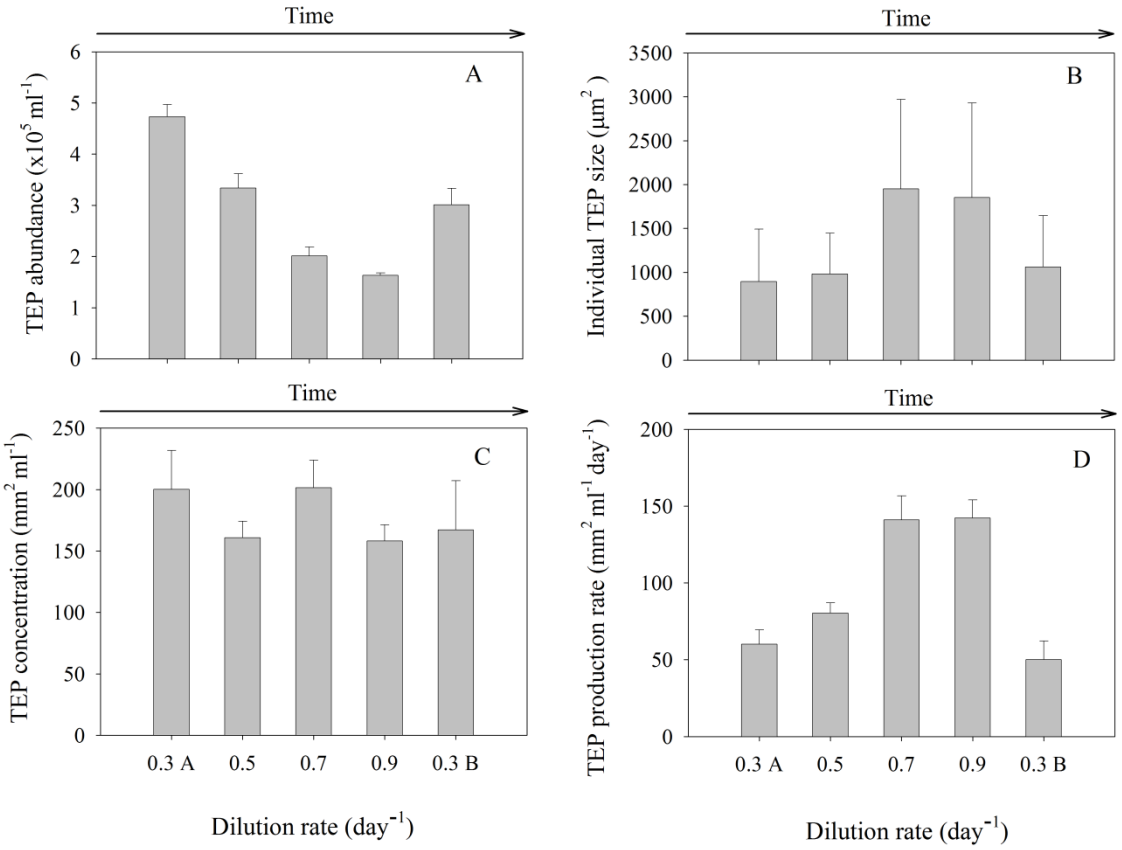

Figure 22. TEP dynamics in steady-state semi-continuous cultures of *Thalassiosira weissflogii*. Bars show mean (+ SD; n = 100) TEP abundance (A), Individual TEP size (B), TEP concentration (C), and TEP production rate (D).

4.3.4 Aggregation

In addition to estimates of biomass in the cultures based on volume concentration, the LISST was also used to determine the degree of aggregation in the cultures. A particle significantly larger than a single *T. weissflogii* cells implies aggregation. Based on visual examination of PSDs measured using the LISST, we assigned volume concentration with an ESD ≥ 63 μm as aggregated and volume concentration in the size bins containing an ESD < 63 μm as unaggregated. A spherical particle with a diameter of 63 μm would have a volume of 98,183 μm^3, which is considerably larger than the greatest mean steady state cell volume of 1,146 ± 128 μm^3 (0.7 day^{-1}), therefore we can be confident that particles ≥ 63 μm were aggregates. The degree of aggregation in the cultures was determined from the ratio of volume concentration ≥ 63 μm ESD to volume concentration < 63 μm ESD (Figure 23). There was a significant difference in the aggregation at different dilution rates dilution ($F_{4, 59} = 79.849$, $p < 0.001$, $n = 60$). Aggregation was positively correlated to dilution rate during steady state ($r = 0.840$, $p < 0.001$, $n = 60$), indicating that the faster growing cultures were more aggregated. Aggregation was negatively correlated with the total area of TEP in the cultures ($r = -0.303$, $p < 0.05$, $n = 60$), therefore the aggregate measurement was not simply a measurement of TEP abundances in the cultures. However, TEP production rate was positively correlated to aggregation ($r = 0.723$, $p < 0.001$, $n = 60$).

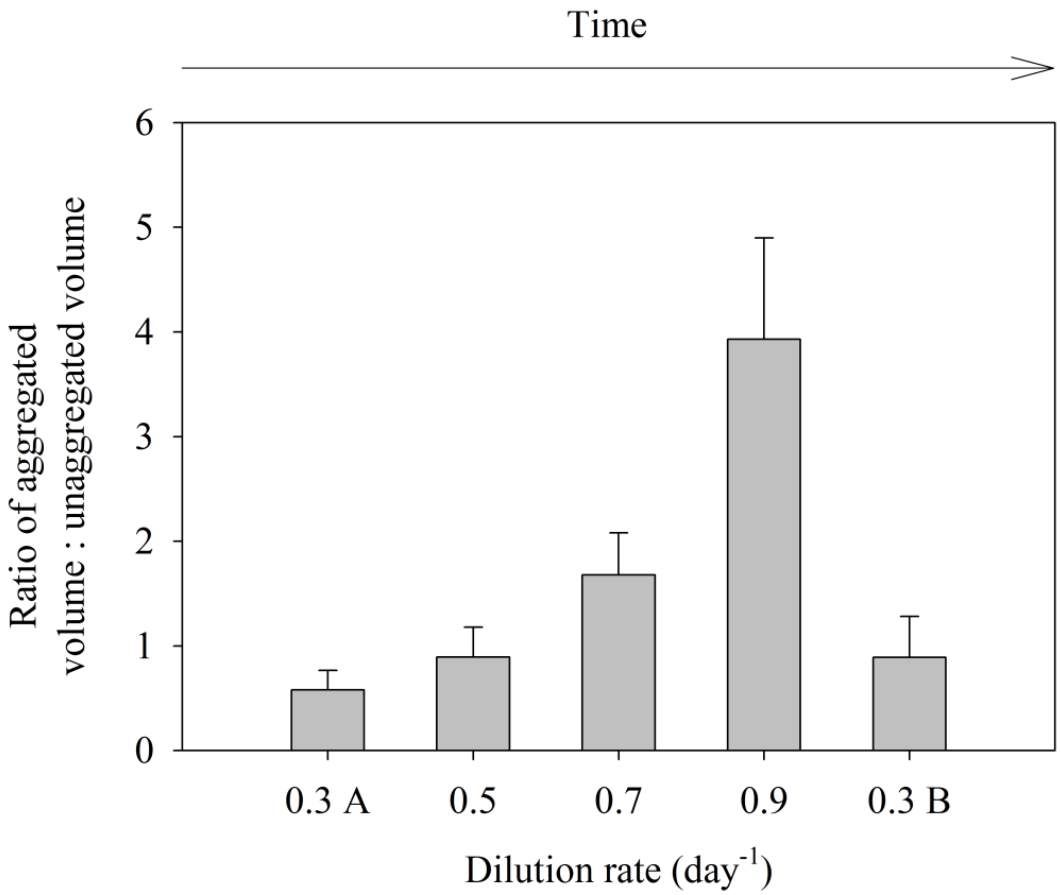

Figure 23. Ratio of aggregated volume to unaggregated particulate volume in the cultures of *T. weissflogii* grown in nitrate limited semi-continuous cultures at different dilution rates. Bars show mean (± SD) ratio at different dilution rate (n = 400).

4.3.5 Cell membrane integrity

SYTOX Green labeling of cells was used to determine whether the cell membranes were intact or compromised at steady state with different dilution rates (Figure 24). The proportion of cells with compromised cell membranes was consistently < 5 %. There was a significant difference ($F_{4, 59} = 142.408$, $p < 0.001$, $n = 60$) in the proportion of the population that had compromised cell membranes at the different dilution rates. However, there was no significant difference between the cultures grown in the two different periods of 0.3 day $^{-1}$ (0.3A and 0.3B). The proportion of cells with compromised cell membranes was inversely correlated to growth rate at steady state ($r = -0.927$, $p < 0.001$, $n = 60$).

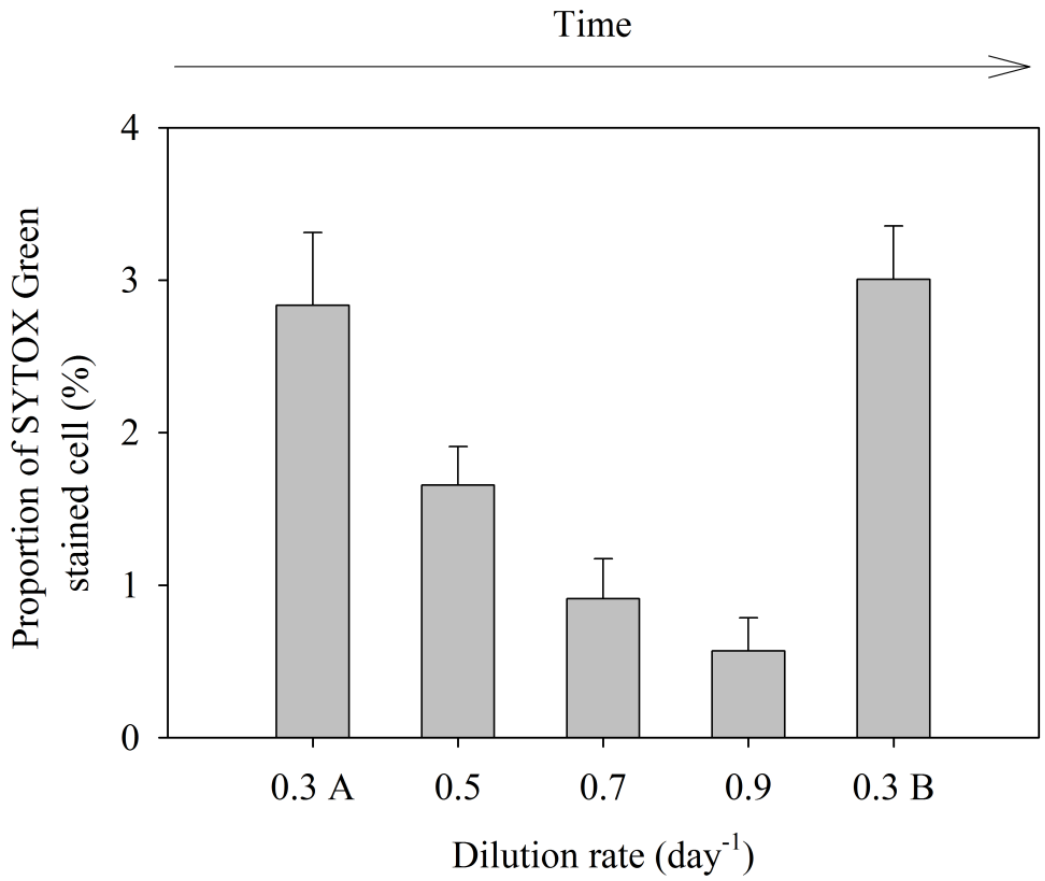

Figure 24. The proportion of SYTOX Green stained cells in cultures grown at different dilution rate. Bars show mean + SD (n = 12).

4.3.6 Bacteria abundance and biomass

Bacteria concentrations were generally low and did not increase to above 10^6 ml^{-1} until the last period of growth at a dilution rate of 0.3 day^{-1} (0.3B). Prior to this period, the mean bacteria concentration was $4.78 \times 10^5 \pm 2.90 \times 10^5$ ml^{-1}). The bacteria concentration in the cultures was negatively correlated with dilution rate (r = -0.661, $p < 0.001$, n = 60) and therefore positively correlated with the concentration of diatoms in

the cultures (r = 0.577, p < 0.001, n = 60). There was a significant difference in the bacteria concentration at the different dilution rates (H = 44.285, p < 0.001, n = 60) and there was a significant difference in the bacteria concentration during the two periods of growth at 0.3 day^{-1}. Although both diatom and bacteria concentrations decreased with dilution rate, there was still a significant difference (H = 38.018, p < 0.001, n = 60) between the ratio of bacteria to diatoms at the different dilution rates (Table 6). The mean number of bacteria per diatom cell was 7.8 ± 5.0 (± SD) over the course of the whole experiment. Bacteria per diatom cell were significantly different at the two dilution periods of 0.3 day^{-1}, increasing from 4.7 ± 2.3 (0.3A) to 15.1 ± 5.0 (0.3B).

Estimates of the carbon content of the diatom and bacterial populations (Table 6) were used to determine how much of the total cell carbon was associated with bacteria. The amount of carbon associated with bacteria was greatest at the end of the experiment during the 0.3B period. The cell carbon associated with bacteria during 0.3B varied from 0.36 ± 0.13 % (mean ± SD) to 4.10 ± 1.47 % using values for bacterial carbon of 12.4 and 149 fg $cell^{-1}$, respectively. Lowest estimates of bacterial carbon occurred at a dilution rate of 0.9 day^{-1}, varying from 0.06 ± 0.03 % to 0.71 ± 0.30 % (mean ± SD). Mean estimates of the amount of carbon associated with bacterial cells was always < 5 %. The greatest estimate of the amount of cell carbon associated with bacteria from any culture on any day was 6.01 % from one of the 0.3B cultures on the last day of sampling.

Table 6. Bacteria abundance and estimates of bacterial biomass in *Thalassiosira weissflogii* cultures grown in nitrate-limited semi-continuous culture at a range of dilution rates. Values are means ± standard deviation (n = 4 replicate cultures). The amount of carbon associated with bacteria was estimated using 3 values of the carbon content for bacteria from the literature: [a] 12.4 fg C per bacterium, [b] 30.2 fg C per bacterium, and [c] 149 fg C per bacterium. Values are means ± SD (n = 4 replicate cultures).

Dilution rate (day^{-1})	Bacteria (cells mL^{-1}) (x 10^6)	Bacteria per diatom	Diatom C (ng mL^{-1})	Bacteria C[a] (ng mL^{-1})	Bacteria C[b] (ng mL^{-1})	Bacteria C[c] (ng mL^{-1})
0.3A	0.626 ± 0.285	4.7 ± 2.3	5814 ± 726	8 ± 4	19 ± 9	93 ± 42
0.5	0.695 ± 0.133	7.0 ± 1.4	4065 ± 527	9 ± 2	21 ± 4	104 ± 20
0.7	0.502 ± 0.153	8.4 ± 2.9	5270 ± 634	6 ± 2	15 ± 5	75 ± 23
0.9	0.086 ± 0.036	3.5 ± 1.5	1839 ± 226	1 ± 0	3 ± 1	13 ± 5
0.3B	1.827 ± 0.619	15.1 ± 5.0	6456 ± 720	23 ±8	55 ± 19	272 ± 92

4.4 Discussion

Figure 19 shows that the diatom cell concentration remained relatively constant at each dilution rate, after an initial transition period. As diatom concentration did not change in the cultures over time (Table 4), the dilution rate must have been equal to the growth rate and therefore the cultures reached a steady-state at each dilution rate (Fogg and Thake 1987). Unlike continuous cultures, fresh medium was not added constantly, but rather in a pulse once a day. Figure 19 is somewhat misleading as it gives the impression that biomass was constant throughout each steady-state period. In reality, the diatom concentration would have followed a pattern over the course of the day, with the minimum occurring immediately after dilution and the maximum occurring at the time of sampling. As the cultures were sampled at the same time every day, this gives the impression of constant diatom cell concentration. Therefore, it is more accurate to describe the cultures as being in a quasi-steady-state; with the mean growth rate equivalent to the dilution rate and the same pattern of change in growth and biomass occurring each day.

While the concentration of nitrate added to the cultures was constant (60 μM), the rate of nitrate supply was not as the total amount of nitrate added depended on volume as well as concentration. The daily additions of nitrogen to the cultures were 18, 30, 42, and 54 μmol at the dilution rates of 0.3, 0.5, 0.7 and 0.9 day^{-1}, respectively. While the addition of nitrate at 0.9 day^{-1} was three times that at a dilution rate of 0.3 day^{-1}, the steady-state diatom concentration was significantly lower. In a chemostat system at

steady state, the biomass is determined by the concentration of limiting nutrient and dilution rate determines the growth rate (Fogg and Thake 1987). We expected the diatom cell concentration in the semi-continuous cultures to remain relatively constant as there was no change in nitrate concentration when the dilution rate was changed. Our results indicate that either nitrogen was not the limiting nutrient in the cultures or that there was a significant difference in the physiology of *T. weissflogii* growing at different rates. To ensure nitrogen limitation, nitrogen was supplied at relatively low concentrations compared with phosphorus and silicon. The Redfield ratio for C: N: P in particulate organic matter in the ocean is 106: 16: 1 (Redfield et al.1963). Deviations from these proportions are often used as an indicator of nutrient limitation (Geider and La Roche 2002). The N and P additions to the culture were made at the ratio of 0.6: 1, compared with Redfield stoichiometry of 16:1. However, the Redfield ratio represents a mean value for marine phytoplankton; there are significant differences in C: N, C: P and N:P requirements by different phyla of phytoplankton (Quigg et al. 2003). Leonardos and Geider (2004) compiled data from the literature on nutrient replete stoichiometry in diatoms and found that the mean C: N ratio approximated to Redfield stoichiometry (6.6) with a value of 6.9 and a range of 5.1 to 9.0. Quigg et al. (2003) found that the C:N ratio of exponentially growing nutrient replete *Thalassiosira weissflogii* (CCMP 1336) approximated to Redfield proportions, with a mean value of 6.3. The mean C:N ratio of our cultures was approximately twice this value (12.38 ± 0.98 (mean ± SD, n = 60)). Similarly, Goldman et al. (1979) grew *Thalassiosira psuedonana* (3H) with a limiting supply of ammonium and found that the C: N ratio was 12.6 (mol: mol). The C:N ratio

of the POM in our cultures supports the conclusion that they were nitrogen limited and this was confirmed by the bioassay experiments.

POC would have been the definitive measure of biomass in the diatom cultures. Unfortunately, there may have been a loss of material from the filters during preparation of the samples for elemental analysis. This potential source of error precluded measuring the POC concentration of the cultures and cell quotas of carbon or nitrogen, as was our original intention. However, we are confident that this potential loss did not affect the determination of the C: N ratio of the particulate organic matter in the culture. Measures of biomass (diatom cell concentration, chl. *a* concentration, and total carbohydrate concentration) indicate that there was a biomass decrease with increasing diatom growth rate. *T. weissflogii* may be less efficient at utilizing the available nitrate at higher growth rates. This hypothesis is supported by the constant steady-state C: N ratios of the cultures, despite more nitrogen per diatom being available at high dilution rates. The nitrogen supply per diatom during steady state with a dilution rate of 0.3 day^{-1} (0.3A) was 133 compared with 2,160 pmol N $cell^{-1}$ (estimated based on the mean steady-state cell concentration at each dilution).

Cell size, in addition to diatom cell concentration, determined the biomass in the cultures. While there was a lower diatom cell concentration in fast growing cultures (0.7 and 0.9 day^{-1}), the cells were significantly larger than in cultures growing at 0.3 and 0.5 day^{-1}. Therefore, biomass volume may be a better proxy for diatom biomass than cell concentration. Measurements of biomass volume made by light microscopy and using the LISST followed the same pattern, but they did not have the same values. The volume

of diatoms based on LISST volume concentration measurements were consistently higher than those made by light microscopy. Using light microscopy, cell volume of individuals can be determined relatively precisely as the length and width of the cells can be measured and the shape of the cell is confers to a cylinder. However, the LISST method does not measure the size and shape of individual cells, but rather the volume concentration of the whole population of particles that scatter light onto a series of 32 detectors equivalent to 32 size bins (Agrawal and Pottsmith 2000). Moreover, the volume concentration is determined based on the assumption that the particles are spheres (Agrawal and Pottsmith 2000). Rzadkowolski and Thornton (2012) found that large peaks on the particle size distributions from diatom monocultures corresponded to the length and widths of the cells. In the case of *Thalassiosira weissflogii*, volume concentrations based on the equivalent spherical diameters of the length and width of the diatom would over and underestimate the biomass of diatoms, respectively. Much of the biomass in the cultures was in the form of aggregates, which may lead to an overestimation of biomass by volume as aggregates tend to be porous (Ploug et al. 2008), which will not be detected by the LISST. Finally, LISST measurements may have included a volume of particles that were not diatoms. There were high concentrations of TEP in the cultures and it is possible that these particles may have contributed to the measured volume concentrations. However, our attempts to measure TEP with the LISST have been unsuccessful as the LISST has not been able to „see" these particles. LISST instruments have been used to measure the concentration of purple sulfur bacteria in a lake (Serra et al. 2001) and therefore it is possible that bacteria may have

contributed to the detected volume concentration. The minimum size of particles detected by the Type C LISST used in this study is 2.5 μm, compared with 1.2 μm for the instrument used by Serra et al. (2001). Therefore, it is unlikely that bacteria directly contributed to the volume concentration measured; however, light scattering by objects smaller and larger than the sizes measured by the LISST does cause errors in the volume concentrations measured in the smallest and largest size bins (Agrawal and Pottsmith 2000).

Most diatom reproduction is by mitotic cell division, with each generation being smaller than the previous as the when the diatom divides into two, one parent valves goes to each daughter cell and the new valve forms inside the old valve, resulting in one cell that is smaller than the parent cell and one cell that is the same size (Armbrust and Chisholm 1992). Cell shrinkage with each generation is obviously unsustainable, therefore sexual reproduction or asexual cell enlargement is used to restore cell size in response to a threshold cell size and/or environmental cues (Armbrust and Chisholm 1992). Armbrust and Chishom (1992) found that the timing of enlargement depended on isolate in *T. weissflogii,* with a range of 120 to 270 generations. We found that cell volume in *T. weissflogii* increased with increasing growth rate at steady state. Similarly, Costello and Chisholm (1981) found that vegetative cell volume increased from 800 to 2800 μm^3, with a concomitant increase in growth rate from 1.6 to 3.4 doublings per day in batch cultures of *T. weissflogii* grown in f/2 medium. Increased cell volume and growth rate occurred after auxospore formation, though the triggering environmental conditions were not clear. Our cells were much smaller than those observed by Costello

and Chisholm (1981); this may reflect phenotypic differences between strains and the difference in growth conditions as our cultures were always growing under nutrient limitation. However, the smallest mean cell size observed in our work was still greater than the minimum modal cell volume of 278 μm^3 observed by Armbrust and Chisholm (1992). Indeed, Armbrust and Chisholm (1992) observed different patterns of cell size change between different isolates of *T. weissflogii,* and differences in the maximum cell volume of different isolates. Our work differs from Costello & Chisholm (1981) and Armbrust & Chisholm (1992) as we were controlling the growth rate, rather than measuring growth rate under nutrient replete conditions. It may be that the larger cell volume we observed in faster growing cultures simply reflects the proportion of cells undergoing mitotic cell division at the time of sampling. This is supported by the elongated shape of many of the cells at high growth rates and the low proportion of dying cells at high growth rates, as indicated by SYTOX Green staining. We did not observe any evidence of sexual reproduction, though this does not mean that it was not occurring in our cultures.

Recent research has shown that bacteria may play a significant role in determining the stickiness and aggregation of diatom cultures (Gärdes et al. 2011, 2012) and therefore the presence of bacteria and their interactions with the diatom cannot be ignored. We estimated the amount of organic carbon associated with the bacteria based on values of carbon per bacterium from the literature. The literature values varied over an order of magnitude, depending on growth conditions (Fukuda et al. 1998, Vrede et al. 2002). Actual mean carbon content of the bacteria was probably somewhere between the

extremes of 12.4 (oceanic conditions) and 149 fg C bacterium^{-1} (nutrient replete conditions). Of the three values used to estimate bacteria carbon, the estimate based on data from coastal waters (30.2 fg C bacterium^{-1}) was probably the most representative of the nitrogen limited conditions in the semi-continuous cultures. Even using the highest value of 149 fg C bacterium^{-1}, the proportion of microbial carbon that was associated with the bacteria was < 5 %, indicating that the bacteria were not a significant biomass in the cultures. Bacterial concentrations were less steady than those of the diatom. For example, while diatom cell concentrations were in steady state during 0.3B, the bacteria concentration increased. On average, there were 3 times more bacteria in 0.3B compared with 0.3A and therefore any significant difference between these two periods could be used to determine whether bacteria had a significant effect on the growth of the diatom. There were fewer diatoms at steady state during 0.3B compared with 0.3A (Table 3). This difference was significant, but relatively small compared to the differences in diatom concentrations between dilution rates. Competition for nitrogen between the bacteria and diatoms may have contributed to this difference due to the high concentrations of bacteria during 0.3B compared with 0.3A. However, other factors such as sexual reproduction of the diatom and selection (of both diatom and bacteria) over many generations may have also contributed to this difference (Armbrust and Chisholm 1992, Collins and Bell 2004).

Gärdes et al. (2011) showed that bacteria are important in the aggregation of *Thalassiosira weissflogii*; aggregation did not occur in axenic cultures of the diatom, whereas bacteria attached to *Thalassiosira weissflogii* cells enhanced aggregation.

Gärdes et al. (2010) isolated the bacterium *Marinobacter adhaerens* from marine particles and subsequently grew it with the diatom *Thalassiosira weissflogii* in a model system (Gärdes et al. 2012). Interaction between the diatom and the bacterium depended on the nutrient status of the culture. When grown under „balanced" conditions (N:P of 16:1), the bacterium enhanced exudation and TEP formation in batch cultures compared with axenic controls. However, *M. adhaerens* did not enhance TEP production when the cultures were grown under conditions that affected nutrient limitation. We do not know which bacteria were in our cultures; however, it may be that TEP formation and aggregation was not affected by the presence of bacteria in the cultures as they were nutrient limited. Furthermore, there was no difference in TEP abundance and proportion of aggregated biomass between the cultures during the two growth periods at 0.3 day^{-1}, despite the fact that the bacteria concentration during 0.3B was three times that during 0.3A.

In situ and in mesocosm experiments with natural populations, TEP formation is often associated with nutrient limitation and the termination of diatom blooms (Passow et al. 1994, Engel 2000, Engel et al. 2002). In general, stresses such as nutrient limitation are associated with extracellular release of DOM by phytoplankton (see Thornton (accepted in 2013) for a review). We hypothesized that there would be more TEP in the cultures diluted at the lowest rate as these were the slowest growing and the most nitrogen limited. Relatively old and nutrient stressed cells were predicted to be the most „leaky" and therefore the greatest producers of TEP precursors, leading to high concentrations of TEP at low dilution rates and high TEP production rates. Our data

showed that *T. weissflogii* were more permeable at low dilution rates as a greater proportion of cells showed SYTOX staining. Furthermore, there were more cells in the cultures at low dilution rates, which meant that the absolute concentration of leaky cells at low dilution rates was relatively high. However, large numbers of leaky cells did not result in greater amounts of TEP in the slow growing cultures. This suggests that most of the TEP production was associated with healthy cells, rather than dying cells and cell lysis. TEP concentrations (by area) were relatively constant in all cultures during steady state; however, when dilution rate was accounted for, TEP production rate was greatest at the highest dilution rate, further evidence that the production of TEP and/or TEP precursors was associated with relatively healthy and rapidly growing cells.

The proportion of biomass in the cultures that was in the form of aggregates increased with increasing dilution rate. This indicates that the faster growing cultures were stickier than the slower growing cultures. Coagulation efficiency (α), is the probability that two particles stick together on collision (Jackson 1990, Engel 2000), with a range of values from 0 (i.e. there is no adhesion between particles on collision) to 1 (all collisions between particles result in adhesion). Diatom coagulation efficiency is variable; for example, Kiørboe et al. (1998) measured α in the range of 0.1 to 0.4 during a bloom of *Chaetoceros* spp. in the Benguela upwelling. Aggregation is not only dependent on the stickiness of particles‟ surfaces, but also their collision rate. Collision rate was determined by the mixing regime within the culture system, the cell concentration, and cell size. The mixing regime in the cultures was constant, so it should not have affected differences in aggregation between cultures. We hypothesized that cell

size and concentration would remain constant in the cultures and therefore any change in aggregation could be directly related to stickiness. However, both cell volume and cell concentration changed. The most dramatic changes were between the cell concentrations at the different dilution rates; there were 5 times more cells at 0.3 day^{-1} compared with 0.9 day^{-1}. Enhanced aggregation at 0.9 day^{-1}, despite a lower concentration of cells and therefore lower collision rates, indicates that the cells growing at 0.9 day^{-1} were much stickier than those growing at 0.3 or 0.5 day^{-1}. TEP are also a major factor contributing to aggregation (Engel 2000, Passow 2002b). TEP numbers at high dilution rates were approximately half those at low dilution rate, but the TEP particles at high dilution rate were larger. As there was no significant increase in TEP area with increasing dilution rate, the increased aggregation in the fast growing cultures was most likely caused by increased stickiness of faster growing cells or an increase in the stickiness of the TEP, or both. This hypothesis requires that the chemical structure of the cell coating or TEP was different at different growth rates. It would be interesting to determine what properties of the cell surfaces and TEP changed and whether these could be related to the generation time of the cells. FITC labeled lectins are an example of a tool that could be used to image different carbohydrate moieties on the surfaces of the diatoms (Böckelmann et al. 2002, Elloway et al. 2004, Wigglesworth-Cooksey and Cooksey 2005).

The physiology of cell death in phytoplankton has been overlooked until relatively recently, but it is apparent that phytoplankton may undergo a process analogous to programmed cell death in metazoans (Bidle and Falkowski 2004, Franklin et al. 2006). Cell death is a process and it is often hard to define cells as clearly dead or

alive (Franklin et al. 2006, 2012). Veldhuis et al. (2001) developed SYTOX Green as an indicator of cell death and hypothesized that death is a significant source of DOM production as cells in the early stages of death have both leaky plasma membranes and the ability to photosynthesize. An extension of this hypothesis is that the production of TEP precursors and/or TEP itself is dominated by the relatively few dying cells in the population. Indirect evidence supporting this hypothesis is the accumulation of TEP in situations where one would expect large numbers of dying cells, such as old cultures in the laboratory and during the termination of blooms *in situ*. However, our data indicates that neither the proportion nor number of diatoms with leaky plasma membranes was the most significant determinant of TEP concentrations in the cultures.

4.5 Conclusions

Aggregation into larger particles is important in carbon cycling as it affects the vertical flux of carbon through the water column and the efficiency of the biological carbon pump. Our experiment revealed that growth rate affected TEP formation and aggregation in cultures of *Thalassiosira weissflogii*, when they grown in nitrogen-limited conditions. All measurements in this study tell us that most of the TEP production was associated with fast growing cells (healthy cells), rather than stressful cells and cell lysis. As growth rate increased, steady-state cell abundances decreased and cell volume became larger than in slow growing cultures, indicating biomass volume may be a better proxy for reveal diatom biomass. In addition, measurement of particle

size distribution (PSD) and volume concentration of particles illustrated greater aggregation formed in cultures grown at higher growth rate. Analysis both in size and abundance of TEP with growth rate indicated a more complete description of TEP formation process affected by growth rate that can be implicated in investigation of mechanism of TEP production and aggregation formation in the laboratory or *in situ*.

CHAPTER V

EFFECT OF GROWTH AND DEATH ON TEP PRODUCTION BY DIATOMS

5.1 Introduction

The growth of microorganisms changes in batch cultures go through a series of phases over time, including lag phase, exponential phase, stationary phase, and death phase. As cultures grow in a new environment, cells need adjust to the environment (Canfield et al. 2005). In the lag phase, there is no fast reproduction, and cell population is constant. Following the lag phase is exponential phase, which is a period of logarithmic cell number increase in the cultures (Canfield et al. 2005). However, nutrient in the environment has a given amount and it is consumed by cells for growth. When nutrients become limit, growth of culture shifts from exponential to stationary phase (Canfield et al. 2005). During stationary phases, cultures contain constants cell number because that cell division rate equals to the rate of cell death. When nutrients in the environment run out and limit growth of cultures, cultures shift into death phase where rate of cell death exceeds rate of cell growth (Canfield et al. 2005).

Diatoms are important oceanic primary producers because of their high productivity (Thornton 2012). They are widespread in global oceans and form blooms through rapid growth. Marine snow formation often associated with termination of diatoms, and support as food source for grazers transport organic matter from surface waters to deeper water (Thornton 2002). In addition, Diatoms exude a lot of DOC, in the

form of EPS (Stal 2003). The EPS produced and released from the cell surface may be TEP precursors, which contribute to TEP formation. TEP are sticky particles that promote aggregate formation by acting as glue (Logan et al. 1995, Passow 2002b). Several studies on TEP revealed that TEP amount were distinct during microalgae growth and death. Fukao et al. (2010) found that the production of TEP varied during different phases of growth by different diatoms. TEP production by *Chaetoceros granii* was enhanced during growth phase. On the other hand, those of *Eucampia zodiacus*, *Rhizosolenia setigera* and *Skeletonema costatum* were low in growth phase and mostly generated during late senescence. In the exponential growth phase, cells reproduced fast and live cells produced lots of EPS. In contrast, there were more dead cells in the stationary phase that accumulated during exponential phase. However, no studies monitor the allocation of resources with growth to determine the kinetics of TEP production. Hence, it is important to investigate how growth conditions influence the production of TEP in diatoms. For example, allocation of resources into carbohydrate may vary with TEP production rate during different phases of growth. Thus, the purpose of this experiment was to understand how the growth and death affect TEP formation and carbohydrate allocation by diatoms.

5.2 Experimental approach

Following the procedure described in the section of 2.1.2, three replicate cultures (refer to 2.1.3.1) of *Thalassiosira weissflogii*, *Skeletonema marinoi* and *Cylindrotheca*

closterium were grown in 500 ml of 0.2 μm filtered sterile artificial sea water (refer to 2.1.2.1). Macronutrient concentrations were modified from the original recipe (Table 2) (refer to 2.1.2.2), with final concentrations of 100 μM of $NaNO_3$, 200 μM of $NaH_2PO_4 \bullet H_2O$, and 200 μM of $Na_2SiO_3 \bullet 9H_2O$ in the cultures. Cultures were grown in batch cultures in a 20°C incubator (Precision Company) with a day/night cycle of 14h: 10 h, and with a photon flux density of 42 μmol m^{-2} s^{-1}. The growth of cultures was followed indirectly using cell turbidity (absorbance at 750 nm) every day and directly by counting cell abundances (refer to 2.2.1) on selected days during the different phases of growth. When cells arrived at exponential, stationary, death growth phase, and death phase, cultures were sampled at least once to determine allocation of carbon in the cultures. Samples were used to measure chlorophyll *a* concentration (2.2.3) and cell size (2.2.1), EPS concentration (refer to 2.2.10); TEP (refer to 2.2.5) and CSP (refer to 2.2.6) concentration and size using Image J method; the allocation of resources into different carbohydrate pools (refer to 2.2.10); the proportion of the population with compromised cell membranes (refer to 2.2.9) and bacteria check (refer to 2.2.2).

5.3 Results

5.3.1 Cell concentrations and cell volumes

The growth of three species was followed using cell turbidity and cell counts. Because cell abundance and cell turbidity had a good correlation ($r > 0.75$) in each

species, we determined the growth phase of the cultures based on turbidity. The growth curves of the three species followed the same model, cell abundance increased in the growth phase and decreased during death phase and arrived to low total cell number in the death phase (Figure 25). I counted total cell numbers including, live and dead cells.

Cells volume in the cultures of *T. weissflogii* increased with increasing cell abundance in the exponential growth phase, from average size of 325 μm^3 to 570 μm^3 (Figure 26). The cell volume in the exponential phase was half of those in other phases. In contrast, there was negative correlation between cell volumes and culture time in the cultures of *S. marinoi* ($r = -0.584$; $P < 0.005$; $n = 24$) and *C. closterium* ($r = -0.436$; $P < 0.005$; $n = 24$) (Figure 26). There was a significant difference in the cell volumes during the different growth phases (*T. weissflogii*: $F_{8, 26} = 7.842$, $p < 0.001$; *S. marinoi*: $F_{7, 23} = 3.891$, $p < 0.001$ and *C. closterium*: $F_{7, 23} = 13.506$, $p < 0.001$).

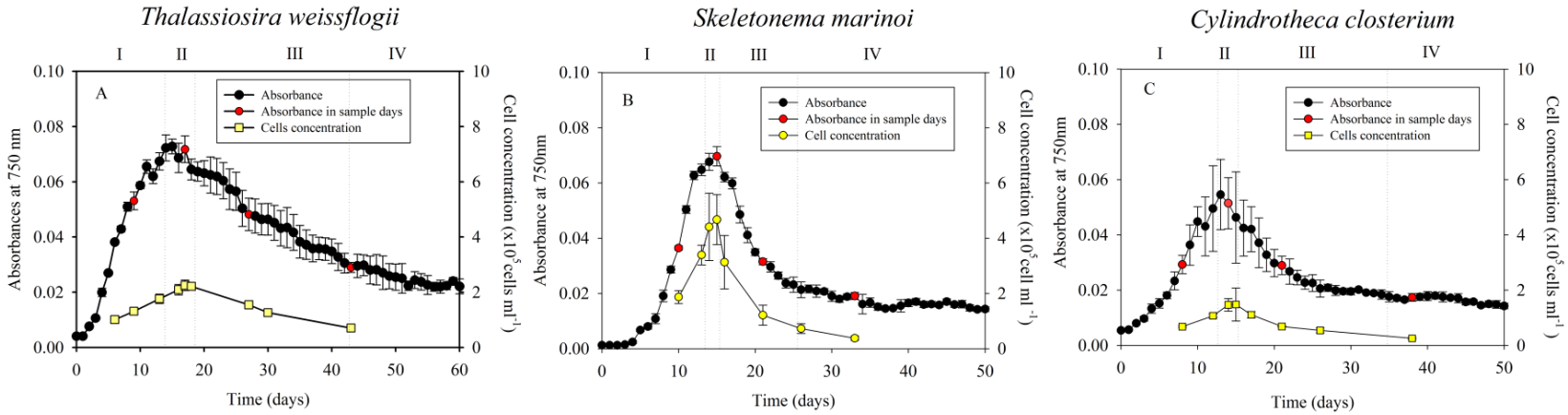

Figure 25. Growth of *Thalassiosira weissflogii*, *Skeletonema marinoi* and *Cylindrotheca closterium* in batch culture. A) *T. weissflogii* B) *S. marinoi* C) *C. closterium*. Black solid circles (●) represent spectrophotometer absorbance of the cultures. Yellow rectangles (■) indicate cell concentrations. Red circles (●) represent cell absorbance of cultures on sampling days. I: exponential growth phase. II: stationary phase. III: death phase. IV: dead. Bars show mean ± SD (n = 3).

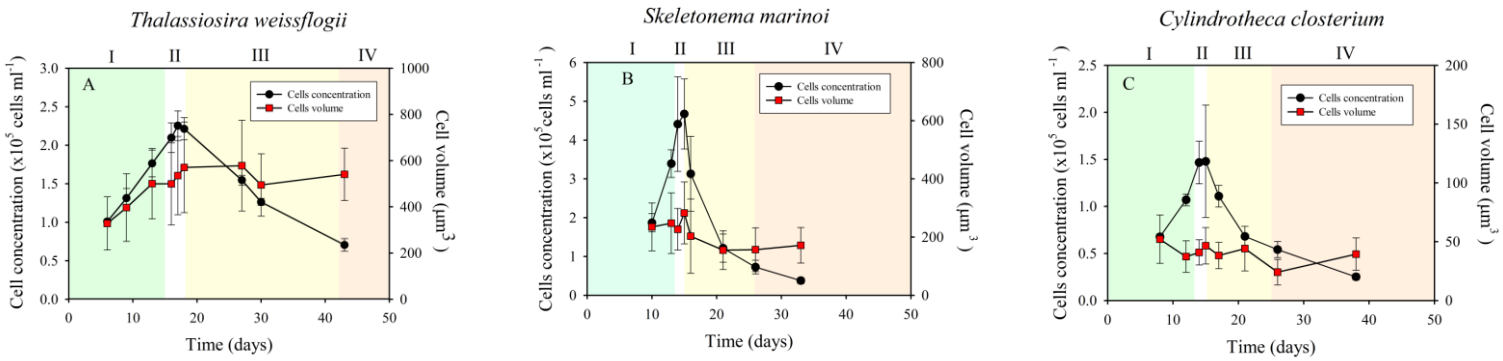

Figure 26. Cell concentration and cell volume with culture time in the cultures of *Thalassiosira weissflogii*, *Skeletonema marinoi* and *Cylindrotheca closterium*. A) *T. weissflogii*. B) *S. marinoi.* C). *C. closterium*. The axes of graphs are not shown on the same scales. Black circles (●) represent cell concentrations, bars show mean ± SD (n = 3). Red rectangles (■) represent cell volumes, bars show mean ± SD (n = 300). Green areas represent exponential growth phase. White areas represent stationary growth phase; yellow areas represent decline growth phase and pink areas represent death phase. I: exponential growth phase. II: stationary phase. III: death phase. IV: dead.

5.3.2 Chlorophyll *a*

The chlorophyll *a* concentration in the cultures of *T. weissflogii* followed the same pattern as cell abundance with culture time, which increased in the exponential growth phase and then decreased in the phase of death (Figure 27). The chlorophyll *a* concentration in the cultures of *S. marinoi* increased very quickly and declined slowly over a long period of time (Figure 27). The chlorophyll *a* concentration in the cultures of *C. closterium* decreased from growth to death phase, from 291.73 ± 82.02 μg l^{-1} to 13.60 ± 1.41 μg l^{-1} (Figure 27). There were significant differences in the chlorophyll *a* concentration in different growth phases in the cultures of *T. weissflogii* ($F_{8, 26} = 3.581$, $p < 0.001$) and in *C. closterium* ($F_{7, 23} = 56.203$, $p < 0.001$), but not in *S. marinoi*.

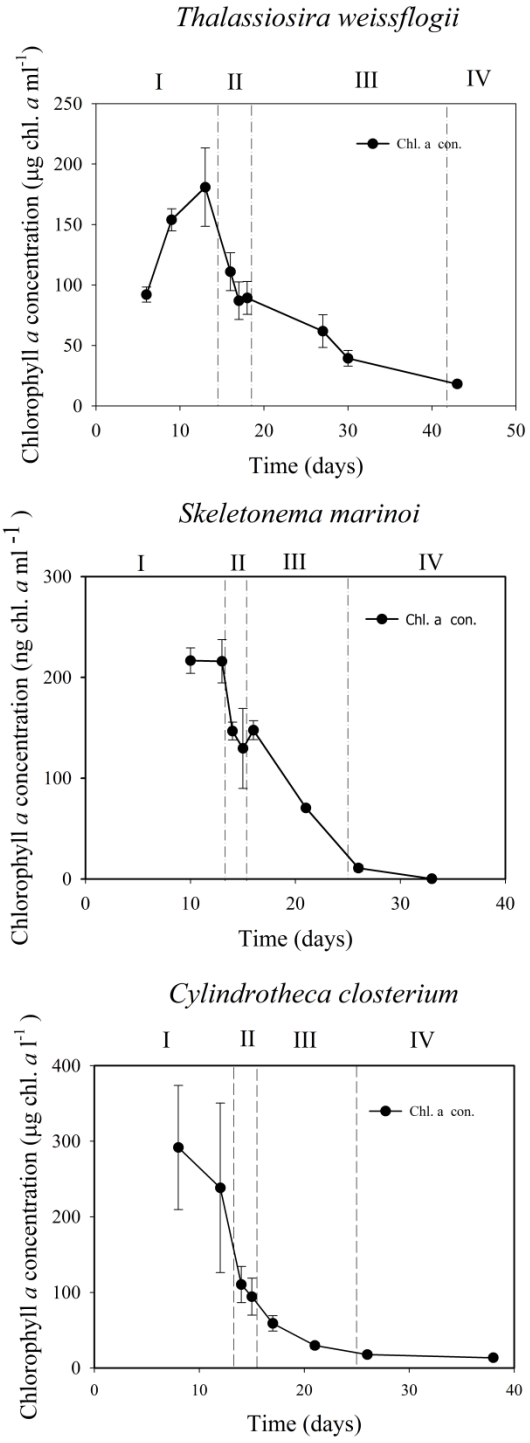

Figure 27. Chlorophyll *a* production in the cultures of *Thalassiosira weissflogii*, *Skeletonema marinoi* and *Cylindrotheca closterium* with culture time. Black circles (●) represent chl. *a* concentration. I: exponential phase. II: stationary phase. III: death phase. IV: dead. Bars show mean ± SD (n = 3).

5.3.3 Carbohydrate fractions were measured by PSA method

Different fractions of carbohydrate, including total carbohydrate, dissolved extracellular carbohydrate, EPS, storage associated carbohydrate (HW extraction), cell wall associated carbohydrate (HB extraction) and residual carbohydrate, were measured using the PSA method. Results of total carbohydrate concentration, HW carbohydrate concentration, HB carbohydrate concentration with culture time are shown in the appendix. In this section, I show results of EPS and carbohydrate allocation in three cultures at different growth phases.

5.3.3.1 EPS concentration

The EPS concentration in three diatom cultures all increased with increasing cell abundances during exponential growth phase and continued to increase during the phase of death, although cell numbers decreased at that time (Figure 28). The EPS concentration per cell was greatest in the death phase in three cultures. The EPS concentration per volume slightly increased during death phase in the cultures of *T. weissflogii*, and rapidly increased in the cultures of *S. marinoi* and *C. closterium* during the death phase (Figure 28).

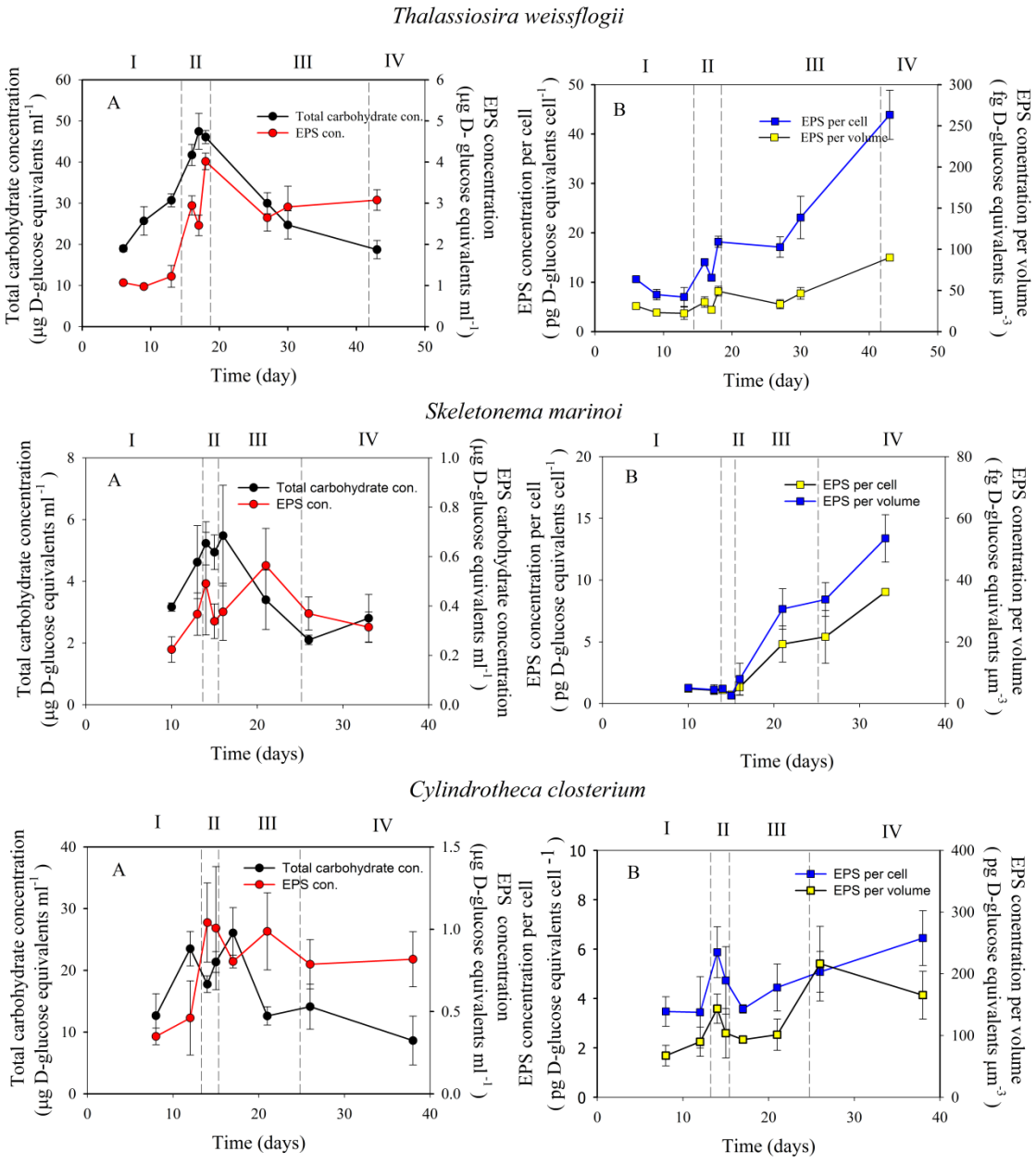

Figure 28. EPS content in cultures of *Thalassiosira weissflogii*, *Skeletonema marinoi* and *Cylindrotheca closterium* with time. A) Total carbohydrate and EPS concentration. B) EPS content per cell and per cell volume. Black circles (●) represent total carbohydrate concentration. Red circles (●) represent EPS concentration. Blue rectangles (■) represent EPS concentration per cell. Yellow rectangles (■) represent EPS concentration per volume. I: exponential growth phase. II: stationary phase. III: death phase. IV: dead. Bars show Mean ± SD (n = 3).

5.3.3.2 Carbohydrate allocation

In this experiment, carbohydrate concentrations of different fractions were measured to determine carbohydrate allocation with growth (Table 7). The carbohydrate fractions associated with different carbon pools were normalized to chlorophyll *a* concentration as cell abundance changed significantly during different growth phases. In addition, the proportions of different carbohydrate fractions in the total carbohydrate at different growth phases are shown in Figures 29~31.

In the cultures of *T. weissflogii*, total carbohydrate concentration was not significantly difference in different growth phases (Figure 29). However, total carbohydrate content per chlorophyll *a* increased over time (Table 7). There was a significant difference in total carbohydrate per chlorophyll *a* concentration in different growth phases ($F_{3,11} = 25.309$, $p < 0.001$, $n = 12$). The proportion of dissolved extracellular carbohydrate to total carbohydrate increased during death phase (Figure 29). On the contrary, the proportion of cell pellet carbohydrate (storage + cell wall + residual) declined during death phase (Figure 29). When carbohydrate was normalized to chlorophyll *a*, dissolved extracellular carbohydrate and cellular carbohydrate were significantly different during different growth phases ($F_{3,11} = 100.265$, $p < 0.001$, $n = 12$; $F_{3,11} = 6.496$, $p < 0.001$, $n = 12$). In the cell pellet, there was a significant negative correlation between carbohydrate associated with storage per chlorophyll *a* and culture time ($r = -0.437$, $p < 0.001$, $n = 12$), and a positive correlation between non-storage carbohydrate per chlorophyll *a* and culture time ($r = 0.929$, $p < 0.001$, $n = 12$). The

production of different carbohydrate fractions with growth suggested that the proportion of total carbohydrate in the form of extracellular carbohydrate, rather than intracellular storage carbohydrate, as the cells transitioned from growth to death.

In the cultures of *S. marinoi*, total carbohydrate concentration markedly increased in the death phase (Table 7; Figure 30). As total carbohydrate increased from growth to the death phase, the dissolved extracellular carbohydrate and cell pellet carbohydrate increased as well (Figure 30). However, in the intracellular carbon pool, carbohydrate associated with storage decreased as cells transitioned from growth to death (Figure 30). There were significant differences in total carbohydrate and cell pellet carbohydrate in different growth phases ($F_{3,11} = 5.765$, $p < 0.001$, $n = 12$; $F_{3,11} = 6.919$, $p < 0.001$, $n = 12$). When different carbohydrate fractions were normalized to chlorophyll *a*, maximum values were in dead cultures because of dead cells with very low Chl. *a* concentration (Table 7).

In cultures of *C. closterium*, the greatest total carbohydrate occurred in the death phase (Figure 31). There was a significant difference in total carbohydrate concentration in different growth phases ($F_{3,11} = 20.065$, $p < 0.001$, $n = 12$). *C. closterium* produced more dissolved extracellular carbohydrate in the exponential growth phase than in other phases (Table 7. Figure 31). When cultures shifted from growth to death, cell pellet carbohydrate increased, especially in the cell non storage carbohydrate (cell wall + residual) (Figure 31). There were significant differences in dissolved carbohydrate and cell pellet carbohydrate in different growth phases ($F_{3,11} = 1.427$, $p < 0.001$, $n = 12$; $F_{3,11} = 74.706$, $p < 0.001$, $n = 12$).

Table 7. Different fractions of carbohydrate in batch cultures of *Thalassiosira weissflogii*, *Skeletonema marinoi* and *Cylindrotheca closterium* during different growth phases. Values are mean ± SD (n = 3 replicate cultures).

		Thalassiosira weissflogii	
Growth phases	Total carbohydrate (μg × ng chl*a*$^{-1}$)	Cell pellet carbohydrate (μg × ng chl*a*$^{-1}$)	Dissolved extracellular carbohydrate (μg × ng chl*a*$^{-1}$)
Exponential	0.17 ± 0.03	0.20 ± 0.01	0.06 ± 0.002
Stationary	0.55 ± 0.07	0.38 ± 0.06	0.14 ± 0.012
Death	0.49 ± 0.10	0.37 ± 0.08	0.25 ± 0.045
Dead	1.05 ± 0.22	0.47 ± 0.11	0.67 ± 0.095
		Skeletonema marinoi	
	Total carbohydrate (μg × ng chl*a*$^{-1}$)	Cell pellet carbohydrate (μg × ng chl*a*$^{-1}$)	Dissolved extracellular carbohydrate (μg × ng chl*a*$^{-1}$)
Exponential	0.015 ± 0.002	0.004 ± 0.001	0.0002 ± 0.0001
Stationary	0.040 ± 0.009	0.044 ± 0.010	0.0063 ± 0.0025
Death	0.048 ± 0.012	0.029 ± 0.009	0.0004 ± 0.0034
Dead	57.516 ± 84.337	16.234 ± 23.687	22.767 ± 34.027
		Cylindrotheca closterium	
	Total carbohydrate (μg × ng chl*a*$^{-1}$)	Cell pellet carbohydrate (μg × ng chl*a*$^{-1}$)	Dissolved extracellular carbohydrate (μg × ng chl*a*$^{-1}$)
Exponential	0.44 ± 0.16	0.07 ± 0.04	0.23 ± 0.16
Stationary	1.93 ± 0.60	1.08 ± 0.09	1.30 ± 0.46
Death	1.30 ± 0.31	0.72 ± 0.13	1.27 ± 0.52
Dead	0.62 ± 0.27	0.38 ± 0.05	0.91 ± 0.19

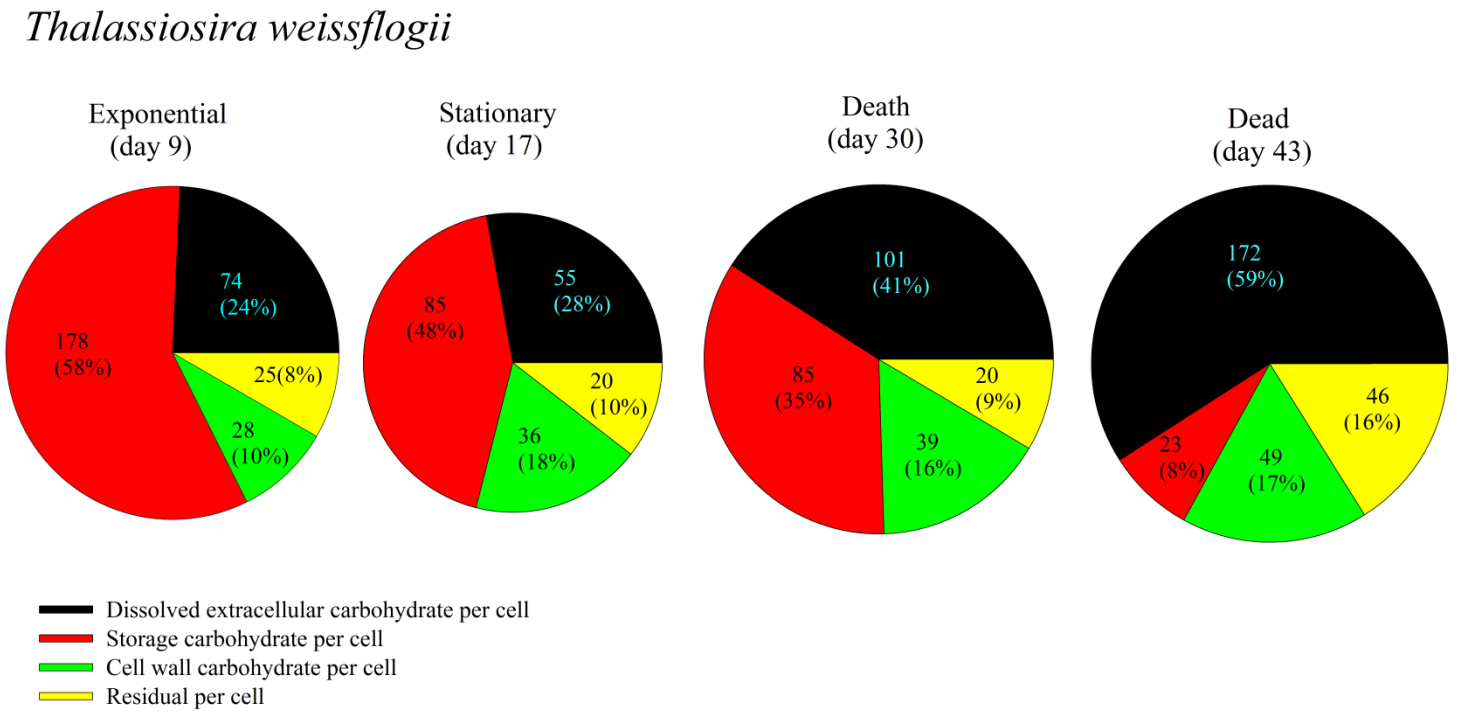

Figure 29. Proportion and concentration of different carbohydrate fractions in diatom species *Thalassiosira weissflogii* in exponential, stationary, death phase and dead. The black areas represent dissolved extracellular carbohydrate in the cultures; red areas represent storage associated carbohydrate. Green areas represent cell wall associated carbohydrate and yellow areas represent residual carbohydrate. The sum of red, green and yellow areas represent intracellular carbohydrate. The total area represents total carbohydrate. Numbers in each fraction represent specific carbohydrate concentration (pg cell^{-1}), and proportion in each fractions represent proportion of specific carbohydrate fraction in total carbohydrate.

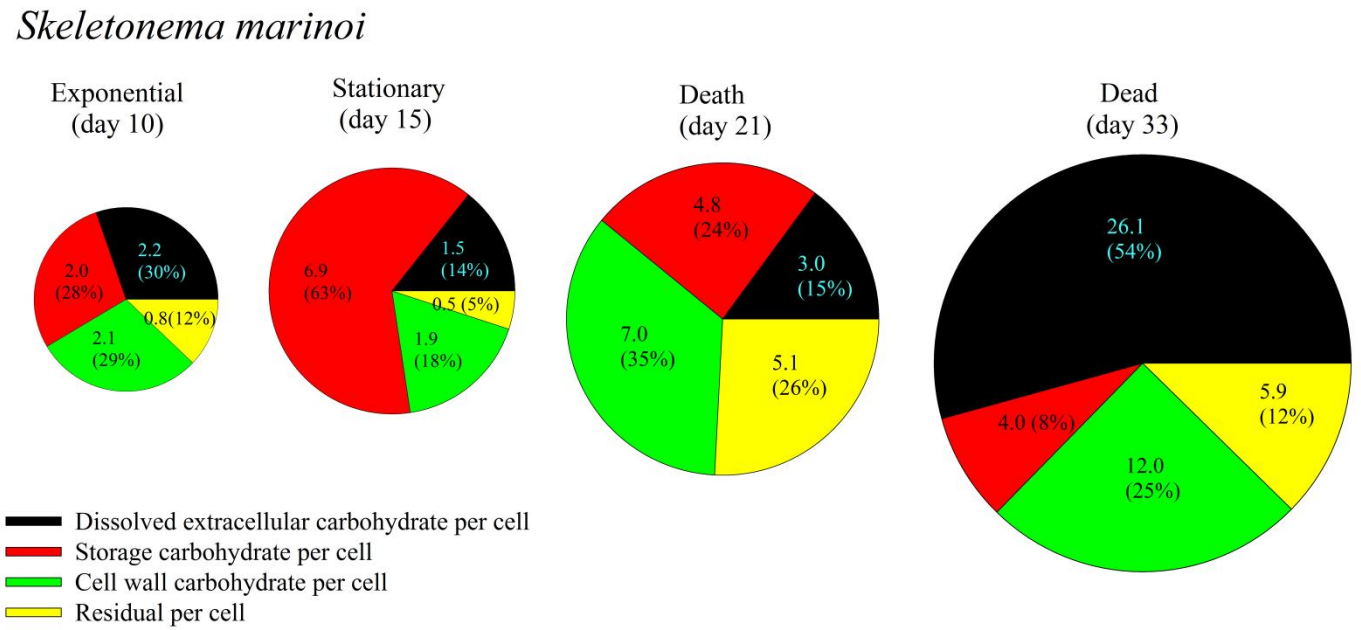

Figure 30. Proportion and concentration of different carbohydrate fractions in diatom species *Skeletonema marinoi* in exponential, stationary, death phase and dead. The black areas represent dissolved extracellular carbohydrate in the cultures; red areas represent storage associated carbohydrate. Green areas represent cell wall associated carbohydrate and yellow areas represent residual carbohydrate. The sum of red, green and yellow areas represent intracellular carbohydrate. The total area represents total carbohydrate. Numbers in each fraction represent specific carbohydrate concentration (pg cell^{-1}), and proportion in each fractions represent proportion of specific carbohydrate fraction in total carbohydrate.

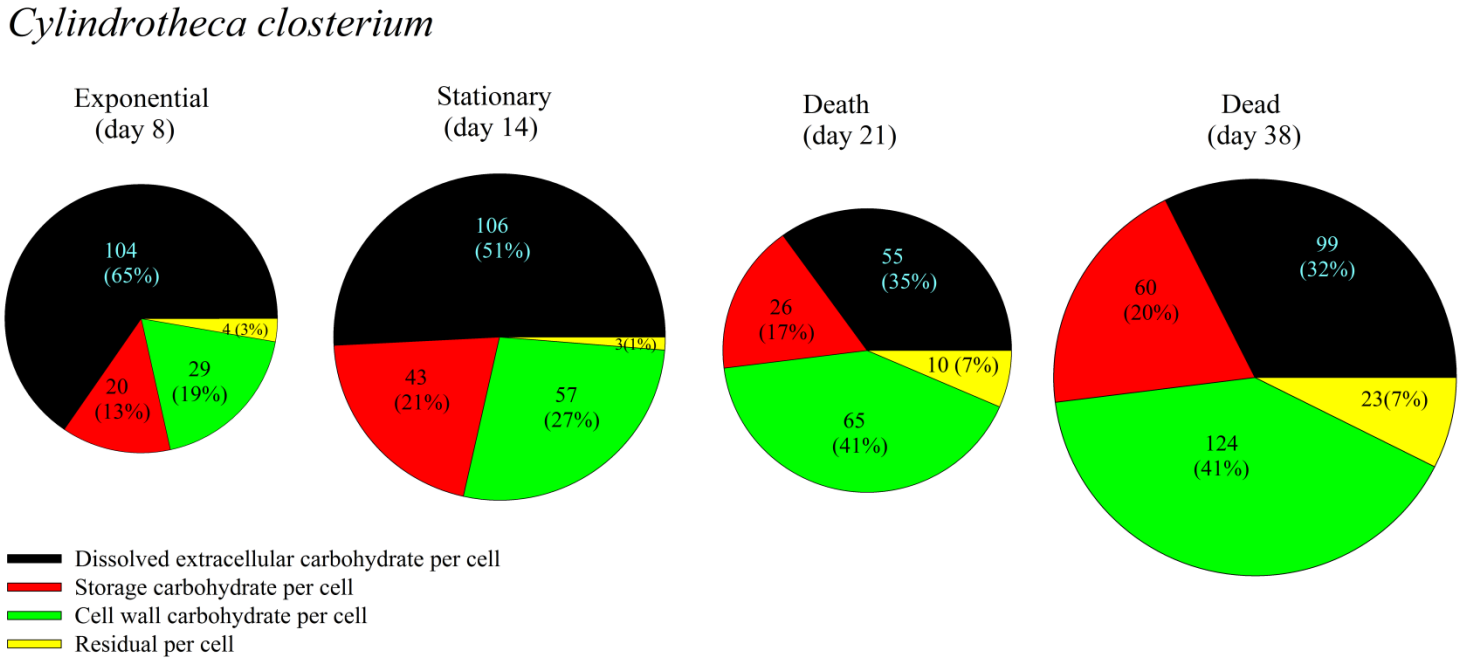

Figure 31. Proportion and concentration of different carbohydrate fractions in diatom species *Cylindrotheca closterium* in exponential, stationary, death phase and dead. The black areas represent dissolved extracellular carbohydrate in the cultures; red areas represent storage associated carbohydrate. Green areas represent cell wall associated carbohydrate and yellow areas represent residual carbohydrate. The sum of red, green and yellow areas represent intracellular carbohydrate. The total area represents total carbohydrate. Numbers in each fraction represent specific carbohydrate concentration (pg cell^{-1}), and proportion in each fractions represent proportion of specific carbohydrate fraction in total carbohydrate.

5.3.4 Carbohydrate fractions were measured by TPTZ method

Monosaccharide and polysaccharide concentrations in the intracellular and extracellular pools were determined using the TPTZ method. In three cultures, intracellular carbohydrate was higher than extracellular carbohydrate. The intracellular monosaccharide and polysaccharide showed a rapid increase from growth to stationary phase and a decrease during death phase (Figure 32). However, extracellular carbohydrate didn‟t decrease, and extracellular polysaccharide even slightly increased in the death phase. Thus, a decrease of intracellular monosaccharide and polysaccharide was correlated with more extracellular polysaccharide as cultures transitioned from the growth to the death phase.

5.3.5 Comparison for PSA and TPTZ methods in carbohydrate fractions analysis on phytoplankton

Carbohydrate fractions collected from three different diatom species, *T. weissflogii, S. marinoi* and *C. closterium,* in different growth phases were measured by PSA and TPTZ methods and the results obtained by the two methods were compared. Carbohydrate fractions included total carbohydrate, extracellular dissolved carbohydrate, and intracellular carbohydrate.

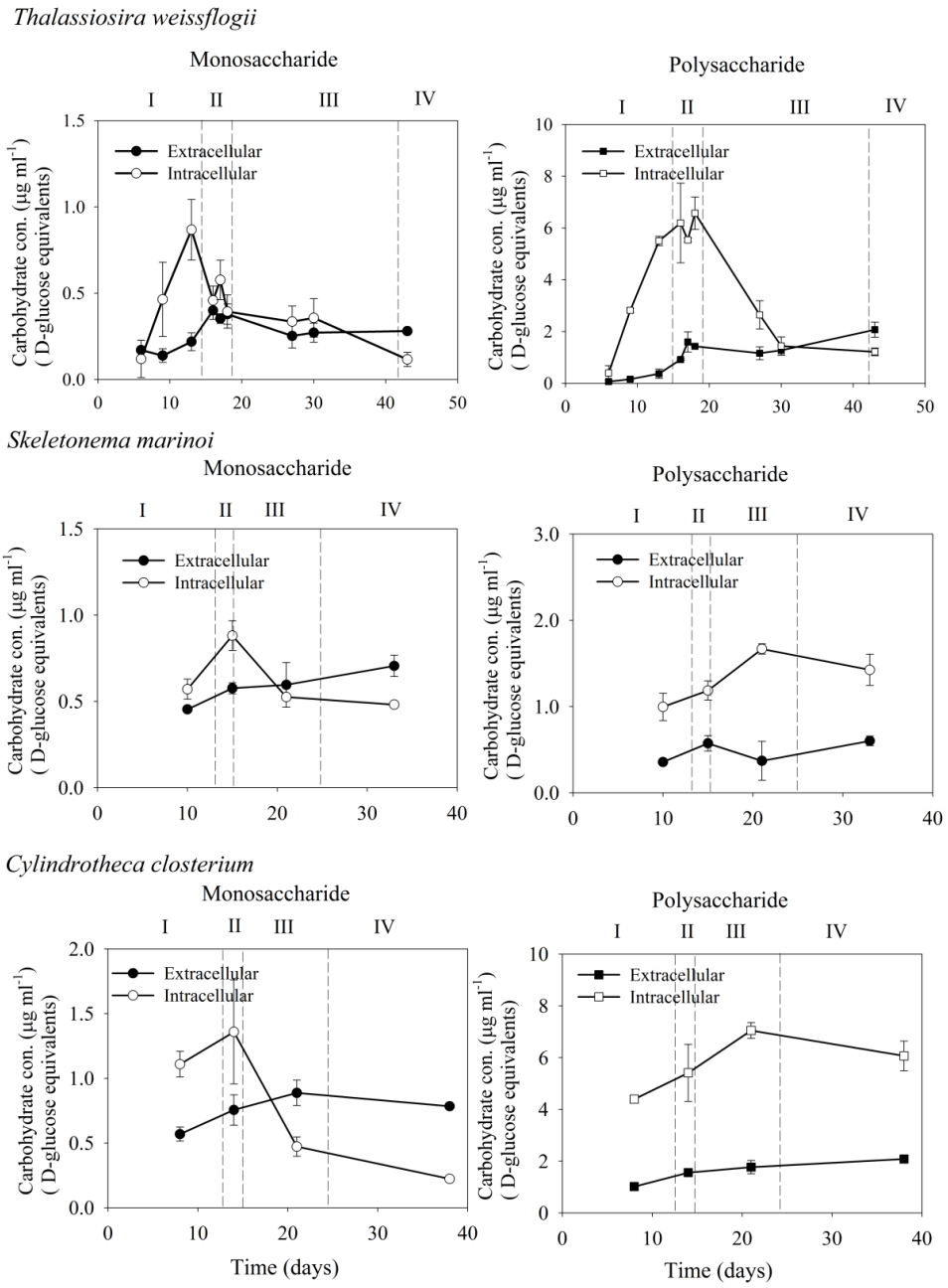

Figure 32. Changes in monosaccharide and polysaccharide concentrations in culture medium in extracellular and intracellular pools in cultures of *T. weissflogii*, *S. marinoi* and *C. closterium* in different growth phases.
extracellular monosaccharide (●); intracellular monosaccharide concentration(○); extracellular polysaccharide (■); intracellular polysaccharide (□). I: exponential growth phase. II: stationary phase. III: death phase. IV: dead. Bars show Mean ± SD (n = 3).

5.3.5.1 Total carbohydrate

Total carbohydrate concentration (TCHO) was determined by summing the extracellular and intracellular carbohydrate measured by the TPTZ method. TCHO carbohydrate was determined directly using the PSA method. Comparing TCHO measured by the PSA and TPTZ method, the PSA method showed higher TCHO than TPTZ (Figure 33). The relationships between the two methods are shown in regression lines. In cultures of *T. weissflogii*, TPTZ and PSA methods all showed an increase of TCHO from exponential to stationary phase and a decrease during death phase (Figure 33). There was a positive correlation between total carbohydrate measured by TPTZ and PSA ($r = 0.887$; $n = 27$; $p < 0.05$) (Figure 34). However, measuring of TCHO by TPTZ method did not show a good agreement with PSA in cultures of *S. marinoi* and *C. closterium* (Figure 34). There was not a significant correlation between TCHO measured by PSA and by TPTZ in *S. marinoi* ($r = 0.206$; $n=12$; $p < 0.05$) and in *C. closterium* ($r = -0.115$; $p > 0.05$).

5.3.5.2 Dissolved extracellular carbohydrate

Dissolved extracellular carbohydrate (DEC) was directly measured by PSA method and TPTZ method. PSA method showed higher concentration of DEC than did TPTZ in cultures of *T. weissflogii* and *C. closterium*, but lower results than TPTZ in *S. marinoi* (Figure 33).There was significant positive correlation between DEC measured

by TPTZ and by PSA in cultures of *T. weissflogii* with r = 0.528; n = 27; $p < 0.05$; and in *S. marinoi* with r = 0.784; n = 12; $p < 0.05$ (Figure 34). However, there was not a significant correlation between DEC measured by TPTZ and by PSA in cultures of *C. closterium* (r = 0.06; n = 12; $p > 0.05$) (Figure 34).

5.3.5.3 Cellular carbohydrate

Cellular carbohydrate was measured by PSA method through the sum of storage associated carbohydrate (HW extraction), cell wall associated carbohydrate (HB) and residual carbohydrate fractions. Cellular carbohydrate was determined by the TPTZ method through measuring carbohydrate concentrations in the intracellular carbon pool. The amount of cellular carbohydrate detected by PSA method was higher than cellular carbohydrate obtained using TPTZ method (Figure 33). There was significant positive correlation with cellular carbohydrate measured by TPTZ and PSA in cultures of *T. weissflogii* (r = 0.871; n = 27; $p < 0.05$) (Figure 34); However, there were not significant correlations between cellular carbohydrate measured by TPTZ and by PSA in cultures of *S. marinoi* (r = 0.504; n = 12; $p > 0.05$) and in *C. closterium* (r = 0.382; n = 12; $p > 0.05$) (Figure 34).

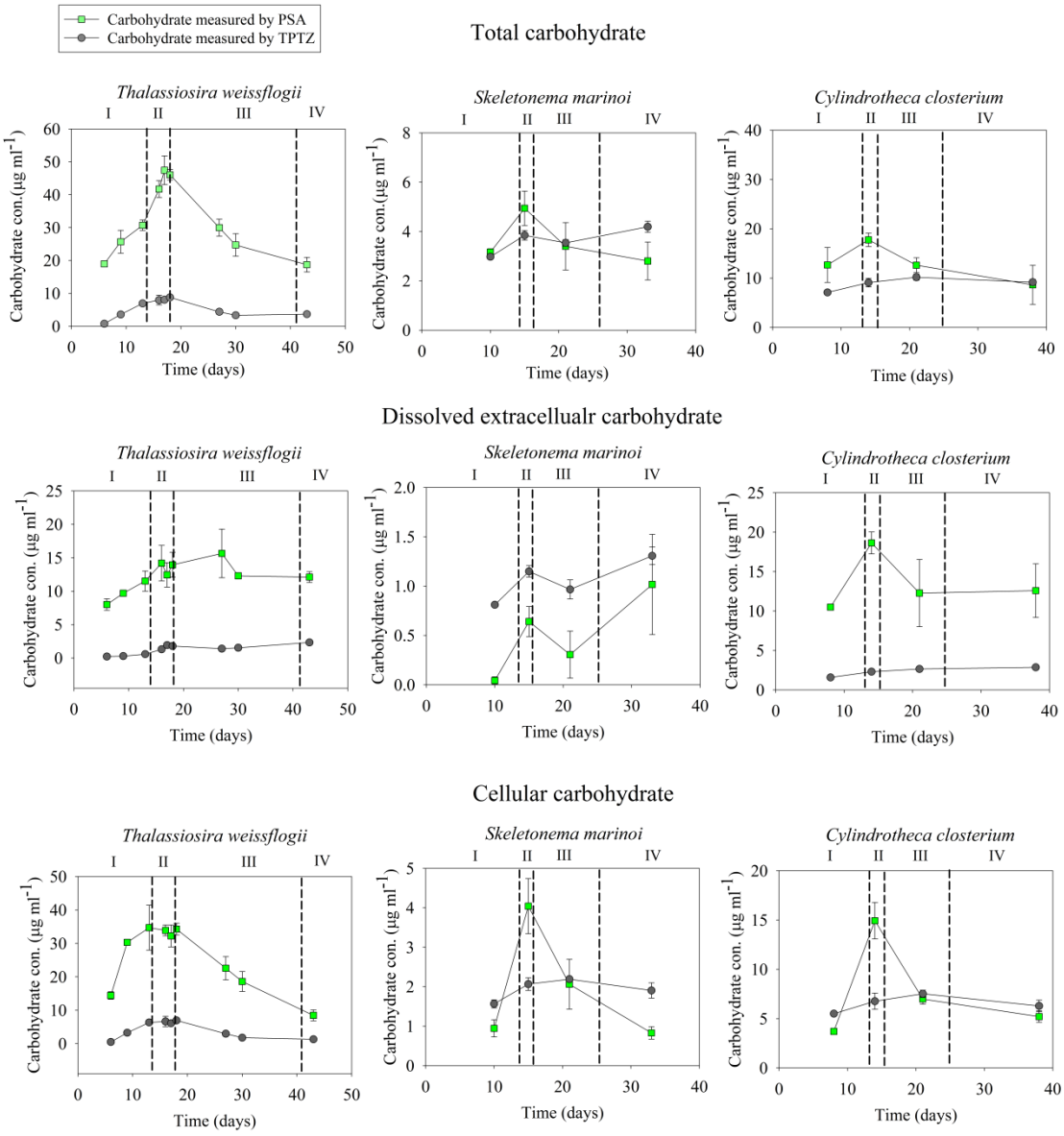

Figure 33. Comparison of different fractions of carbohydrate measured by the PSA and TPTZ methods in cultures of *Thalassiosira weissflogii*, *Skeletonema marinoi* and *Cylindrotheca closterium.* Total carbohydrates were measured by PSA (green rectangles (■)) and TPTZ methods (black circles (●). Data points show mean ± SD (n=3).

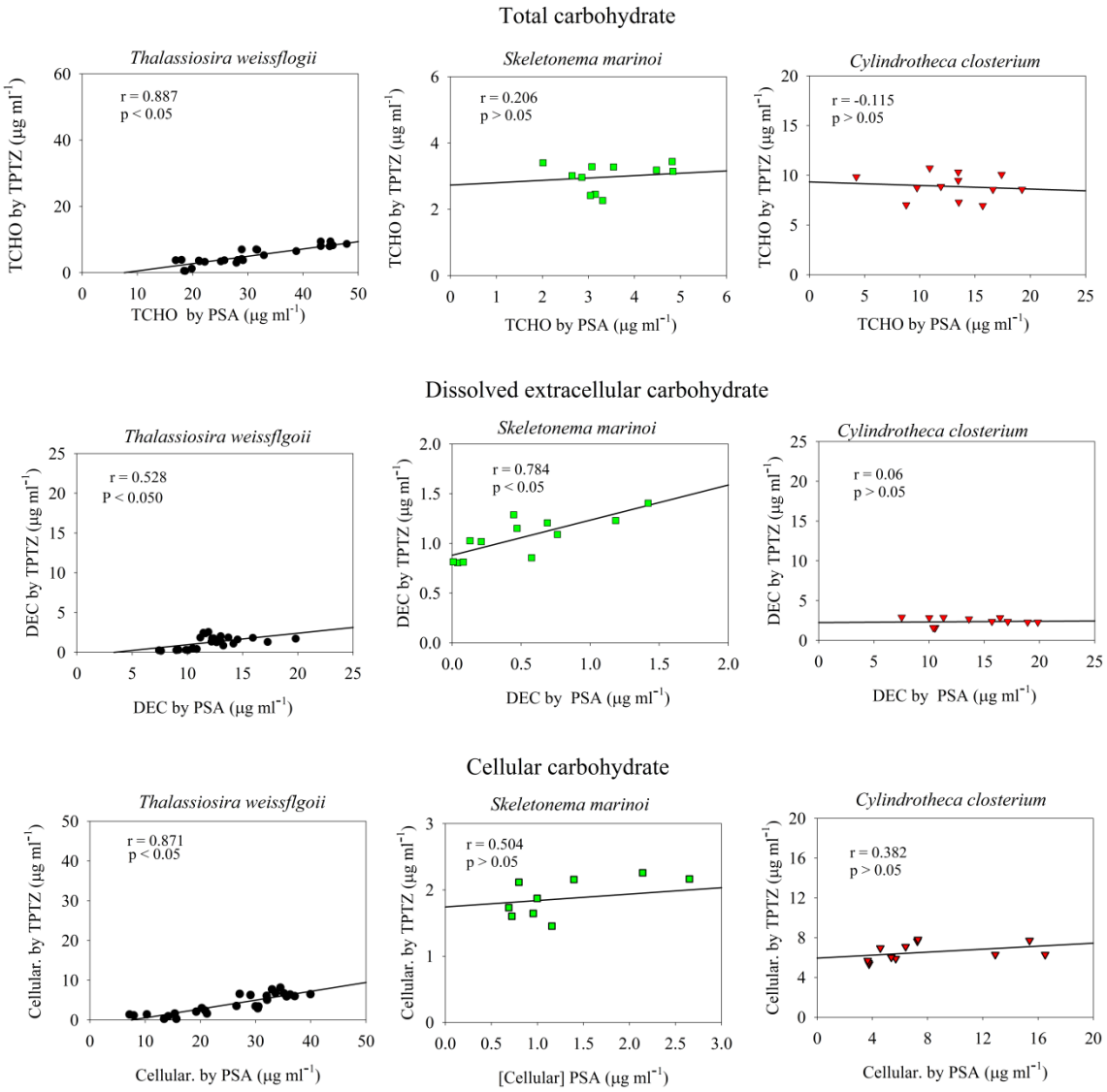

Figure 34. Comparison of PSA and TPTZ method for determining different fractions of carbohydrate in diatom cultures of *Thalassiosira weissflogii* (●), *Skeletonema marinoi* (■), and *Cylindrotheca closterium* (▼). Solid lines represent regression line between the PSA and TPTZ methods.

5.3.6 TEP formation

Total TEP area per ml was used to indicate TEP production. In the cultures of *T. weissflogii*, TEP abundance and total area of TEP increased during stationary phase to death phase, although cell numbers had a rapid decline during that phase (Figure 35). As cells died, TEP abundance declined in the cultures. Therefore, TEP was mainly formed during stationary to death phase. The particle size distributions indicated that TEP particle size was shifted from smaller size (0 to 40 μm^2) in the exponential phase to larger size (40 to100 μm^2) in the stationary phase, and then reduced back to smaller size in the death stage (Figure 35).

In the cultures of *S. marinoi*, TEP abundance remained constant in all phases (Figure 35). However, TEP total area increased with decreasing cell abundance from stationary to death phase, from $1.51 \pm 0.81 \times 10^2$ mm^2 ml^{-1} (mean ± SD) to $17.96 \pm 10.65 \times 10^2$ mm^2 ml^{-1} (mean ± SD). There were more large TEP particles in the stationary phase than in the other phases (Figure 35). Therefore, TEP formation was greatest in stationary to death phase.

Unlike to *T. weissflogii* and *S. marinoi*, total TEP area dramatically increased during the exponential growth phase in cultures of *C. closterium*, from $4.41 \pm 0.85 \times 10^2$ mm^2 ml^{-1} to $7.60 \pm 0.19 \times 10^2$ mm^2 ml^{-1}. The TEP abundance was greatest in the death phase with an abundance of $2.61 \pm 0.81 \times 10^5$ ml^{-1}. There were more TEP particles with bigger size in the stationary phase than in other phases. Thus, TEP production was enhanced during the growth phase in *C. closterium* cultures (Figure 35).

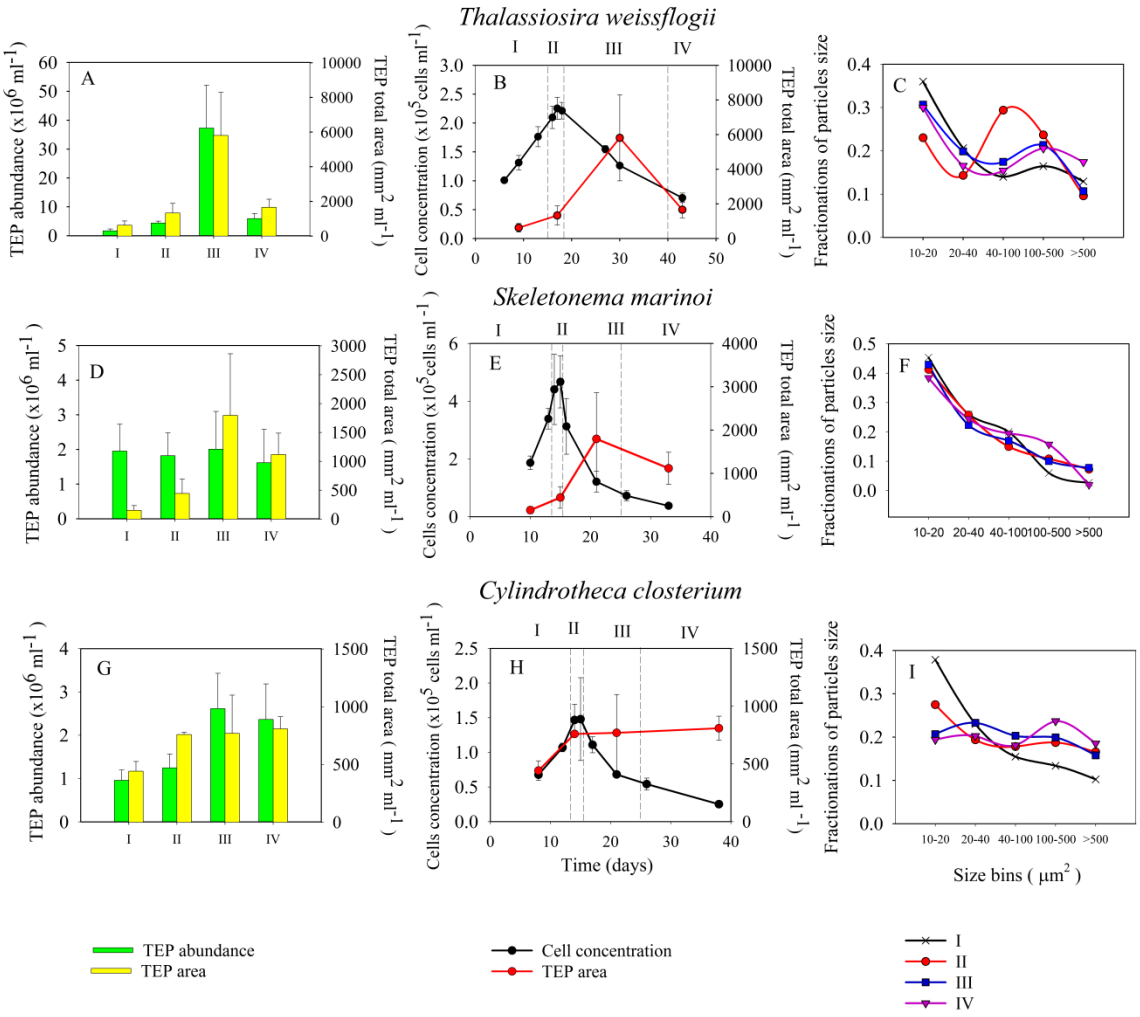

Figure 35. TEP concentrations and abundance in exponential, stationary, death phase and dead cultures of *Thalassiosira weissflogii*, *Skeletonema marinoi* and *Cylindrotheca closterium*. A,D,G) TEP abundance and TEP total area. B,E,H) TEP total area and cell abundance with culture time. C,F,I) TEP size distribution in different growth phases. In graphs A, D, G, green bars represent mean TEP abundance. Yellow bars represent mean total TEP area.
In graphs B. E. H., black circles (●) represent mean cell abundances. Red circles (●) represent mean TEP total area.
In graphs C. F. I., Crosses (×) represent TEP size distribution in the exponential phase. Red circles (●) represent TEP size distribution in the stationary phase. Rectangles (■) represent TEP size distribution in the death phase. Triangles (▼) represent TEP size distribution in dead cells.
I: exponential growth phase. II: stationary phase. III: declining growth phase. IV: death phase. Error bars show ± SD (n = 3).

5.3.7 CSP formation

In the cultures of *T. weissflogii* and *S. marinoi*, CSP production enhanced during the stationary and death phases, because total CSP area and CSP abundance elevated during those phases (Figure 36). When cells became dead, CSP abundance reduced in these two cultures. Thus, CSP was mostly formed in the stationary to death phase in these two diatom cultures. However, in the cultures of *C. closterium*, the total area of CSP markedly increased over time, even cell abundance decreased in the death phase. Therefore, the CSP was mainly produced in the exponential to declining growth phase in cultures of *C. closterium*. Moreover, most CSP particles in cultures of *T. weissflogii* significantly shifted to a larger size (20 ~500 μm^2) in the stationary phase. In the cultures of *S. marinoi* and *C. closterium*, CSP particles slightly increased in size to 100 ~ 500 μm^2 in the stationary phase in the cultures of (Figure 36).

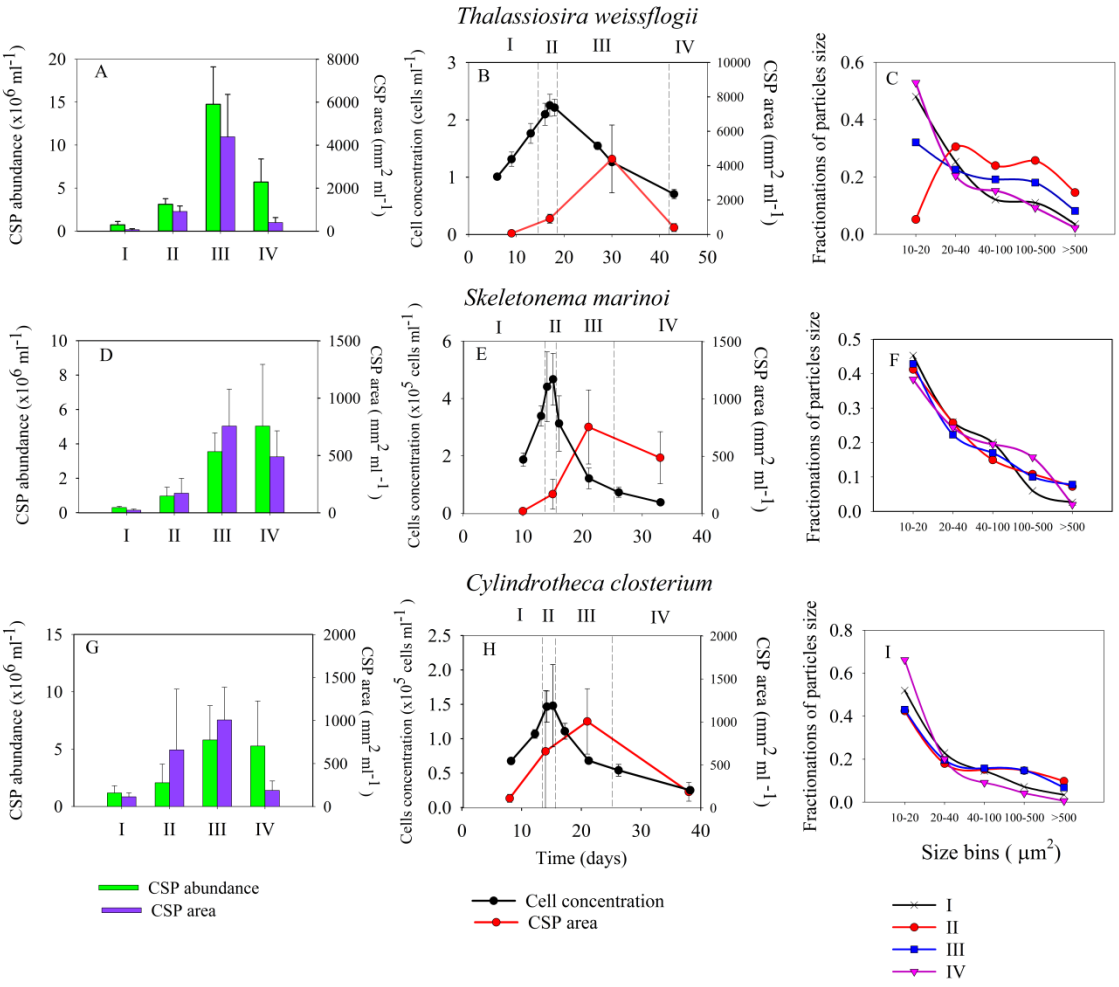

Figure 36. The CSP productions in cultures of *Thalassiosira weissflogii*, *Skeletonema marinoi* and *Cylindrotheca closterium* during exponential, stationary, death phases and dead. A.D.G) CSP abundance and CSP area. B.E.H) Total CSP area and cell abundance with culture time. C.F.I) CSP size distribution in different phases.
In graphs A.D.G, green bars represent CSP abundance. Purple bars represent total CSP area.
In graphs B.E.H, black circles (●) represent cell abundances. Red circles (●) represent total CSP area.
In graphs C.F.I, crosses (×) represent size in exponential phase. Red circles (●) represent size in the stationary phase. Rectangles (■) represent size in the death phase. Triangles (▼) represent size when cells dead.
I: exponential growth phase. II: stationary phase. III: death phase. IV: dead. Deviation bars show Mean ± SD (n = 3).

5.3.8 Cell permeability

In all three diatom cultures, there was a significant increase in the fraction of SYTOX Green labeled cells from death phase to dead (Figure 37). The greatest proportion of SYTOX Green labeled cells occurred when cells were dead; 65.4 ± 5.2 % in the cultures of *T. weissflogii*, 88.5 ± 2.8 % in the cultures of *S. marinoi*, and 92.4 ± 4.3 % in the cultures of *C. closterium*.

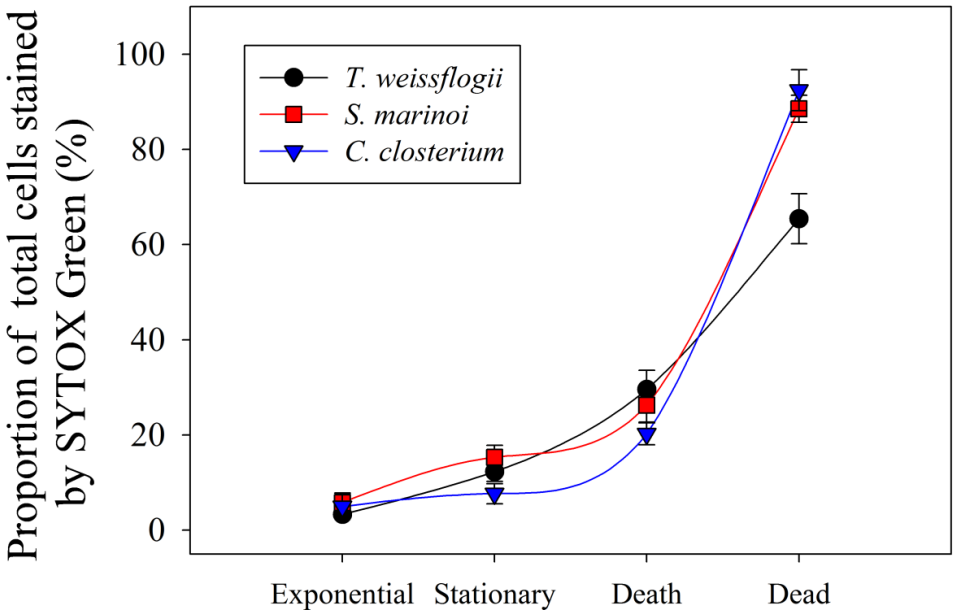

Figure 37. Proportion of SYTOX Green labeled cells in total 400 cells in the cultures of *Thalassiosira weissflogii*, *Skeletonema marinoi* and *Cylindrotheca closterium* during different phases. Deviation bars show Mean ± SD (n = 12). Solid circles (●) represent *T. weissflogii* cells. Red rectangles (■) represent *S. marinoi* cells and blue triangles (▼) represent *C. closterium* cells.

To clarify the contribution of nucleic acids to TEP formation, TEP was stained by SYTOX Green and Alcian Blue at the same time. SYTOX Green is a nucleic acid dye, which can indicate extracellular DNA and RNA. Alcian Blue is an acidic polysaccharide dye, which is used to stain TEP. Our results revealed that some parts of TEP also stained with SYTOX Green, indicating that extracellular nucleic acids are associated with TEP (Figure 38).

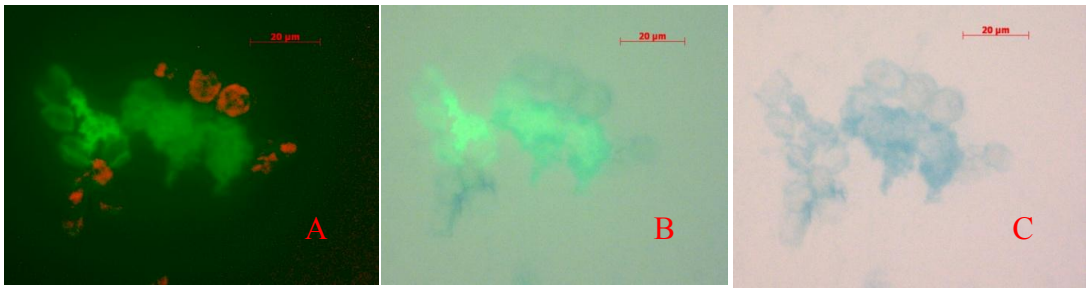

Figure 38. Images of TEP stained by SYTOX Green and Alcian Blue in cultures of *Thalassiosira weissflogii*. Nucleic acid was stained by SYTOX Green and fluoresce green. TEP were stained by Alcian Blue and show blue under brightfield light. Chlorophyll *a* fluorescence is shown in red.

A) Stacked images captured using a GFP filter (showing SYTOX Green fluorescence), and DAPI filter (show chl. *a* fluorescence)
B) Stacked image combining a photo taken with the GFP fluorescence filter (showing SYTOX Green fluorescence) and a brightfield image of TEP.
C) Brightfield (showing TEP).

5.3.9 Bacteria

Bacteria concentrations were very low at the beginning time of cultures (*T. weissflogii*: 5972 cells ml^{-1}; *S. marinoi*: 6098 cells ml^{-1}; *C. closterium*: 7086 cells ml^{-1}). However, bacteria concentration was high in the death phase after 50 days of culturing (*T. weissflogii*: 2.08×10^5; *S. marinoi*: 6.30×10^5; *C. closterium*: 5.78×10^5). The bacteria concentration in the cultures was positively correlated with culture times (*T. weissflogii*: $r = 0.961$, $p < 0.001$, $n = 12$; *S. marinoi*: $r = 0.969$, $p < 0.001$, $n = 12$; *C. closterium*: $r = 0.984$, $p < 0.001$, $n = 12$). There was a significant difference in the bacteria concentration at the different culture date (*T. weissflogii:* $F_{3,11} = 114.143$, $p < 0.001$, $n = 12$; *S. marinoi:* $F_{3,11} = 722.142$, $p < 0.001$, $n = 12$; *C. closterium:* $F_{3,11} = 409.201$, $p < 0.001$, $n = 12$).

5.4 Discussion

5.4.1 Growth and death phases affect TEP production

Our results showed that TEP production depended on growth phase and was species-specific in different diatoms. In batch cultures, nutrient availability is the main factor limiting the growth of cultures. Nutrients in batch culture shifted from replete to limit as cultures transitioned from growth to death phase (Canfield et al. 2005). Nutrient stress influences the metabolic pathways of cells and how they store carbohydrate

(Miller et al. 1988). Many studies indicate that diatoms exude more TEP under nutrient stress because of metabolic imbalance (Passow et al. 1994, Engel 2000). Under nutrient limitation, carbon is often fixed in excess of requirements and cells release fixed carbon into the surrounding medium as extracellular carbohydrates (Myklestad and Haug 1972, Fogg et al. 1983, Staats et al. 2000). In my experiment, TEP production changed significantly in three diatom species from growth to death, indicating cells‟ metabolism varied during different phases of growth. I found a rapid increasing of TEP concentration in the cultures of *Thalassiosira weissflogii* and *Skeletonema marinoi* during stationary to death growth phases, as nutrients limit growth. Thus, TEP production was enhanced by nutrient stress during stationary to death phases in these two diatom species. On the other hand, most of the TEP produced by *Cylindrotheca closterium* was produced during exponential growth phase, when nutrients were replete in the culture medium. This indicated that the production of TEP was associated with rapidly growing cells in *C. closterium*. My results are consistent with observations by others. Engel (2000) and Fukao et al. (2010) found that high concentrations of TEP production were generated by *Skeletonema costatum* during stationary to death phases. Underwood et al. (2004) suggested that more exopolymers (EPS) were produced by benthic diatoms (*Cylindrotheca spp.*) during growth phase. Why TEP should be formed during different growth phases by different species? It can be explained by life history and TEP functions in species. *Thalassiosira weissflogii* and *Skeletonema marinoi* are coastal diatoms. TEP synthesis could be a mechanism to protect these diatoms from bacteria or viral attack and assist in cell flow in the oceans (Passow et al. 2003).

However, *Cylindrotheca closterium* is a benthic diatom (Smith and Underwood 1998; Staats et al. 2000). The exudation of exopolymers helps them to attach and move on sediments, which gives them advantage in adapting to changing environmental conditions of the shallow benthic environment (Underwood and Paterson 2003).

Analysis of allocation of carbon and TEP production during different phases of growth and death suggested that TEP production was associated with carbon allocation. In the cultures of *T. weissflogii* and *S. marinoi*, the most TEP production occurred during stationary to death phases and that TEP may be transformed from stored carbohydrate. However, an opposite pattern of TEP production associated with carbon allocation showed in the cultures of *C. closterium*. High concentration of TEP production was associated with enhanced exudation of dissolved extracellular carbohydrate by *C. closterium* during growth phase. My results were supported by Smith and Underwood (1998), who tracked process of carbon allocation using ^{14}C as tracer. They revealed that intracellular storage glucan can be reallocated into EPS during the growth phase in *Cylindrotheca closterium* (Smith and Underwood 1998). Similarly, Wetz and Wheeler (2007) grew planktonic and benthic diatom in batch culture and found that *Chaetoceros decipiens* (a planktontic species) released more DOC during death phases, but DOC release rate in the cultures of *Cylindrotheca closterium* (benthic species) decreased to 0 in the death phase.

TEP precursors (DOM) could be contributed actively by cell exudation or passively by cell lyses (Bhaskar and Bhosle 2005). In the exponential growth phase, healthy cells exuded lots of EPS, which can be used in form of TEP. In contrast, cells

lost vitality and there were more dead cells with low integrity during stationary to death phase, which was predicted to more easily leak intracellular DOC and TEP precursors to the outside and subsequently in the form of TEP. Thus, there might be exist two mechanisms of TEP formation. One way is abiotic formation of TEP from leakage DOC and TEP precursors from permeable cells, such as formation of TEP by *T. weissflogii* and *S. marinoi* during death phase. The other way is biotic formation by exudation of DOC from healthy cells, such as generation of TEP by *C. closterium* during exponential growth phase. Fukao et al. (2010) indicated that increased TEP production during death phase by *Rhizosolenia setigera* and *Skeletonema sp*. maybe caused by dissolved polysaccharides released from dying cells. However, the TEP formation pathway is still not clearly understood and I cannot prove the relationship between cell lyses and TEP formation in this study. I knew that some parts of TEP also can be stained with SYTOX Green, indicating that nucleic acids exported by lyses cells are associated with TEP.

TEP are sticky particles which stimulate aggregate formation. If species generated TEP during exponential growth phase of cells, aggregation would occur during blooms of cells. For example, many aggregations were recorded during the bloom of *Cylindrotheca closterium*, which produced TEP during growth phase (Staats et al. 2003). On the other hand, species that tend to form TEP during decline phase would onset aggregation during termination of bloom. Several records pointed out aggregation occurrences after *Skeletonema costatum* blooms, because *S. costatum* generated TEP during death phases (Kiørboe and Hansen 1993, Engel 2000). Focus on time scale of TEP formation and aggregation will be important in study of carbon flux exported to

ocean interior. Hence, the effects of growth and death phases on TEP formation in different species are interesting for further investigation.

5.4.2 DOM release by phytoplankton cells

Phytoplankton can release lots of DOM, which consists of a wide range of organic molecules, including carbohydrates, nitrogen compounds, and lipids (Lancelot & Mathot 1985). There are many processes that affect the release of DOM from inside of phytoplankton to the outside environment, which include physical process (sloppy feeding by predators, and viral attraction) (Møller 2007, Franklin et al. 2006), and physiological process (release from phytoplankton cells) (Veldhuis et al. 2001, Berman-Frank et al. 2007, Claquin et al. 2008). Anderson and Williams (1998) divided the physiological loss of DOM from phytoplankton into two processes: the exudation of excess carbon from cells in response to changing environmental factors, and the loss of DOM by leakage from cells. Research has demonstrated that that healthy phytoplankton cells can exude a significant amount of DOM in response to changing environmental factors (Myklestad & Haug 1972, Myklestad 1974). Under nitrogen limitation, more DOM is exuded by diatoms in form of EPS (Staats et al. 2000, Passow 2002a, Wetz and Wheeler 2007). Recently, there have been several studies on the relationship between phytoplankton cell integrity and the release of DOM. Permeable cells were more „leaky" and easily released intracellular DOM to the outside (Franklin et al. 2006). Franklin et al. (2006) demonstrated that cell death results in increased permeability of the cell

membrane. My result is consistent with Franklin‟s observation. In my batch culture experiment, cells in the death phase were aged and nutrient stressed. SYTOX green results indicated that these dying and dead cells were more permeable. However, there was no evidence to prove that whether cell leakage contributed to TEP precursors. TEP formation is a complex pathway that might link to both exudation by healthy cells and leakage by permeable dying cells. The mechanism of TEP formation needs further investigation. Furthermore, TEP formed by DOM associated with different release processes may be of different compositions. Some studies illustrated that permeable cell membranes more easily leak small molecular compounds (amino acids, monosaccharides) than big chemical compounds (Myklestad 2000). In contrast, healthy cells preferentially exude big molecular compounds, such as polysaccharides (Myklestad 2000). Therefore, different pathways of DOM release may lead to different compositions of TEP and subsequently to diverse chemical and/or physical properties. Unfortunately, I did not measure composition of TEP during different growth phases. Other studies suggested that composition of EPS was distinct during different growth phases among species, which resulted in variable EPS types (Bellinger et al. 2005, Abdullahi et al. 2006). As a subgroup of EPS, TEP production probably has different types with different structures and characteristics formed by different mechanisms. Therefore, it is important to investigate carbohydrate composition of TEP associated with TEP formation mechanisms among diatom species.

5.4.3 Comparison of the PSA and TPTZ methods for the analysis of carbohydrates from phytoplankton

TPTZ and PSA methods were two popular methods in analysis of carbohydrate. They have been used in many carbohydrate analyses of natural samples (Underwood et al. 1995, Witter and Luther 2002; Panagiotopoulos and Sempéré 2005). In a comparison of these two methods, PSA method had a better regression coefficient in measurement of higher concentration of carbohydrate (20 μg C ml^{-1} ~100 μg C ml^{-1}) than TPTZ method. Carbohydrate concentration measured using TPTZ method is not linear at higher concentrations (≥ 20 μg C ml^{-1}). Thus, the PSA method is better for measuring high concentration carbohydrate samples, such as batch culture samples, than the TPTZ method. In this experiment, I revealed that hydrolysis efficiency had a strong relationship with acid types and hydrolysis time (Figure 2 & 4). The hydrolysis efficiency of two methods all increased with time until to a maximum and then decreased with longer hydrolysis time (Figure 2 & 4; Dubois 1956, Liu et al. 1973). The maximal hydrolysis efficiency was higher in the PSA method (80~100 % for 30 minutes hydrolysis) than in the TPTZ method (78 % from 24 hours hydrolysis). This may be because the PSA method used sulphuric acid, and the TPTZ method used hydrochloric acid for hydrolysis. Many studies state that sulphuric acid is much more effective in the hydrolysis of polysaccharides, especially high molecular weight compounds, than hydrochloric acid (Pakulski and Benner 1992, Borch and Kirchman 1997). However, using sulphuric acid to hydrolyse polysaccharide in the TPTZ method always causes the

explosion of sealed samples, so hydrochloric acid was selected to hydrolysis samples in the TPTZ method. Moreover, results in this study demonstrated that monosaccharides decomposed during the hydrolysis procedure at high temperature (Figure 5). Decomposition of monosaccharides during hydrolysis would lead to an underestimate of the size of the carbohydrate pool and the amount of carbon associated with it. Many studies showed consistent results, which indicates that acid hydrolysis may destroy some monosaccharides, such as fructose and ribose (Mopper 1977, Borch and Kirchman 1997).

In my measurements, salinity did not interfere with the PSA and TPTZ measurements (Figure 3 & 6). However, previous studies indicated that high salinity could influence carbohydrate analysis by the PSA method and not affect the TPTZ method (Huang & Santschi 2001). Thus, PSA method was suggested for use in measuring carbohydrate in low salinity samples, such as river and sediment (Liu et al. 1973, Underwood et al. 1995), and TPTZ method was used in measuring carbohydrate in seawater samples (Myklestad et al. 1997).

In this experiment, carbohydrate fractions collected from three diatom species, *T. weissflogii, S. marinoi* and *C. closterium* during growth and death phases, were measured by the PSA and TPTZ methods, respectively. The amount of carbohydrate (total carbohydrate, extracellular dissolved carbohydrate and cellular carbohydrate) measured by the PSA method were always higher than those obtained by the TPTZ method. Results from the two methods were consistent in cultures of *T. weissflogii*, but not in cultures of *S. marinoi* and *C. closterium* (Figure 31 & 32). Several factors contributed to these discrepancies. Firstly, hydrolysis by sulphuric acid (used in PSA) is

much more effective than hydrochloric acid (used in TPTZ) in the analysis of some polysaccharides (Pakulski and Benner 1992, Hanisch et al. 1996). Hanisch et al. (1996) found similar results. They recovered a higher concentration of total carbohydrate and extracellular dissolved carbohydrate after hydrolysis by H_2SO_4 using the PSA method compared with hydrolysis by hydrochloric acid using the TPTZ method. In addition, the TPTZ reagent may break some chemical structures and lead to different results than the PSA method (Witter & Luther 2002). Also, strong acids decompose monosaccharide, but HCl and H_2SO_4 used in two methods may destroy different monosaccharide compositions. In our experiment, D- glucose decomposed during hydrolysis by hot hydrochloric acid during the TPTZ method. Maybe some kinds of monosaccharides are easily decomposed during the PSA method. Decomposition of different monosaccharide by two methods could result in different concentrations of the different carbohydrate fractions measured by the two methods (Panagiotopoulos and Sempéré 2005). In my experiment, the slope of regression line between TPTZ and PSA method is different in different species. This may be related to the different composition and concentrations of carbohydrates produced by diatoms, which are highly species–specific (Myklestad 1995, Panagiotopoulos and Sempéré 2005). From the results observed above, I propose that PSA method is more sensitive and suitable in determining carbohydrate fractions in phytoplankton cultures than the TPTZ method.

5.5 Conclusions

In this experiment, analysis of different carbohydrate fractions indicated carbohydrate allocation as cultures from growth to death change. TEP production is strongly associated with carbohydrate allocation. Measurements in different species did not show the same relationship between TEP formation and cell growth. My results showed that benthic diatom species, such as *Cylindrotheca closterium* released most DOM and produced TEP during growth phases, indicating benthic diatom TEP was produced by healthy cells. In contrast, coastal diatom species, *Thalassiosira weissflogii* and *Skeletonema marinoi* produced the most TEP during stationary to death growth phases, indicating the most of the TEP was produced by dying and aged cells in planktonic diatoms. The different life styles between coastal and benthic species influence their TEP production pathway. From this study, I still do not know whether permeable cells can leak more DOM from inside of the cell in the form of TEP. In this experiment, I compared PSA and TPTZ methods for analysis of carbohydrates in different cultures, because they always have been used in carbohydrate analyses of lab or field samples. From my results, PSA method showed higher hydrolysis efficiency and is the better one for analyzing high carbohydrate concentration samples, such as lab culture samples and sediment samples. Compared to PSA method, TPTZ method is the better one to determine carbohydrate concentration in monosaccharides and polysaccharides but it is only suitable in the analysis of low carbohydrate concentrations. Thus, I

suggested that using TPTZ method in low carbohydrate measurements, such as POM and DOM *in situ* samples.

CHAPTER VI

EFFECT OF OXIDATIVE STRESS ON CELL DEATH AND TEP PRODUCTION BY DIATOMS AND CYANOBACTERIUM

6.1 Introduction

Diatoms and cyanobacteria are important primary producers in the oceans and have high primary productivity. Diatom and cyanobacteria can excrete large amounts of exopolymers (EPS) (Engel 2000, Wetz and Wheeler 2007, Pereira et al. 2011), which can coagulate into transparent exopolymer particles (TEP) (Passow 2002a). Due to the stickiness of TEP, they can coagulate with cells to promote aggregates and marine snow formation (Passow 2002a, Thornton 2002, Verdugo et al. 2004). The sinking of marine snow transports biological carbon from surface ocean to its interior (Passow and Carlson 2012). Therefore, TEP formation plays an important role in carbon cycling (Passow and Alldredge 1994). It is documented that TEP is accumulated during the termination of phytoplankton blooms (Passow and Alldredge 1994, Engel 2002). However, there are few studies that relate TEP production and demise of blooms.

Recently, several studies on phytoplankton have shown that autocatalytic cell death occurs in prokaryotic and eukaryotic unicellular phytoplankton (Berges et al.2001, Berman–Frank et al. 2004, Franklin and Berges 2004), and autocatalytic cell death may induce bloom termination in the ocean (Berman-Frank et al. 2004). Autocatalytic cell death is analogous to programmed cell death (PCD). PCD is “cell suicide,” which lead to

cell lyses and a distinctive morphology (apoptosis) of the cell (Franklin and Berges 2004). A specific class of proteases, caspases, has an important role in the initiation and activation of PCD through cleavage of the caspase specific substrates. Thus, caspase is used as a cellular indicator of PCD (Berge et al.2001, Frankin and Berges 2004, Berman-Frank et al. 2007). Many studies have proposed that PCD can be triggered by environmental factors, such as nutrient limitation (Berge et al.2001, Berman –Frank et al. 2004, Bidle and Bender 2008), oxidative stress (Qian et al. 2010, Bouchard and Purdie 2011), and high light levels (Bouchard and Purdie 2011).

The process of respiration and photosynthesis by photosynthetic organisms could cause oxidative stress (Apel and Hirt 2004). Oxidative stress is a physiological status when oxidant production exceeds the antioxidant defensive mechanisms in the cells (Latifi et al. 2009). During oxidative stress, reactive oxygen species (ROS) are produced that result in damage to the cells (Apel and Hirt 2004). Hydrogen peroxide is one such ROS, and is toxic to cyanobacteria and eukaryotic microalgae (Kay 1982), causing them to express caspase and activate PCD (Bouchard and Purdie 2001).

Berman- Frank et al. (2007) found a positive coupling between PCD and TEP production in cyanobacteria grown under oxidative stress. However, the role that PCD and the resulting cell membrane leakiness play in TEP production is largely unknown. For example, there has been no work on the role of PCD in TEP production by diatoms. The aim of this study was to investigate PCD in the diatom *Thalassiosira weissflogii* and the cyanobacterium *Synechococcus elongatus* in response to oxidative stress and compare the effect of oxidative stress on TEP production in the two different species.

My hypothesis was that PCD results in enhanced cell membrane permeability and subsequently enhanced TEP production.

6.2 Experimental approach

6.2.1 Culture condition

A diatom (*Thalassiosira weissflogii)* and a cyanobacterium (*Synechococcus elongatus_cf*) were obtained from the National Center for Culture of Marine Algae and Microbiota (NCMA). Three replicate cultures (refer to 2.1.3.1) were grown in 2000 ml of 0.2 μm filtered sterile artificial sea water (refer to 2.1.2.1). Macronutrient concentrations were modified from the original recipe (Table 2, refer to 2.1.2.2), with final concentrations of 400μM of $NaNO_3$, 25 μM of $NaH_2PO_4 \bullet H_2O$, and 400μM of $Na_2SiO_3 \bullet 9H_2O$ in the cultures. Batch cultures were grown in a 20°C incubator (Precision Company) with a day/night cycle of 14 h: 10 h, and a photon flux density of 42 μmol m^{-2} s^{-1}.

When cultures were grown to the exponential phase (at least 7×10^4 cells ml^{-1} in *T. weissflogii* and 2×10^6 cells ml^{-1} in *S. elongatus*), each stock culture was transported to three replicate bottles, which were exposed to oxidative stress by the addition of hydrogen peroxide at three concentrations: control (0 μM H_2O_2 final concentration), low (10 μM H_2O_2) and high (100 μM H_2O_2). Each treatment had three replicates. Each

treatment was sampled over four days (Day 0, Day 1, Day 2 and Day 3). Day 0 sample was collected at the time of H_2O_2 addition into the cultures.

6.2.2 Measures of phytoplankton abundance and biomass

Cell counts in *T. weissflogii* cultures were performed using the method of Guillard and Sieracki (2005) (refer to 2.2.1). *T. weissflogii* cell counts were made by light microscopy at 10 × magnification. Because *Synechococcus* cells are small and form aggregates in the cultures, cells were counted by light microscopy at 100 × magnification and a pipettor was used to break up aggregates into individual cells before cell counting. Samples were flushed in and out of a 1 ml pipette tip 20 times to ensure that the aggregates were broken apart. In addition, cell turbidity in the cultures was measured (absorbance at 750 nm) to indirectly indicate changes in cell abundance. Cells collected from each treatment were observed using light microscopy at 100 × magnification. Chlorophyll *a* concentrations in the cultures was determined by fluorescence (refer to 3.3.2).

6.2.3 Photosynthetic efficiency

The photosynthetic efficiency was indicated by photochemical quantum yield of PSII fluorescence ($Ø_{PS\ II}$). In this study I did not use dark-adapted samples to determine the maximum photochemical quantum yield of PSII. Diatom and cyanobacteria samples

collected from test cultures were directly used to measure $Ø_{PS\ II}$ under ambient light conditions. Measurements of yield value were conducted at the same time (11:00 am) in each day. $Ø_{PS\ II}$ was determined by the saturation pulse method using a pulse amplitude modulated chlorophyll fluorometer (PAM-210, Heinz Walz GmbH, Germany) according to Genty et al. (1989). A strong pulse of light causes photochemical energy conversion in PS II becomes saturated, the quantum yield transiently decreases to 0. The fluorescence yield increased to a maximum value. The effective PS II quantum yield ($Ø_{PS\ II}$) can be determined following equation 1(Genty et al. 1989):

$$Ø_{PS\ II} = (F_m‟ – F_t) / F_m‟ = Δ F / F_m‟ \quad \text{(Equation 1)}$$

Fm‟ is defined as relative maximal fluorescence yield of illuminated samples induced by a saturating pulse with short wavelength red emission peak (650 nm). F_t represents the fluorescence yield excited by ambient light at a given time, which is measured before the saturation pulse. Δ F represent variation fluorescence after saturation pulse, which determined by $F_m‟ – F_t$. The $Ø_{PS\ II}$ is determined by normalizing Δ F against the $F_m‟$, which represent proportion of light absorbed by chlorophyll associated with PS II that is used in photochemistry.

During preliminary experiments, I found that $Ø_{PS\ II}$ value in same sample remained constant over a range of F_t. However, F_t above the range would cause a decline of $Ø_{PS\ II}$. It is because that sample was collected on filters and too much cell may induce self- shading. Thus, samples used to measure $Ø_{PS\ II}$ need to remain in a specific range of F_t for the same species. Firstly, cells were filtered onto 0.4 μm pore size polycarbonate filters (Whatman). After that, filters were used to measure $Ø_{PS\ II}$ immediately by PAM. A

filter blank was used to zero the instrument. The sensitivity of fluorescence detector in instrument was set at a low GAIN (GAIN 1 was selected). It was found that F_t maintained within the range 230 to 280 for *S. elongates* produced sufficient signal without evidence of self-shading. F_t was maintained within the range 340 to 380 for *T. weissflogii*. Ensuring that F_t was maintained within the optimized range for each species eliminated biomass artifacts and therefore variations in yield could be related to oxidative stress.

6.2.4 Measurements of caspase activity

Caspase activity was determined by cleavage of a caspase substrate. Measurement of caspase activity was modified from Bouchard and Purdie (2011). A 100 ml of the cultures were centrifuged at 20 °C for 20 minutes (4000*g*), and then supernatant was removed. The pellet was resuspended in 40 ml of phosphate buffered saline (PBS) (100 mM, pH = 7.0) and centrifuged cell pellet down at 20 °C (20 minutes, 4000*g*). After three cycles of resuspend- centrifuge, cells were washed well. The pellet was stored at -20 °C until the measurement of caspase-like activity within one week of sample collection. The cells were lysed in a buffer (50 mM HEPES, 1 mM EDTA, 100 mM NaCl at pH = 7.3) modified from Bouchard and Purdie (2011). When a sample was measured, the frozen pellet was defrosted at room temperature, and then resuspended in the cell lyses buffer (0.6 ml), and sonicated on ice (Qsonica, 125 Watts, 20 kHz) for 1 minute with the amplitude set at 50 % in 5 second pulses. After sonication, the sample

was immediately frozen in liquid N_2 and stored at -20 °C for 10 minutes and then thawed. For optimal lyses, the sample was frozen, thawed, and sonicated three times. The lysed sample was centrifuged at 4 °C for 30 min (10,000 *g*). The supernatant contained the protein extract. Lysed protein concentration was measured using bovine serum albumin as a standard protein (Sigma Aldrich Company). The method of protein measurement followed a 1.5 ml assay protocol shown in a technical bulletin (Sigma Aldrich Company). Bradford Reagent (1.5 ml) and sample (50 µl) were added into a cuvette. Samples were incubated in a dark place at room temperature for 30 minutes and then the absorbance of the sample was measured at 595 nm to determine protein concentration in the sample.

The capase-3 like protein activity was determined using Enzcheck Caspase-3 Assay Kit #1(Invitrogen Inc.). Cell extract (75 µl of supernatant per well) was transferred onto a black 96 well microplate (Greiner bio-one). A caspase-3 substrate (Z-DEVD-AMC, 10 mM final concentration; 75 µl per well) was added into wells containing cell extract. The sample was incubated for 48 hour in the dark, at a temperature of 25 °C. Z-DEVD-AMC does not fluoresce, but AMC, produced by caspase-3 cleavage of Z-DEVD-AMC, does fluoresce. The fluorescence of AMC was measured using a microplate reader (SPECTRAmax, GeminiEM) with excitation at 368 nm and emission at 467 nm.

6.2.5 Cell permeability

The proportion of the population with compromised cell membranes was determined using SYTOX Green staining (refer to 2.2.9).

6.2.6 TEP and CSP staining and analysis

TEP (refer to 2.2.5) and CSP (refer to 2.2.6) concentration and size were observed using light microscopy and image analysis was performed with Image J (National Institutes of Health).

6.2.7 Bacteria check

Bacteria concentrations in the cultures were determined on the last day of the experiment (refer to 2.2.2.).

6.3 Results

6.3.1 Cell concentrations

Figure 39 shows changes of cell abundance and chlorophyll *a* in cultures of *Thalassiosira weissflogii* and *Synechococcus elongatus* under different oxidative stress

levels. Cell abundance markedly increased before cultures were submitted to different treatments. After three days of incubation in H_2O_2 supplement, mean cell abundance of *T. weissflogii* in the control (0 μM H_2O_2) increased to 1.38×10^5 cells ml^{-1}, which was slightly higher than the cell abundance in cultures under oxidative stress (in 10 μM H_2O_2: 1.36×10^5 cells ml^{-1}; in 100 μM H_2O_2: 1.28×10^5). There was no significant difference in cell abundance between the control and oxidative stress cultures ($P > 0.05$). However, in cultures of *Synechococcus elongatus*, cell abundance in the cultures exposed to oxidative stress was significantly lower than the cell abundance in the control (7.03×10^6 cells ml^{-1}). The cell abundance in 10 μM H_2O_2 cultures was 5.97×10^6 cells ml^{-1} and in 100 μM H_2O_2 cultures it was only 3.02×10^6 cells ml^{-1}. There was a significant difference in cell abundance between the control and 100 μM H_2O_2 cultures on day 1 and day 3 ($P < 0.001$).

Chlorophyll *a* concentration showed similar patterns between oxidative stress and non- oxidative stress cultures (Figure 39). In the cultures of *T. weissflogii*, chlorophyll *a* concentration was not significantly different between control cultures and cultures under oxidative stress from day 0 to day 2 ($P > 0.05$). On day 3, chl. *a* in cultures with H_2O_2 additions was lower than it was in the control cultures. There was a significant difference between chl. *a* in the control and oxidative stressed cultures ($p < 0.001$) on day 3. However, in cultures of *Synechococcus elongatus*, chlorophyll *a* concentration in the 100 μM H_2O_2 culture was four times lower than in the control after four days of culturing. Greater oxidative stress cultures (100 μM H_2O_2) were significantly different ($p < 0.001$) from control cultures in all cultures every day.

Cultures under less oxidative stress (10 µM H_2O_2) started to have significant differences with control and with higher oxidative stress (10 µM H_2O_2) after day 1.

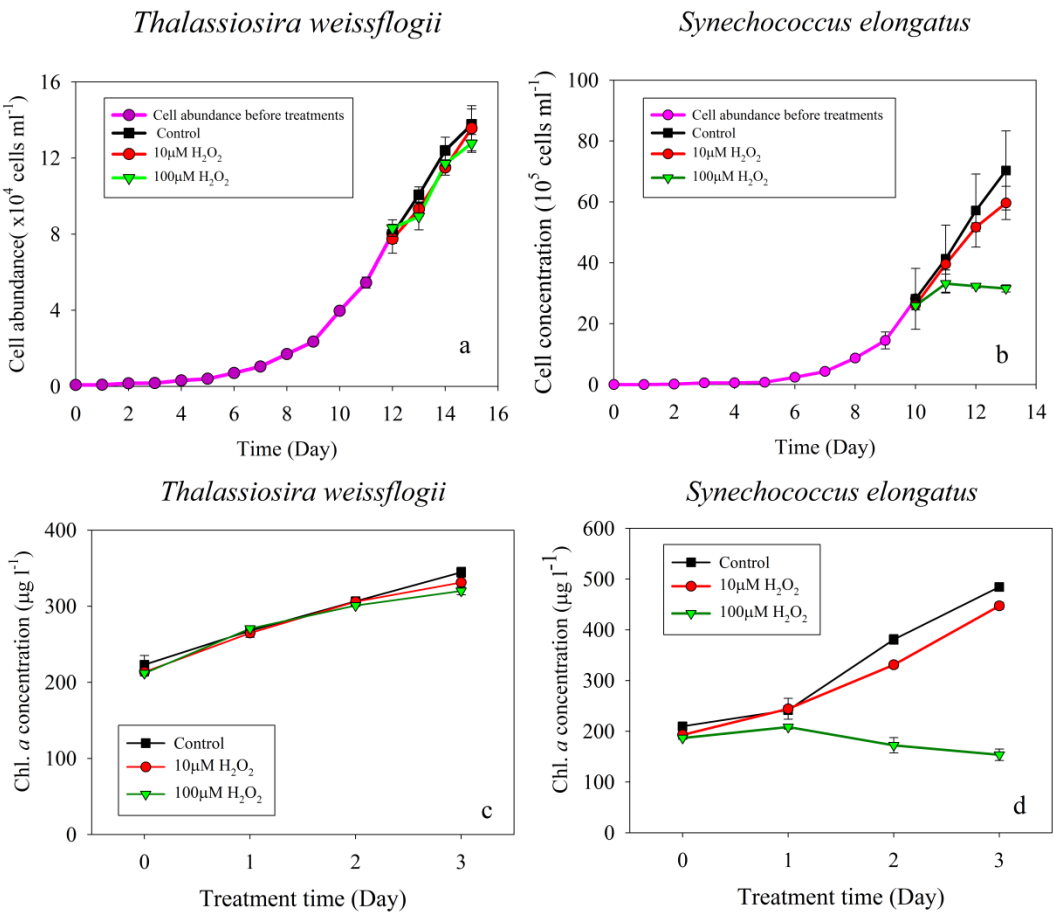

Figure 39. Variation in cell abundance (a; c) and chlorophyll *α* (b; d) with time in the cultures of *Thalassiosira weissflogii* and *Synechococcus elongatus* under control (0 µM H_2O_2), and H_2O_2 treatments (10 µM H_2O_2 and 100 µM H_2O_2). Purple circles (●) represent cell abundances before treatments. Black rectangles (■) represent control, Red circles (●) represent 10 µM H_2O_2, and green triangles (▼) represent 100 µM H_2O_2. Points show mean ± SD (n = 3).

6.3.2 Photosynthetic efficiency

Photosynthetic efficiency was expressed as the quantum yield of photosyntem II ($Ø_{PS\ II}$) in ambient light conditions. Photosynthetic efficiency of *Thalassiosira weissflogii* was higher than that of *Synechococcus elongatus* (Figure 40). In cultures of *Thalassiosira weissflogii*, the $Ø_{PS\ II}$ in the control cultures did not significantly change over time ($P > 0.05$), remaining at a value of 0.65 ± 0.02 (Mean ± SD; n = 12). The photosynthetic efficiency of cultures under oxidative stress was slightly lower than that in the control, the mean photosynthetic efficiency value in the 10 μM H_2O_2 cultures decreased from 0.63 to 0.57, and in the 100 μM H_2O_2 cultures it decreased from 0.66 to 0.53 after four days (Figure 40). In the cultures of *Synechococcus elongatus*, the $Ø_{PS\ II}$ value under oxidative stress (100 μM H_2O_2) was significantly lower than that in the controls and 10 μM H_2O_2 cultures (Figure 40). The yield value in control and low oxidative stress (10 μM H_2O_2) cultures remained between 0.45 and 0.53. However, the $Ø_{PS\ II}$ value in greater oxidative stress (100 μM H_2O_2) cultures decreased significantly from 0.50 to 0.21 after four days of treatment.

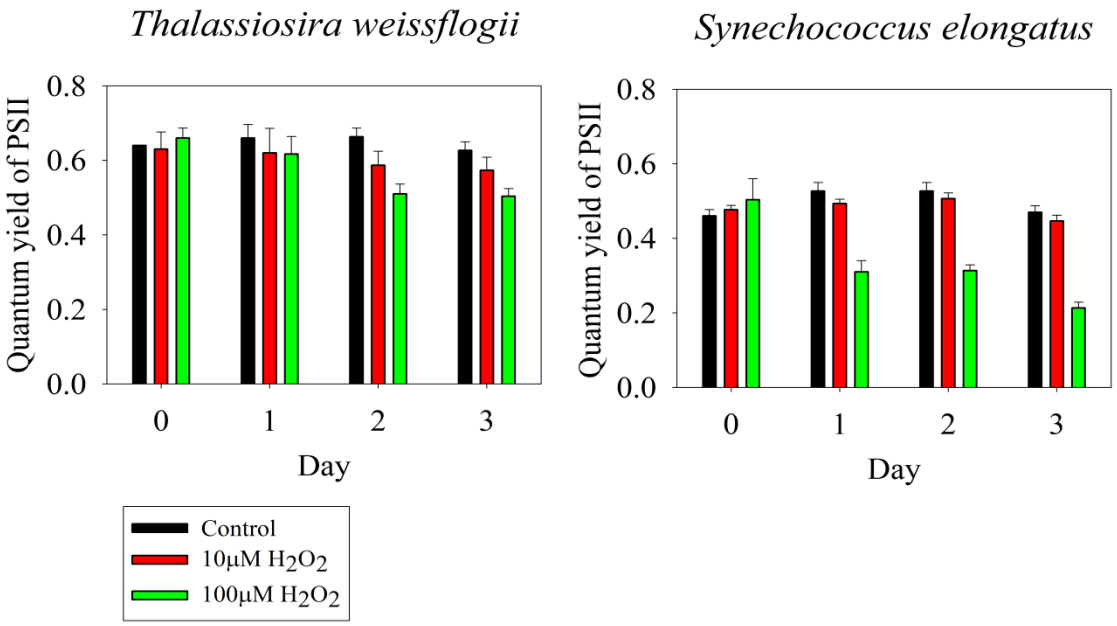

Figure 40. Variation in quantum yield of PSII fluorescence Ø $_{PS\ II}$ in cultures of *Thalassiosira weissflogii* and *Synechococcus elongatus* under oxidative stress and control conditions. Black bars represent Ø $_{PS\ II}$ in control cultures. Red bars represent Ø $_{PS\ II}$ in cultures with 10 µM H_2O_2. Green bars represent Ø $_{PS\ II}$ in cultures with 100 µM H_2O_2. Bars showed in Mean + SD, n = 3.

6.3.3 Caspase activity

Cultures under oxidative stress showed higher caspase 3-like protein activity than the control cultures (Figure 41). In the cultures of *Thalassiosira weissflogii*, caspase 3-like protein activity was low in the control and 10 µM H_2O_2 cultures, in which it remained between 97.06 RFU mg protein^{-1} h^{-1} and 115.06 RFU mg protein $^{-1}$ h^{-1} (Figure 41). However, the caspase 3- like protein activity in cultures with 100 µM H_2O_2 increased significantly to 172.70 RFU mg protein^{-1} h^{-1} after four days exposure. There was a significant difference between caspase activity in the cultures with 100 µM H_2O_2

and 10 μM H_2O_2 ($F_{1,5} = 16.365$, $p < 0.01$) and in the control cultures ($F_{1,5} = 19.891$, $p < 0.01$).

In the cultures of *Synechococcus elongatus*, the caspase 3- like protein activity in the cultures under control and oxidative stress increased with culturing time (Figure 41). The caspase activity in three different treatments was close to equal during the first two days, after which caspase activity increased in the cultures exposed to H_2O_2 relative to the controls. Caspase activity increased significantly to 1184.29 RFU * mg protein $^{-1}$ h^{-1} in the 10 μM H_2O_2 cultures and reached 1628.46 RFU * mg protein $^{-1}$ h^{-1} in the 100 μM H_2O_2 cultures. There were significant differences between caspase activity in the control cultures and cultures with 10 μM H_2O_2 ($F_{1,5} = 22.378$, $p < 0.01$), and between control cultures and cultures with 100 μM H_2O_2 ($F_{1,5} = 49.746$, $p < 0.01$).

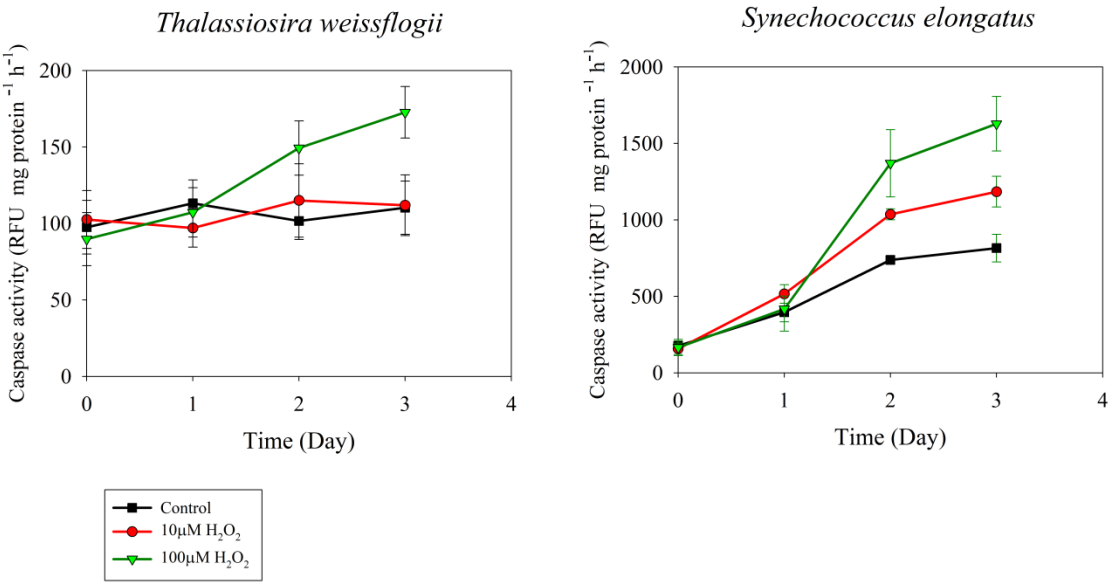

Figure 41. Variation of caspase- 3 like protein activity with culture times in the cultures of *Thalassiosira weissflogii* and *Synechococcus elongatus* under control (0µM H_2O_2), and H_2O_2 additions (10µM H_2O_2 and 100µM H_2O_2). Black rectangles (■) represent control, Red circles (●) represent 10µM H_2O_2, and green triangles (▼) represent 100µM H_2O_2. Each data point shows mean ± SD (n = 3).

6.3.4 Cell permeability

The proportion of SYTOX Green labeled cells followed the same pattern as caspase activity with culture time in the different oxidative treatments for both species. This indicates that an increase in cell permeability was associated with dying cells. In the culture of *T. weissflogii*, the proportion of SYTOX Green labeled cells was not significantly different between control cultures and 10µM H_2O_2 supplemented cultures. The proportion of SYTOX Green labeled cells in these cultures increased slightly during culture time, from 4 % to 10 % (Figure 42). The proportion of SYTOX Green labeled

cells in 100 µM H_2O_2 supplemented cultures increased markedly from day 2, and reached 39 % at the end (Figure 42). In the cultures of *Synechococcus elongatus*, there was a greater proportion of SYTOX Green labeled cells in cultures under oxidative stress than in control cultures (Figure 42). The proportion of SYTOX Green labeled cells in the cultures under oxidative stress increased dramatically to 78 % (in 100 µM H_2O_2 culture) and 47 % (in 10 µM H_2O_2 culture) over time (Figure 42). Although the proportion of SYTOX Green labeled cells in the control cultures slight increased, the increase was very low and no more than 24 % in the final.

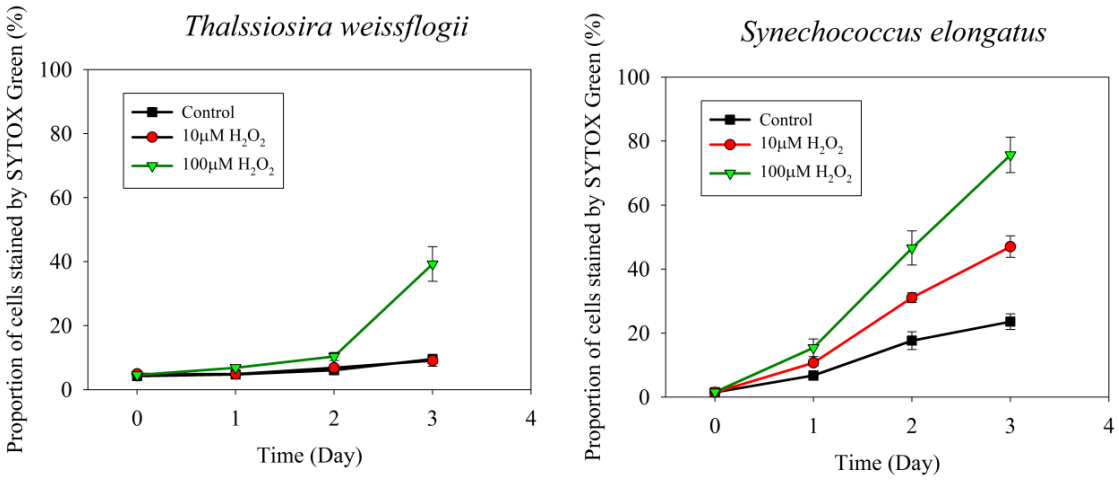

Figure 42. Proportion of SYTOX Green labeled cells in a total of 400 cells in the cultures of *Thalassiosira weissflogii* and *Synechococcus elongatus* under oxidative stress and in control over culture time. Deviation bars show Mean ± SD (n = 3). Black rectangles (■) represent control cultures. Red circles (●) represent cultures under 10 µM H_2O_2 and green triangles (▼) represent cultures under 100 µM H_2O_2.

6.3.5 TEP formation

As TEP was attached to cell surfaces and it was difficult to remove cells from the TEP image, TEP concentration was normalized to chl. *a* concentration. In cultures of both species, those grown with 100 μM H_2O_2 showed higher TEP concentration than at 10 μM H_2O_2 and in the control cultures after three days (Figure 43). In the cultures of *T. weissflogii*, TEP abundance did not show a significant difference between control cultures and cultures under oxidative stress over culture time. However, TEP were larger in the 100 μM H_2O_2 cultures than in the 10 μM H_2O_2 and in control cultures. Therefore, TEP concentration (total TEP area) was greater in the 100 μM H_2O_2 cultures than in the 10 μM H_2O_2 and control cultures (Figure 43). In cultures of *Synechococcus elongatus*, TEP abundance in the three treatment cultures remained constant in first two days, and then TEP abundance started to increase in cultures with 100 μM H_2O_2, but not in control cultures or those containing 10 μM H_2O_2. The size of TEP particles did not change with culture time. Thus, I found that total TEP concentration normalized to chl. *a* significantly increased in high oxidative stress (100 μM H_2O_2) cultures, but not in low oxidative stress cultures and in control cultures (Figure 43).

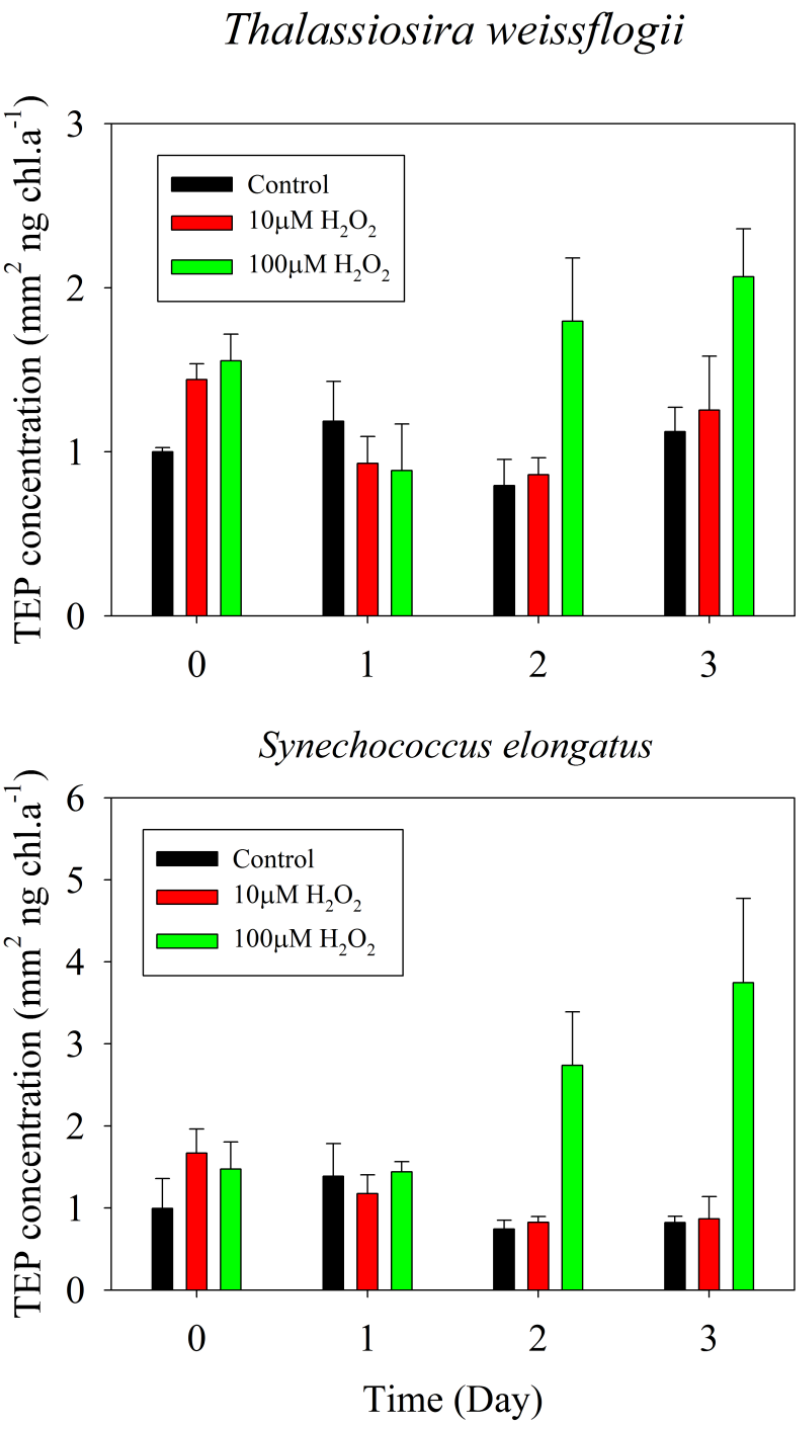

Figure 43. TEP concentration with culture time in cultures of *Thalassiosira weissflogii* and in *Synechococcus elongatus* under oxidative stress. Black bars represent control cultures. Red bars represent cultures with 10 µM H_2O_2. Green bars represent cultures with 100 µM H_2O_2. Bars show mean + SD, n = 3.

6.3.6 CSP formation

In the cultures of *T. weissflogii*, there was no pattern of CSP abundance and CSP size change over culture time in different treatments (Figure 44). The CSP concentration in the cultures of *T. weissflogii* was not significantly different between cultures under oxidative stress and in control cultures (Figure 44). In the cultures of *Synechococcus elongatus*, CSP abundance in 100 μM H_2O_2 was greater than those in other treatments on the last culture day (day 3). The size of CSP particles increased in all treatments over culture time, and there were larger sized particles in the control and 10 μM H_2O_2 than in 100 μM H_2O_2 cultures. Therefore, CSP concentration increased in all treatments during the course of experiment, and there was lower concentration of CSP in 100 μM H_2O_2 cultures than in others (Figure 44).

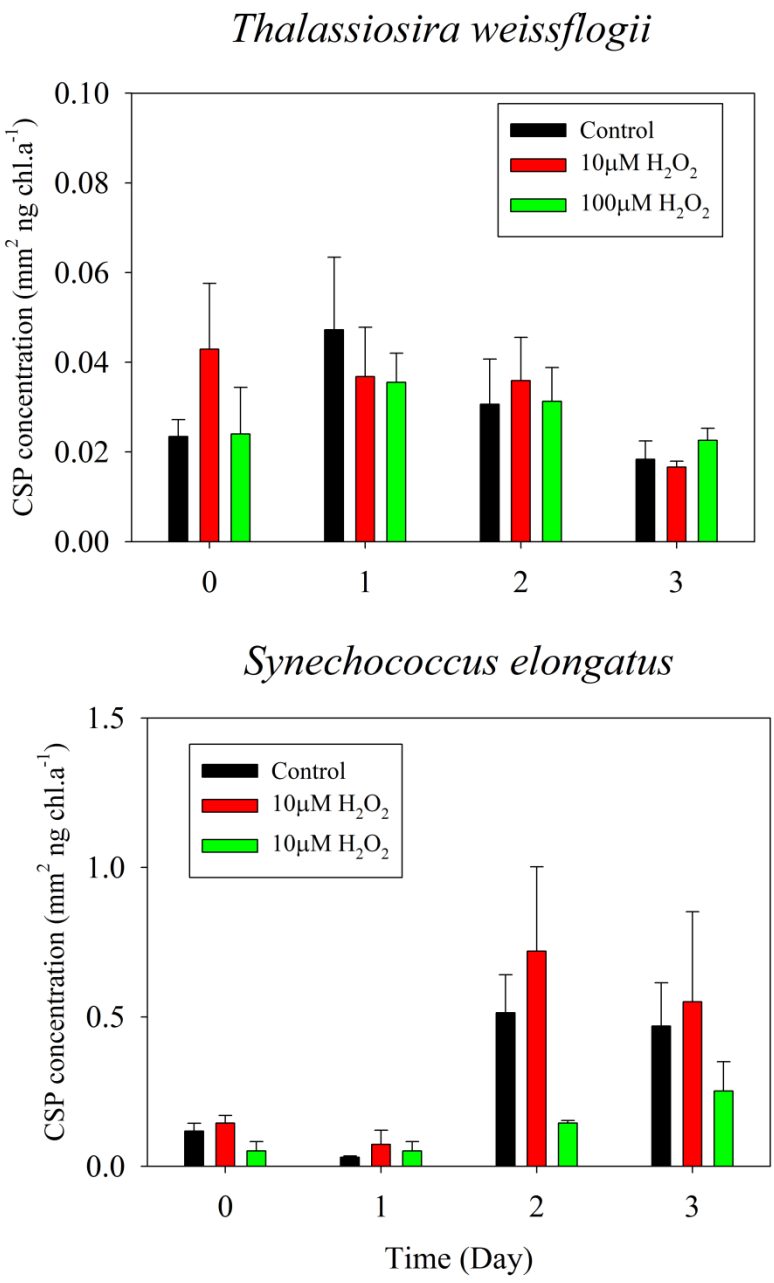

Figure 44. CSP concentration with culture time in cultures of *Thalassiosira weissflogii* and *Synechococcus elongatus* under oxidative stress. Black bars represent control cultures. Red bars represent cultures with 10 µM H_2O_2. Green bars represent cultures with 100 µM H_2O_2. Bars show mean + SD, n = 3.

6.3.7 Cell observation

Morphological changes were observed in cells exposed to H_2O_2. On day 3, *T. weissflogii* cells in the control cultures had intact membranes and chloroplasts (Figure 45 A). In the cultures grown with 10 μM H_2O_2, cells showed a stressed shape (Figure 45 B). In the cultures grown with 100 μM H_2O_2, the cells were characterized by more cell lyses and empty frustules that did not contain organelles (Figure 45 C). In the cultures of *Synechococcus elongatus*, cells in control cultures had less lyses and cells looked greener indicating that the cells contained higher amounts of chlorophyll (Figure 45 D). Cells collected from 10 μM H_2O_2 cultures contained low chlorophyll concentrations (Figure 45 E). In the cultures with 100 μM H_2O_2, most cells appeared empty. In addition, there were sticky gels that stuck the cells together (Figure 45 F).

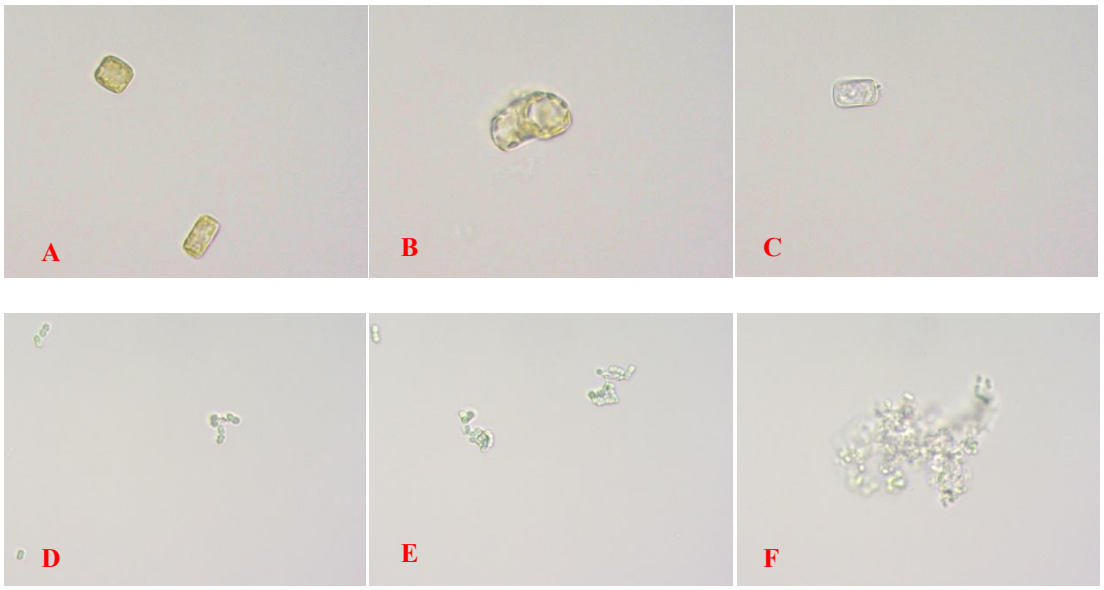

Figure 45. Morphology of *Thalassiosira weissflogii* and *Synechococcus elongatus* under oxidative stress and in control treatments after three days. A: *T. weissflogii* in the control. B: *T. weissflogii* in the 10 µM H_2O_2. C: *T. weissflogii* in 100 µM H_2O_2. D: *S. elongatus* in the control. E: *S. elongatus* in 10 µM H_2O_2 . F: *S. elongatus* in 100 µM H_2O_2.

6.3.8 The correlation between TEP production and photosynthetic efficiency and caspase activity

The correlation between TEP production, photosynthetic efficiency (quantum yield of PSII fluorescence $Ø_{PS\ II}$), and caspase activity in the diatom *Thalassiosira weissflogii* and cyanobacterium *Synechococcus elongatus* under differing oxidative stress is shown in table 8. There were significant positive correlations between TEP production and $Ø_{PS\ II}$ in the diatom *T. weissflogii* and cyanobacterium *S. elongatus* under 100 μM H_2O_2, indicating TEP production increased in cultures with greater oxidative stress. In addition, TEP production increased with increasing caspase activity in *T. weissflogii* in100 μM H_2O_2 cultures. In the cyanobacterium, there was a positive correlation between TEP production and caspase activity at both 10 and 100 μM H_2O_2. There was higher correlation between TEP production and caspase activity in the *S. elongatus* than in the *T. weissflogii*. Thus, cyanobacteria have stronger responses to reactive oxidative stress than do diatoms. In addition, there was good correlation between $Ø_{PS\ II}$ and caspase activity in *T. weissflogii* and *S. elongatus* under 100 μM H_2O_2.

Table 8. The correlation coefficient between TEP production and quantum yield of PSII fluorescence ($Ø_{PS\ II}$); TEP production and caspase activity; $Ø_{PS\ II}$ and caspase activity in cultures of *Thalassiosira weissflogii* and *Synechococcus elongatus* under control, 10 μM H_2O_2 and 100 μM H_2O_2. When $P \geq 0.05$, coefficients shown as ; * represent $0.001 < P < 0.05$; ** represent $P < 0.01$.

	Thalassiosira weissflogii			***Synechococcus elongatus***		
H_2O_2 concentration	**0μM**	**10μM**	**100μM**	**0μM**	**10μM**	**100μM**
TEP v.s. $Ø_{PS\ II}$	/	/	-0.765*	/	/	-0.603*
TEP v.s. Caspase activity	/	/	0.804*	/	0.803**	0.886**
$Ø_{PS\ II}$ v.s. Caspase activity	/	/	-0.777*	/	/	-0.762*

6.4 Discussion

6.4.1 Relationship between TEP formation and cell death

Oxidative stress is an important factor influencing phytoplankton physiology (Apel and Hirt 2004). Many studies have shown that oxidative stress causes a decrease in photosynthetic efficiency and an elevation in caspase activity (Qian et al. 2010, Bouchard and Purdie 2011). My result is consistent with their observations, lower cell abundance and photosynthetic efficiency ($Ø_{PS\ II}$) was associated with an increase in caspase activity in the *Thalassiosira weissflogii* and *Synechococcus elongatus* cultures under oxidative stress.

ROS are toxic to many species andreact with a large variety of biomolecules cause damage to cells. ROS may change regulator gene expression, such as activation of Mitogen-Activated Protein Kinase (MAPK) (Gustin et al. 1998) and inhibition of Protein Phosphatases (van Montfort et al. 2003) and onset of PCD. On the other hand, ROS are deliberately generated within cells under some circumstances to serve as signaling molecules to help regulate processes within the cell. ROS influence the expression of a number of genes and signal transduction pathways, which play a central role in plant pathogen defense (Klessig et al. 2000, Apel & Hirt 2004). Many studies indicated that modified regulator genes of stressed cells have evolved as strategies during acclimation tolerance (Pandolfil et al. 1995, Gasch et al. 2000, Chen et al. 2003). Thus, stress acclimation protects cells from the same stress at a later time.

In this study, I also found that TEP production was enhanced with greater oxidative stress (100 μM H_2O_2) in both species. Berman-Frank et al. (2007) found that caspase activity was strongly correlated with TEP production in the cyanobacterium *Trichodesium spp*. Claquin et al. (2008) showed a good correlation between TEP production and photosynthetic efficiency ($Ø_{PS\ II}$) in the diatom *T. pseduonana* at different temperatures. From microscope observations and TEP analysis, I found that cultures under oxidative stress had more permeable cell membranes and larger TEP were released around stressed cells. Under oxidative stress, high production of TEP in cultures was properly associated with leakage of TEP precursors from stressed cells and as a result of cell lysis. However, the way in which TEP produced by diatoms and cyanobacteria responded to oxidative stress was different. *T. weissflogii* produced larger

TEP particles with oxidative stress. TEP produced by *S. elongatus* did not vary in size, but more was produced under oxidative stress. My results are supported by Vardi et al. (2012), who found that more TEP was produced by the coccolithophore *E. huxleyi* as cells underwent PCD under stressed growth conditions. Similarly, Kahl et al. (2008) also found larger particles and more TEP production in the diatom *Thalassiosira pseudonana* during cell death. My results are different from observations by Berman-Frank et al (2007), who demonstrated that the increase in TEP production by the cyanobacterium *Trichodesmium* was derived from an increase in TEP size, not in TEP abundance. This difference from my results may reflect physiology differences between genera and the difference in stress factors as my cultures were under oxidative stress, but their experiment was under iron starvation. Whether increased TEP production was due to increased particle size or abundance, oxidative stress triggered PCD and caused a significant increase in TEP production by both species. Thus, I propose that the TEP production mechanism can be influenced by oxidative stress.

It is well established that TEP are sticky and can affect aggregation (Passow 1994). Therefore, the increase of TEP production with PCD may play an important role in enhancing aggregate formation and the transport of biological carbon into the ocean interior. Indeed, in lab and *in situ* studies showed higher stickiness and sedimentation rate occurred as PCD lead to diatom and cyanobacterium bloom termination (Berman-Frank 2007, Kahl et al. 2008, Vardi et al. 2012).

6.4.2 The relationship between photosynthetic efficiency and cell death

In this study, a decline in photosynthetic efficiency was correlated with elevated levels of caspase activity, indicating cells with PCD had an unhealthy physiological condition, such as photosynthetic stress. My result is supported by other observations. Franklin et al. (2012) found that photosynthesis in the diatom *Thalassiosira pseudonana* decreased during cell death. Bidle and Bender (2008) also reported a decrease in quantum yield of photosynthesis II ($Ø_{PS\ II}$) in the diatom *T. pseudonana*, from 0.6 to 0.3 after 6 days of culturing in iron starvation conditions. Bouchard and Purdie (2011) grew the cyanobacterium *Microcystis aeruginosa* in oxidative stress conditions and found that $Ø_{PS\ II}$ decreased to 0. Furthermore, an increase in caspase activity consistent with greater permeability of cells and lower cell abundance appeared in cultures under oxidative stress. Cells under stress were identified by cell lyses and weak fluorescence, suggesting caspase activity induced cell mortality. My results are supported by the findings of Jiménez et al. (2009), who found a good correlation between caspase activity and cell death. In their study, cell death was defined by the distinct morphology of cell lysis. Thus, cells under stress always have low photosynthesis efficiency and high cell permeability. However, in this study cultures with high proportions of permeable cells and high caspase activity still had a high $Ø_{PS\ II}$ value. For example, in *S. elongatus* under 100 μM H_2O_2, $Ø_{PS\ II}$ did not decline to 0, but 78 % of cells with permeable cell membrane under stress. $Ø_{PS\ II}$ was 0.2 in the stress cultures, which was not significantly lower than that in a healthy culture with a quantum yield of 0.5. The $Ø_{PS\ II}$ value in this

experiment is greater than in other studies. This may be because the effect of oxidative stress on the photosynthetic efficiency may be different between strains. Franklin et al. (2009) measured photosyntem II efficiency in stressed dying cells among different species and found that the effects of dying cells on photosynthetic efficiency were specific to species.

6.4.3 Comparison of the effect of oxidative stress on a diatom and cyanobacterium

Many studies indicate that oxidative stress can cause a physiological change from healthy to unhealthy in cyanobacteria and diatoms, and influence them to release caspase and trigger programmed cell death (PCD) (Berman-Frank et al. 2004, Qian et al. 2010, Bouchard and Purdie 2011). However there is no report comparing the effect of oxidative stress on TEP production and caspase activity and photosynthetic efficiency in a cyanobacterium and diatom under the same conditions. In this study, the cyanobacterium showed a caspase activity that was10 times higher and a value of $Ø_{PS\ II}$ that was half that in the diatom. There was a higher correlation between TEP production and $Ø_{PS\ II}$ in the cyanobacterium than that in the diatom species, indicating the cyanobacterium has a stronger response at each level of oxidative stress. Many studies on cell death in phytoplankton showed similar results. Under oxidative stress, F_v/F_m in the diatom *Phaeodactylum tricornutum* decreased from 0.6 to 0.4 (Domingues et al. 2012). In the diatom *Thalassiosira pseudonana*, it decreased from 0.7 to 0.6 (Rijstenbil 2002). Bouchard and Purdie (2011) found a lower value of $Ø_{PS\ II}$, which decreased from

0.3 to 0, in the cyanobacterium *Microcystis aeruginosa* than in the diatom. Moreover, in this study low H_2O_2 concentration (10μM) caused significant physiological variation in the cyanobacterium *S. elongatus*, but not in the diatom *T. weissflogii*, indicating the diatom is more tolerant to oxidative stress than the cyanobacterium. This can be explained by different stress effects on different cell volumes. The diatom *T. weissflogii* has a larger cell volume between 800 to 2800 μm^3 (Costello and Chisholm 1981), whereas the cell volume of the cyanobacterium *S. elongatus* was much smaller, only 15μm^3 (calculated using length and width information showed on the NCMA website). As the volume of the diatoms is larger, the amount of H_2O_2 needed for a physiological change would likely be higher in the diatom than in the cyanobacterium. In addition, surface area to volume ratio of the cells is higher in the cyanobacterium than in the diatom (Snoeijs et al. 2002), which consequently increases H_2O_2 stress for cyanobacteria relative to the diatom at similar H_2O_2 concentrations. There may also be physiological differences that explain why H_2O_2 is more toxic to cyanobacteria. Perhaps internal membranes around the organelles help protect eukaryotes or maybe eukaryotes have better developed enzyme systems etc. to deal with oxidative stress (Hunter 2008). The cells that survived under oxidative stress were properly related to the adjustment of metabolism to stress (Wu et al. 2008).

In this study, H_2O_2 was used as a regent to cause oxidative stress. It was reported that H_2O_2 is toxic to most phytoplankton (Kay 1982). In the environment, hydrogen peroxide is formed in surface water exposed to high light and also can be delivered into the ocean by rainfall (Cooper and Zika 1983).The hydrogen peroxide concentration can

reach 250 nM in the open ocean (Miller et al. 2005), and 800 nM in the coastal areas like the Gulf of Mexico (Cooper et al. 1987). In fresh water, the concentration of H_2O_2 can reach up to 10 μM (Cooper and Zika 1983). In this experiment, H_2O_2 concentrations were 10 μM and 100 μM, which is close to the concentration in the coastal ocean and 10 and 100 times the concentration in coastal ocean. My results suggested that 10 μM H_2O_2 is high enough to trigger cell death and induce more TEP formation in the cyanobacterium *S. elongatus*, whereas greater oxidative stress (100 μM H_2O_2) is needed to effect cell death and influence TEP production in the diatom *T. weissflogii*. Therefore, the effect of H_2O_2 on phytoplankton depends on species.

Under oxidative stress, oxidant lead to photosynthetic electron transport and rubisco catalysis and the generation of ROS is in chloroplasts and peroxisomes. However, the release of ROS by different organisms is chemically distinct or is generated in different cellular compartments (Neill et al. 2002). Different inorganic carbon concentration mechanisms (CCMs) exist in different genera (Raven & Larkum 2007), which may induce specific responds to same level of oxidative stress. There are many evolutionary origins of CCMs. Diatom and cyanobacteria with specific origin histories implicate different CCMs. In cyanobacteria, the CCM occurs in the cytosol, where HCO_3 is transport into the carboxysomes and conversion to CO_2 (Badger et al. 2002; Price et al. 2007, Raven et al. 2008). CCM occurs in the chloroplast stroma and contain rubisco, where active transport of CO_2 (Raven & Larkum 2007; Raven et al. 2008). Many studies indicated that algal photosynthetic biochemistry included C_3 or C_4 photosynthetic biochemistry. For example, recent tracer carbon data suggested that the

diatom *Thalassiosira weissflogii* has C_3-C_4 intermediate biochemistry (Roberts et al. 2007a & b, McGinn & Morel 2008). CCMs in different genera with different photosynthetic mechanism are associated with different functions. For C_4 or C_3-C_4 intermediate organisms, their photosynthesis is constitutive, CCMs show many acclimation mechanisms, including variations in the supply of CO_2 and nutrients (Raven et al. 2008). Cyanobacterial CCMs regulation evolved to decrease CO_2 availability and increase the O_2 concentration in cells, which leads to reactive oxygen species (Raven et al. 2008). In my experiment, the greater response to oxidative stress shown in cyanobacteria compared with the diatom was probably influenced by cyanobacterial CCMs. Greater oxygen production and higher photosynthetic quantum yield by the cyanobacterium generated more ROS compared to the diatom, and caused greater damage to the cyanobacterial cells. My results are consistent with Raven& Larkum (2007), who suggested that higher concentrations of O_2 around the photosynthetic apparatus lead to rubisco catalysis and the generation of reactive oxygen species and injury cells (Raven & Larkum 2007).

In addition, caspase activity measured in diatom cultures in this study was much lower than results reported by others. Bidle and Bender (2008) showed a caspase activity up to 2000 RFU mg protein^{-1} h^{-1} after 8 days of culturing the diatom *T. pseudonana* under iron starvation, which is three times higher than my results. RFU means „relative fluorescence units", which is arbitrary and depends on the measuring instrument. Different instruments may give different relative fluorescence units. The difference in the effect of oxidative stress on TEP production and cell death between a diatom and a

cyanobacterium has important implications in understanding the demise of blooms and vertical flux of organic matter into the ocean interior. Under the same level of oxidative stress, the cyanobacterium may induce a more intense demise of a bloom and cause a faster carbon flux into ocean depth than the diatom. Thus, the effect of oxidative stress on PCD of cyanobacteria need be given attention for their important role in carbon flux in the ocean. When diatoms were exposed to oxidative stress, their caspase activity was used as a cellular indicator of PCD. Whether or not the cells really possessed a PCD pathway, it must be determined by the gene coding for caspase. Bidle and Bender (2008) published the specific gene sequence coding for caspase in the diatom *T. pseudonana*. In the future, we can define the PCD by investigating the presence of the metacaspase gene to prove whether or not cells activate PCD. In addition, we could use a fluorescent probe, eg. caspaseACE, to bind to cells to indicate variation in PCD (Franklin et al. 2012).

6.5 Conclusions

In this study, I compared the effect of oxidative stress on TEP production and cell death in the diatom *T. weissflogii* and in the cyanobacterium *S. elongatus*. My results indicated that the cyanobacterium was more sensitive to oxidative stress than the diatom. However, the results from diatom and cyanobacteria cultures all indicated that oxidative stress enhance TEP production, which was associated with increases in cell permeability. Oxidative stress triggered high caspase activity, a decline in photosynthetic efficiency, and induced cell mortality. In addition, TEP production was enhanced under

oxidative stress indicating that oxidative stress influenced the mechanism of TEP formation. This would consequently influence aggregate formation and carbon cycling in the ocean.

CHAPTER VII

SUMMARY AND CONCLUSIONS PRODUCTION BY DIATOMS AND CYANOBACTERIUM

In conclusion, my study investigated different factors (temperature, nutrient availability, oxidative stress, and growth) affecting the release of EPS by diatoms, and their role in aggregation. The formation of TEP is strongly associated with EPS production and affects the formation of aggregates and marine snow, which consequently influence the biological carbon pump and global carbon cycle. This research contributed to our understanding of the dynamics of TEP production by diatoms and improved our understanding of the fate of primary production and carbon cycling in the ocean.

7.1 Result summary

In lab experiments to investigate the effect of temperature on TEP production, results from semi-continuous cultures of *Thalassiosira weissflogii* and *Skeletonema marinoi* were not consistent. Increased temperature caused a decrease of cell abundance in *S. marinoi*, but not in *T. weissflogii* (Figure 7). *S. marinoi* grows better in cooler water and the range of thermal tolerance for *T. weissflogii* was wider than *S. marinoi*. This observation is consistent with the distribution of these two species in the ocean. My hypothesis for this experiment was that more EPS and TEP would be produced and more

aggregates would form in cultures at higher temperatures. My results indicated that diatoms produced more EPS and TEP at higher temperatures, supporting my hypothesis. Compared with TEP, CSP did not correlate with temperature. That may be because TEP and CSP have different formation mechanisms as they are composed, respectively, of acidic polysaccharides and protein. More aggregates occurred in *S. marinoi* cultures at higher temperatures, indicating cells become stickier at warmer temperatures. On the contrary, fewer aggregates formed in the cultures of *T. weissflogii* at higher temperatures. This was associated with high TEP production and indicates that TEP are not very important in aggregate formation, and perhaps it has more to do with the stickiness of the cells. In addition, temperature may affect TEP composition and consequently influence their chemical or physical properties. Aggregation is a source of marine snow. Therefore, the response of aggregation to temperature may lead to different levels of vertical flux of carbon in the ocean. My results suggested that temperature increase did not affect different species in the same way. Thus, we cannot make a generalization about diatoms and temperature increase. We cannot say that all diatoms will be more likely to form aggregation as temperature increases.

In the experiment for determining the effects of growth rate on TEP production and aggregate formation by *T. weissflogii* under nitrogen limitation, my experiment revealed that growth rate affected both TEP formation and aggregation when cultures were grown under nitrogen-limited conditions. The hypotheses for this experiment was that cultures with low growth rates would be the most nutrient limited and therefore produce more TEP and more aggregations than fast growing cultures, and that cells with

low growth rate would have higher permeability than cells in high growth rate cultures. My results suggested that *T. weissflogii* cells were more permeable at low dilution rates, supporting this hypothesis. We know that DOM is a precursor of TEP and therefore higher permeability of cells and higher cell abundances in slow growing cultures would probably lead to more DOM leakage from lysed cells into outside. This would lead to greater TEP production. However, total TEP concentration in slow growing cultures did not increase and there was a greater rate of TEP production in fast growing cultures, suggesting that most TEP production was associated with fast growing cells (healthy cells), rather than stressed cells and cell lyses. In addition, measurement of particle size distribution (PSD) and volume concentration of particles illustrated greater aggregate formation in cultures grown at higher growth rates. Increased stickiness of cells or an increase in the stickiness of the TEP all could lead to an increase of aggregation in the fast growing cultures. However, it is challenging to define the major factor in influencing aggregate formation and the relationship between TEP and aggregation in my study.

In a lab experiment investigating the effect of growth and death on TEP production in three different diatom species, I found a significant difference between two coastal species (*Thalassiosira weissflogii*; *Skeletonema marinoi*) and a benthic species (*Cylindrotheca closterium)*. In this experiment, I hypothesized that there would be more EPS production in dying cultures, and allocation of carbon into different carbohydrate pools would change during different growth phases. In addition, cell permeability was hypothesized to increase during stationary and death phase. My results indicated that

TEP production was strongly associated with how the cells allocated carbon into carbohydrate. TEP produced by *T. weissflogii* and *S. marinoi* may be produced using intracellular carbohydrate. In coastal species (*T. weissflogii* and *S. marinoi*), the dissolved extracellular carbohydrate and EPS production increased in cultures during stationary and death phases. The most TEP was produced by these two species during stationary to declining growth phase, which was associated with greater a proportion of permeable cells in these two species. In contrast, the benthic species *Cylindrotheca closterium* produced most dissolved extracellular carbohydrate and TEP during exponential growth phases, when the cultures contained many healthy cells. Thus, I conclude that TEP production in benthic diatom species is associated with healthy cells, and planktonic diatoms produced the most TEP when the cultures contained relatively old and dying cells.

In addition, I predicted that there might be two TEP formation pathways. One is associated with leakage of DOC and TEP precursors from lyses and dying cells. The other is a biotic way of forming TEP by exudation from healthy, rapidly growing cells. Although, I cannot prove this hypothesis in this experiment, observations by other researchers, such as Fukao et al. (2010), support this idea. Why should TEP be formed during different growth phases by different species? It can be explained by differences in life history and TEP functions between coastal and benthic species. *T. weissflogii* and *S. marinoi* are planktonic species. TEP helps planktonic diatoms float in the oceans. *C. closterium* is a benthic species, which adheres to and moves through seafloor. TEP is a sticky particle which assists benthic diatoms in attaching to the seafloor.

In the experiments to investigate the effect of oxidative stress on TEP production and relationship with cell death I compared oxidative stress effects on TEP production and cell death in the diatom *Thalassiosira weissflogii* and in the cyanobacterium *Synechococcus elongatus*. My results indicated that the cyanobacterium was more sensitive to oxidative stress than the diatom. Oxidative stress triggered high caspase activity and a decline in photosynthetic efficiency and increased cell mortality. In addition, TEP production was enhanced with increased caspase activity under oxidative stress, indicating that oxidative stress influenced mechanisms of TEP formation. This would consequently influence aggregate formation and the carbon cycle in the ocean.

7.2 Conclusions and future work

7.2.1 Active exudation and passive leakage of DOM

DOM can be released from diatom cells by active exudation and passive leakage. Some DOM particles are TEP precursors, their release from diatoms may contribute to TEP production. Our experiments indicated that diatoms produced more extracellular dissolved carbohydrate as EPS under stressful growth conditions, such as high temperature, oxidative stress and nitrogen limitation. In addition, these stresses increased the proportion of cells in the cultures that had permeable cell membranes, as indicated by SYTOX Green staining. Permeable cells are predicted to more easily release intracellular DOM and nucleic acids to the outside environment than intact cells. The

passive leakage of DOM from permeable cells may contribute to the outside DOM pool, which could be used in the form of TEP and support for grazers (Bhaskar and Bhosle 2005, Thornton 2013). The good correlation between TEP production and cell permeability in cultures under stress conditions suggests that the mechanism of passive leakage may contribute to TEP precursors. However, my work did not determine whether cell lyses can release more TEP precursors than cell leakage. However, other work has shown that TEP precursors could be contributed actively by cell exudation or passively by cell lyses (Bhaskar and Bhosle 2005). Thus, I propose that there might be two mechanisms of TEP formation (Figure 46). One way is the formation of TEP from passive leakage of DOC and TEP precursors by permeable cells, such as the formation of TEP by the diatoms *T. weissflogii* and *S. marinoi* and the cyanobacterium *Synechococcus elongatus* during the death phase. The second mechanism is formation by active exudation of DOC by healthy cells, such as the production of a lot of TEP by *C. closterium* during exponential growth phase. DOM release by passive and active process may consist of different compositions of small or large molecular compounds (Myklestad 2000). The different compositions of TEP precursors could cause diversity in chemical and / or physical properties. However, I still do not know the relative production levels of TEP from the two pathways or what factors will trigger which TEP production pathway.

Hence, it would be interesting to investigate the mechanisms of DOM release from cells and to clarify TEP formation related to carbon allocation. I propose using isotopes as tracers to indicate the processes of DOM release and define which

carbohydrate fractions were transformed into TEP. In addition, I could study TEP composition by staining TEP with different fluorescent probes, such as lectins, to show the presence of a particular saccharide.

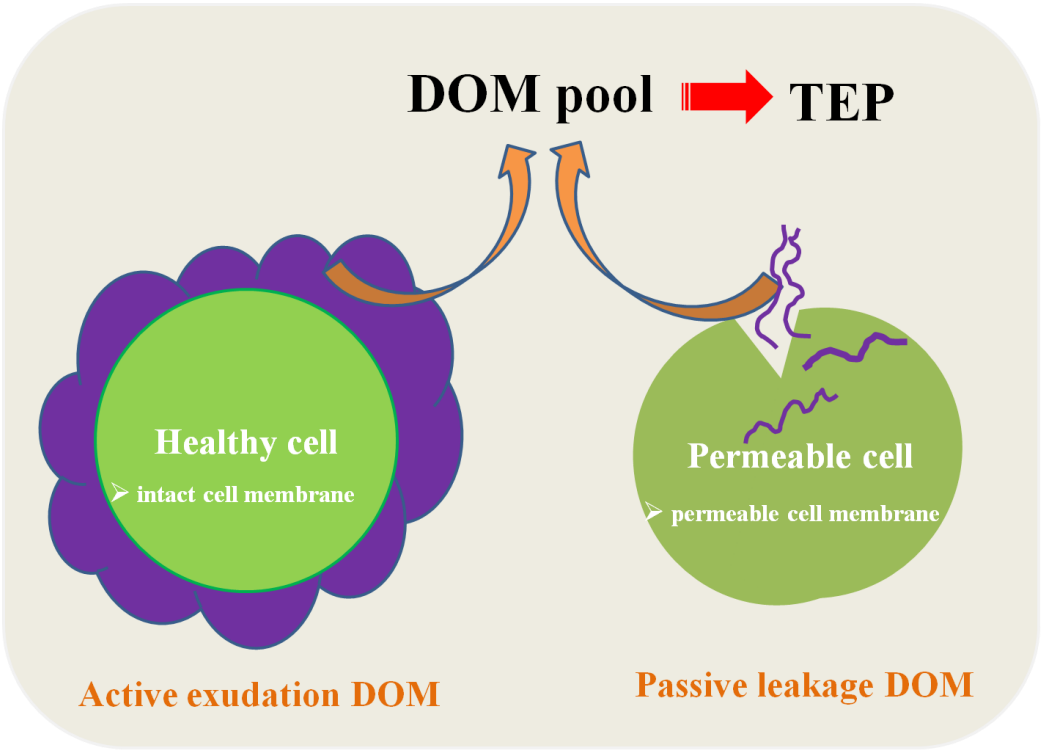

Figure 46. A hypothesis for two TEP formation pathways. One pathway is the formation of TEP from passive leakage of DOC and TEP precursors from permeable cells. The second pathway is the formation of TEP by active exudation of DOC by healthy cells. The purple area represents DOM, which can be actively exuded by healthy cell or passively released from permeable cell into the outside DOM pool. DOM contributes to TEP formation.

7.2.2 Factors influencing aggregation

According to coagulation theory, aggregation is dependent on stickiness. TEP are very sticky particles, so they promote formation of aggregates and marine snow. Aggregation is determined by a combination of TEP production and stickiness of the particles. Results from the growth rate and temperature experiments suggest that temperature and growth rate influence both of these factors. Many studies demonstrated that stickiness of particles could vary with different factors, such as temperature and growth phase (Kiørboe and Hansen 1993, Thornton and Thake 1998). Kiørboe et al. (1998) pointed out that the stickiness of particles varied during a bloom of *Chaetoceros spp*. in the Benguela upwelling. In addition, variation in stickiness among species also influences aggregate formation. Sticky cells, such as *Skeletonema costatum*, would tend to aggregate during blooms and result in the fast sinking of organic carbon. Many observations of aggregation of *S. costatum* in the coastal ocean and sequential sedimentation have been documented (Crocker 1993).

On the contrary, if the cells have low stickiness, such as *T. weissflogii*, they will remain in surface waters for a long time during the bloom. The sinking of diatom aggregates and marine snow plays a critical role in the rapid transfer of primary production from the euphotic zone to deeper water.

The increase of stickiness in fast growth cultures and at warm temperatures may relate to the chemical structure of the cell surface or changes in TEP composition. In the future, it would be interesting to study the chemical composition of the cell surface and

TEP and investigate whether any change in them is related to stickiness. For example, I could use FITC labeled lectins as a tool to label different carbohydrates on cell surfaces of the diatoms (Böckelmann et al. 2002, Elloway et al. 2004, Wigglesworth-Cooksey and Cooksey 2005).

7.2.3 TEP and CSP analysis method

TEP and CSP are transparent gel particles which mean that they cannot be seen by light microscopy. Based on their major composition, scientists developed techniques for the visualization of TEP and CSP. Alldredge et al. (1993) found that TEP are formed from acid polysaccharides, which can be stained using Alcian Blue (Alldredge et al. 1993). Long and Azam (1996) found that CSP are proteinaceous, these protein particles can be stained by Coomassie Brilliant Blue. Up to now, three methods have been used to measure TEP and CSP concentrations.

The first method is determining the concentration of TEP colorimetrically (Passow and Alldrege 1995). The second method requires the measurement of individual TEP and CSP particles during observation by light microscopy (Logan et al. 1994). TEP and CSP concentration and area were analyzed from light micrographs using Axio Vision 4.8 software (Carl Zeiss MicroImaging, details in 2.2.5 and 2.2.6). The third method is quantification of TEP and CSP concentration and area from light micrographs using semi-automated procedures in Image J software (National Institutes of Health, details in 2.2.5 and 2.2.6) (Engel 2009). Table 9 summarizes advantages and

disadvantages of these three methods. Results from my experiment suggest that TEP abundance and individual TEP particles did not change consistently. For example, TEP numbers decreased with increasing growth rate in cultures of *Thalassiosira weissflogii*, whereas the size of TEP particles was larger at higher growth rates. Thus, the total area of TEP (TEP number × TEP size) remained constant at different growth rates. In this case, counting TEP abundance or measuring TEP particle size alone does not provide sufficient information to determine changes in the amount of TEP in the cultures. Thus, the total area of TEP may be a better proxy to reveal TEP concentration.

When I analyzed TEP or CSP using the Image J method, I removed cells in the image using the „pencil" or „brush" tools in the Image J to paint these cells out to match the background color. This ensured that cells were not counted as exopolymer particles during subsequent processing of the images. However, in situations where cells are imbedded in TEP or CSP it can be difficult to accurately and consistently define what is exopolymer particles and what is cell on the images. This is compounded by the fact that TEP and CSP are naturally three dimensional structures that are enumerated by processing two-dimensional images of exopolymer particles collected on filters. Furthermore, in very sticky species, such as the cyanobacterium *Synechococcus sp.*, TEP and CSP were coating the cells" surface and many cells were stuck together to form a mixture of TEP (or CSP) and cells. It is difficult to remove cells from TEP using „pencil" or to extract TEP out through splitting the image into different color channels because the color of TEP and CSP are similar to the color of the cells. Therefore, we need improve TEP and CSP analysis methods in the future. For example, a better threshold

method may help in extraction of TEP or CSP and give more accurate results. In addition, automated programs could be developed to analyze TEP and CSP automatically by computer, which would save labor time and increase efficiency during work on exopolymer particles. Furthermore, the method of collection TEP and CSP needs improve. For example, if we need measure some samples which are stickiness, such as cyanobacteria, or benthic diatoms, we needs pipette many times (at least 20 times) to break up TEP or CSP and cells aggregates into individual cells and particles in a micro contribute tube. After that, filtered unaggregated samples (cells were not attached on sticky particles before extraction of TEP of CSP.

Table 9. Summary of TEP measurement methods.

TEP Methods	Description	Suitable	Advantage	Disadvantage
Colorimetrical	Dye binding assay	All species	Fast and simple	Not truly quantitative, standard is different from TEP.
Light microscopy	Manually draw around particles and count number	All species	quantitative straightforward	Labor intensive, time consuming.
Image J	Remove cells and automatically measure size and abundance	Big cells (eg. diatom, dianoflagellate)	Accuracy	Time consuming

7.2.4 Bacterial interaction with diatoms

The interaction between bacteria and diatoms is summarized in Figure 47. Bacteria can produce TEP and TEP precursors and affect TEP formation. They also decompose TEP and DOM and utilize them as a carbon source (Mari and Kioboe 1996; Passow 2002b; Engel 2004). Many studies indicate that the interaction between bacteria and diatoms determines the stickiness and aggregation of diatom cultures (Gärdes et al. 2011, 2012). Thus, the presence of bacteria in experimental cultures and their interactions with diatoms cannot be ignored. In my results, carbon associated with bacteria was < 5 % of the total microbial carbon in the cultures, suggesting that bacteria did not have a significant effect on biomass in the cultures. Gärdes et al. (2011) showed that the bacterium *Marinobacter adhaerens* causes aggregation in cultures of *Thalassiosira weissflogii* in nutrient replete cultures. But in nutrient limited conditions, Gärdes et al. (2011) found that *M. adhaerens* did not enhance TEP production. My growth rate and temperature experiments were conducted under nitrogen limitation and I do not know which bacteria existed in my cultures. It may be that the presence of bacteria did not have a significant effect on TEP formation and aggregation in diatom cultures, or their effect was relatively small compared to diatom influences.

However, it is not clear how bacteria affected TEP production and aggregate formation in my cultures. Therefore, we need to investigate the mechanisms by which bacteria affect aggregation and TEP formation in different types of bacteria and microalgae.

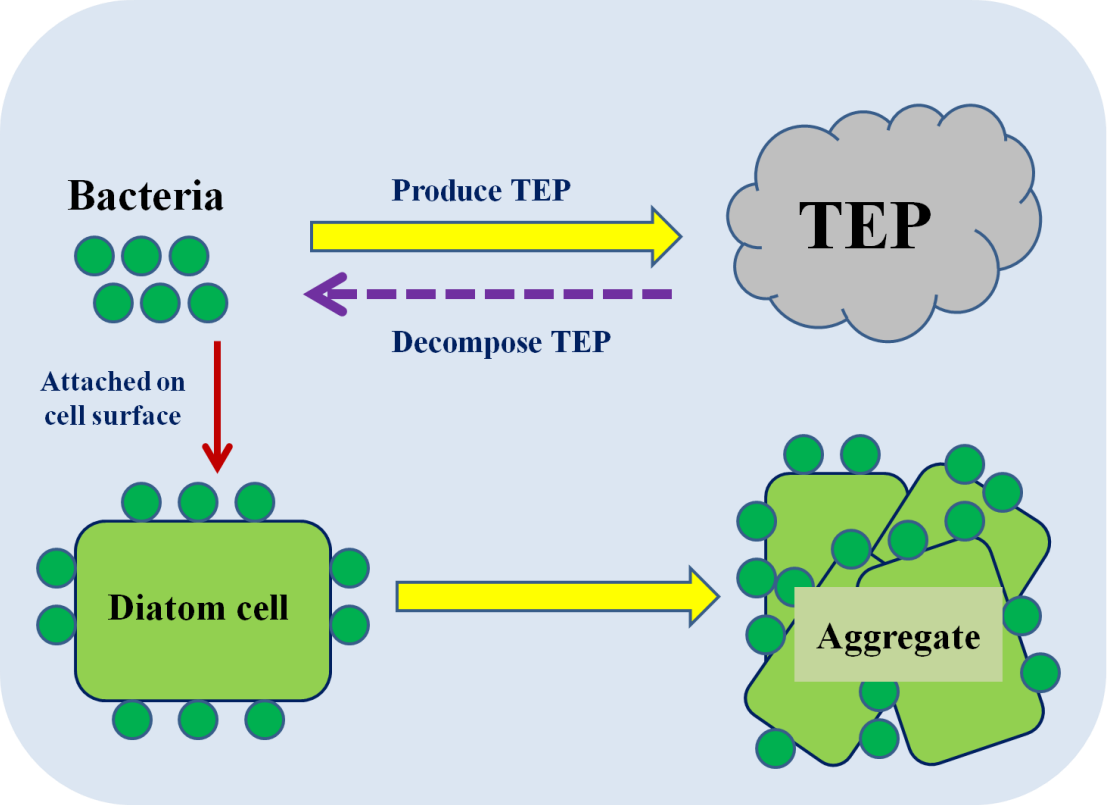

Figure 47. Interaction between bacteria and diatom cells. Bacteria can produce TEP and they also decompose TEP. Bacteria attached to diatom surfaces may enhance aggregate formation.

7.2.5 Comparison of PSA and TPTZ method

In my experiments, carbohydrate fractions measured by the PSA and TPTZ methods for phytoplankton were compared to each other. The amount of carbohydrate measured by the PSA method was always higher than those obtained by the TPTZ method. Two probable reasons for these differences are different compositions and concentrations of polysaccharides exuded by the diatoms and a difference in hydrolysis

efficiency of these two methods. In the future, we need to more thoroughly investigate differences between these two methods and improve both methods in order to apply them to natural sample measurement and to enable direct comparisons between data collected using these two common methods for bulk carbohydrate analysis.

7.2.6 Summary of microbial pathway in marine ecosystem

My work contributed to understanding of the microbial pathway in the ocean which is shown in the figure 48. In the euphotic zone, phytoplankton carry out primary production through photosynthesis (Thornton 2012). A large fraction of organic matter that is synthesized by primary producers becomes DOM and POM. Larger amount of fixed organic carbon are transported by carbon cycling in the ocean. Diatoms are important primary producers which have an important role in the oceanic carbon cycle. They exude large amounts of EPS from healthy cells, or use programmed cell death (PCD) or other cell death pathways to release DOM from the lysis of cells, which contribute to the DOM pool in the ocean. EPS can coagulate into transparent exopolymer particles (TEP), which belong to the POC size range. Therefore, TEP formation transforms DOC into POC. TEP are sticky gel-like particles which promote aggregate formation and sinking of marine snow (Passow 2002b; Thornton 2002; Verdugo et al. 2004). Therefore, TEP formation causes a fast vertical carbon flux from the euphotic zone to the deep ocean and increases the efficiency of the biological carbon pump.

In the ocean, sinking of marine snow decreased with depth (Passow and Carlson 2012). Fixed organic matter is remineralized to dissolve inorganic matter and nutrients and return back to surface oceans. The total time for return back to the sea surface is longer for remineralization at greater depths (Passow and Carlson 2012). If the aggregate sinks into the deep ocean or is buried in the seafloor, it needs thousands or even millions of years to remineralize and return CO_2 back to the surface of the ocean (Thornton 2012). Therefore, strengthening of the biological pump by diatom production of TEP has a critical influence in changing global carbon cycling time and carbon storage in the ocean.

In addition, bacteria have important interactions with phytoplankton and affect biogeochemistry in the ocean (Gärdes et al. 2011, 2012). Aggregates and POM can be hydrolyzed by bacteria to form DOM. DOM in the ocean (from exudation, cell lyses, and hydrolysis of POM) can be utilized by bacteria for their growth. In contrast, the interaction between bacteria and microalgae also helps in the formation of aggregates. Bacteria participate in the microbial loop to remineralize organic matter into inorganic matter (C, N, P, Fe, Si) and return carbon dioxide to the ocean surface by respiration. Therefore, diverse microorganism activities participate in biochemical pathways and interactions between them modify the marine ecosystem and the carbon cycle.

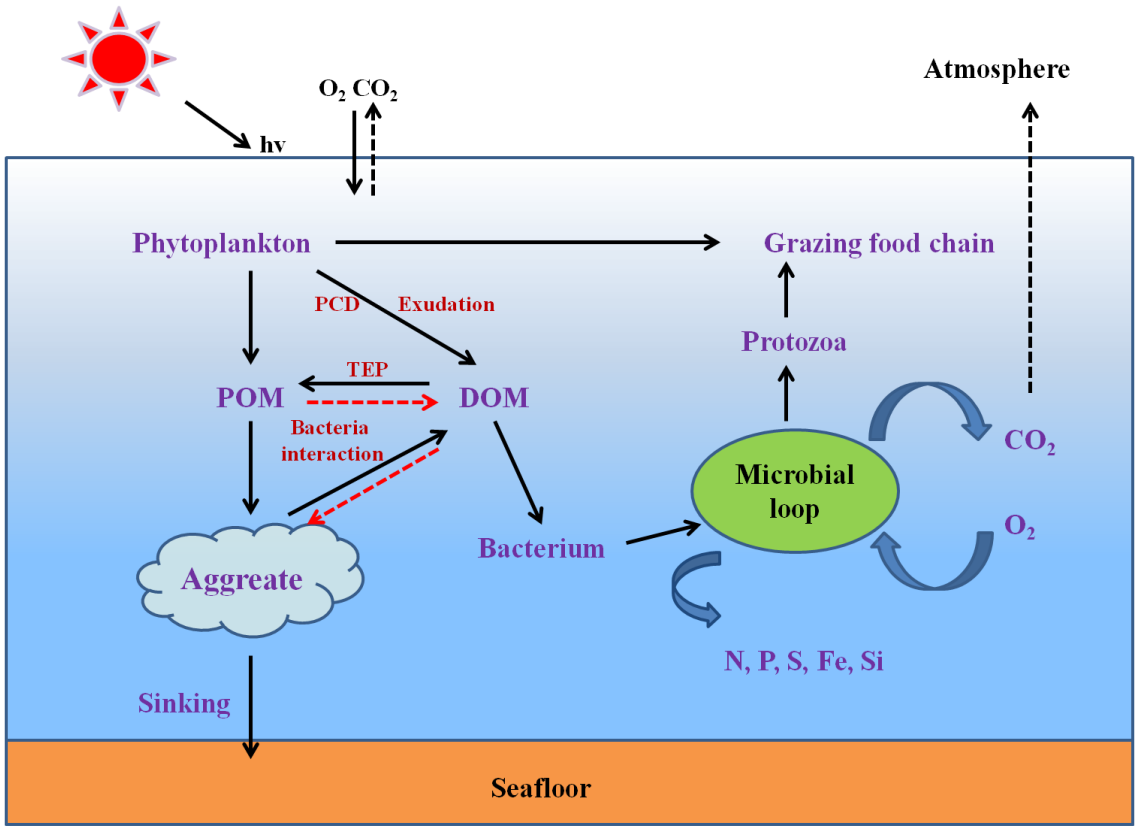

Figure 48. Microbial pathways in the marine ecosystem. Modified from Azam and Malfatti 2007. Primary producers carry out primary production via photosynthesis and transport by the grazing food chain. Large fractions of fixed organic matter become POM and DOM and are transported to the ocean interior by the biological carbon pump. Diatoms contribute large amounts of DOM through exudation of EPS and lysis of DOM from PCD or other cell death. Coagulation of EPS into TEP transports carbon from DOM to POM. TEP glues POM to form aggregates, which enhance biological carbon pump efficiency. If remineralized at a deeper depth, a longer time is required to remineralize DOM to DIC and return CO_2 back to the surface. Therefore, TEP increasing the sinking of aggregates may influence carbon cycling time. Bacteria have interactions with phytoplankton, including producing TEP and influencing aggregate formation. POM also can be hydrolyzed to DOM by bacteria and used in their growth. In addition, bacteria participate in the microbial loop and remineralize inorganic matter and return CO_2 back to the surface of the ocean.

REFERENCES

Abdullahi, A. S., Underwood, G. J. C. & Gretz, M. R. 2006. Extracellular matrix assembly in diatoms (*Bacillariophyceae*). V. environmental effects on polysaccharide synthesis in the model diatom, *Phaeodactylum Tricornutum*. *Journal of Phycology* 42(2):363-378.

Agrawal, Y. C. & Pottsmith, H. C. 2000. Instruments for particle size and settling velocity observations in sediment transport. *Marine Geology* 168: 89-114.

Alldredge, A. L. & Gotschalk, C. 1988. In situ settling behavior of marine snow. *Limnology and Oceanography* 33:339-351.

Alldredge, A. L. & Silver, M. W. 1988. Characteristics, dynamics and significance of marine snow. *Progress Oceanography* 20:41-82.

Alldredge, A. L., Passow, U. & Logan, B. E. 1993. The abundance and significance of a class of large, transparent organic particles in the ocean. *Deep-Sea Research Part I-Oceanographic Research Papers* 40:1131-1140.

Aluwihare, L. I. & Repeta, D. J. 1999. A comparison of the chemical characteristics of oceanic DOM and extracellular DOM produced by marine algae. *Marine Ecology Progress Series* 186:105-117.

Anderson, T. R. & Williams, P. J. L. 1998. Modeling the seasonal cycle of dissolved organic carbon at station E-1 in the English Channel. *Estuarine Coastal and Shelf Science* 46: 93-109.

Apel, K. & Hirt, H. 2004. Reactive oxygen species: metabolism oxidative stress, and signal transduction. *Annual Review Plant Biology* 55:373-399.

Arar, E. J. & Collins, G. B. 1997. Method 445.0. In vitro determination of chlorophyll *a* and pheophytin. *Marine and Freshwater Algae by Fluorescence*, pp 1-20. Environmental Protection Agency, Cincinnati, Ohio.

Armbrust, E.V. & Chisholm, S.W. 1992. Patterns of cell-size change in a marine centric diatom- variability evolving from clonal isolates. *Journal of Phycology* 28(2):146-156.

Armbrust, E. V. & Galindo, H. M. 2001. Rapid evolution of a sexual reproduction gene in centric diatoms of the genus *Thalassiosira*. *Applied Environmental Microbiology* 67:3501-3513.

Aspinall, G. O. 1970. Pectins, plant gums, and other plant polysaccharides. *The Carbohydrates*; *Chemistry and Biochemistry*, edited by Pigman, W. & Horton, D., pp 515-536. Academic Press, New York.

Aspinall, G. O. 1983. CRC handbook of chromatography-carbohydrates. *Journal of the American Chemical Society* 105(1):5963-5964.

Azam, F. & Long, R. A. 2001. Sea snow microcosms. *Nature* 414:495-497.

Badger, M. R, Hanson, M. & Price, G. D. 2002. Evolution and diversity of CO_2 concentrating mechanisms in cyanobacteria. *Functional Plant Biology* 29:161-173.

Barofsky, A., Simonelli, P., Vidoudez, C., Troedsson, C., Nejstgaard, J. C., Jakobsen, H. H. & Pohnert, G. 2010. Growth phase of the diatom *Skeletonema marinoi* influences the metabolic profile of the cells and the selective feeding of the copepod *Calanus* spp. *Journal of Plankton Research* 32:263-272.

Bellinger, B. J., Abdullahi, A. S., Gretz, M. R. & Underwood, G. J. C. 2005. Biofilm polymers: relationship between carbohydrate biopolymers from estuarine mudflats and unialgal cultures of benthic diatoms. *Aquatic Microbial Ecology* 38:169-180.

Benner, R., Pakulsi, J. D., Mccarthy, M., Hedges, F. & Hatcher, P. 1992. Bulk chemical characteristics of dissolved organic matter in the ocean. *Science* 255:1561-1564.

Berges, J. A., Franklin, D. J. & Harrison, P. J. 2001. Evolution of an artificial seawater medium: improvements in enriched seawater, artificial water over the last two decades. *Journal of Phycology* 37:1138-1145.

Berman-Frank, I., Rosenberg, G., Levitan, O., Haramaty, L. & Mari, X. 2007. Coupling between autocatalytic cell death and transparent exopolymeric particle production in the marine cyanobacterium *Trichodesmium*. *Environmental Microbiology* 9:1415-1422.

Bhaskar, P. V. & Bhosle, N. B. 2005. Microbial extracellular polymeric substances in marine biogeochemical processes. *Current Science* 88:45-53.

Bidle, K. D. & Falkowski, P. G. 2004. Cell death in planktonic, photosynthetic microorganisms. *Nature Reviews Microbiology* 2(8):643-655.

Bidle, K. D. & Bender, S. J. 2008. Iron starvation and culture age activate metacaspases and programmed cell death in the marine diatom *Thalassiosira pseudonana*. *Eukaryot Cell* 7(2):223-236.

Billett, D. S. M., Lampitt, R. S., Rice, A. L. & Mantoura, R. F. C. 1983. Seasonal sedimentation of phytoplankton to the deep-sea benthos. *Nature* 302:520-522.

Böckelmann, U., Manz, W., Neu, T. R. & Szewzyk, U. 2002. Investigation of lotic microbial aggregates by a combined technique of fluorescent in situ hybridization and lectin-binding-analysis. *Journal of Microbiological Methods* 49(1):75-87.

Borch, N. H. & Kirchman, D. L. 1997. Concentration and composition of dissolved combined neutral sugars (polysaccharides) in seawater determined by HPLC- PAD. *Marine Chemistry* 57:85-95.

Borchard, C. & Engel, A. 2012. Organic matter exudation by *Emiliania huxleyi* under simulated future ocean conditions. *Biogeosciences* 9:3405-3423.

Bouchard, J. N. & Purdie, D. A. 2011. Effect of elevated temperature, darkness, and hydrogen peroxide treatment on oxidative stress and cell death in the bloom-forming toxic cyanobacterium *mirocystis aeruginosa*. *Journal of Phycology* 47:1316-1325.

Burney, C. M. & Sieburth, J. M. 1977. Dissolved carbohydrates in seawater. II. A spectrophotometric procedure for total carbohydrate analysis and polysaccharide estimation. *Marine Chemistry* 5:15-28.

Canfield, D. E., Thamdrup, B. & Kristensen, E. 2005. Structure and growth of microbial populations. *Aquatic Geomicrobiology*, edited by Southward, A. J., Tyler, P. A., Young, C. M. & Fuiman, L. A., pp 29-64. Elsevier Academic Press, San Diego, California.

Chen, D., Toone, W. M., Mata, J., Lyne, R. & Burns, G. 2003. Global transcriptional responses of fission yeast to environmental stress. *Molecular Biology of the Cell* 14:214-229.

Chin, W. C., Orellana, M. W. & Verdugo, P. 1998. Spontaneous assembly of marine dissolved organic matter into polymer gels. *Nature* 391:568-571.

Christina, L., Rocha, D. L. & Passow, U. 2007. Factors influencing the sinking of POC and the efficiency of the biological carbon pump. *Deep-Sea Research II* 54:639-658.

Claquin, P., Probert, I., Lefebvre, S. & Veron, B. 2008. Effects of temperature on photosynthetic parameters and TEP production in eight species of marine microalgae. *Aquatic Microbial Ecology* 51:1-11.

Collins, S. & Bell, G. 2004. Phenotypic consequences of 1,000 generations of selection at elevated CO_2 in a green alga. *Nature* 431(7008):566-569.

Conway, H. L., Harrison, P. J. & Davis, C. O. 1977. Marine diatoms grown in chemostats under silicate or ammonium limitation. IV. Transient response of *Chaetoceros debilis*, *Skeletonema costatum*, and *Thalassiosira gravida* to a single addition of the limiting nutrient. *Marine Biology* 43:33-43.

Cooper, W. J. & Zika, R. G. 1983. Photochemical formation of hydrogen peroxide in surface and ground waters exposed to sunlight. *Science* 220:711-712.

Cooper, W. J., Saltzman, E. S., Zika, R. G. & William, J. 1987. The contribution of rainwater to variability in surface ocean hydrogen peroxide. *Journal of Geophysical Research* 92:2970-2980.

Costello, J. C. & Chisholm, S. W. 1981. The influence of cell size on the growth rate of *Thalassiosira weissflogii. Journal of Plankton Research* 3:415-419.

Crocker, K. M. 1993. Diatom aggregation and dimethylsulfide production in phytoplankton blooms. Ph.D. dissertation. University of California, Santa Barbara, California.

Crocker, K. M. & Passow, U. 1995. Differential aggregation of diatoms. *Marine Ecology Progress Series* 117:249-257.

Dam, H.G. & Drapeau, D. T. 1995. Coagulation efficiency, organic matter glues and the dynamics of particles during a phytoplankton bloom in a mesocosm study. *Deep Sea Research II* 42:111-123.

Decho, A. W. 1990. Microbial exopolymer secretions in ocean environments, their role(s) in food webs and marine processes. *Oceanography and Marine Biology* 28:73-153.

Ding, Y. X., Chin, C. H., Peter, H. S., Pedro, V. & Wei, C. C. 2009. Spontaneous assembly of exopolymers from phytoplankton. *Terrestrial*, *Atmospheric & Oceanic Sciences* 20(5):741-747.

Domingues, N., Matos, A. R., Marques da Silva, J. & Cartaxana, P. 2012. Response of the diatom *Phaeodactylum tricornutum* to photooxidative stress resulting from high light exposure. *PLoS ONE* 7(6):e38162. doi:10.1371/journal.pone.0038162.

Droop, M. R. 1970. Vitamin B_{12} and marine ecology, continuous culture as an approach to nutritional kinetics. *Helgolander Wissenschaftliche Meeresunters* 20:629-636.

Droop, M. R. 1983. 25 years of algal growth kinetics. A personal view. *Botanic Marina* 26:99-112.

Dubois, M., Gilles, K. A., Hamilton, J. K., Rebers, P. A. & Smith, F. 1956. Colorimetric method for determination of sugars and related substances. *Analytical Chemistry* 28:350-356.

Elloway, E. A. G., Armstrong, R. A., Bird, R. A., Kelly, S. L. & Smith, S. N. 2004. Analysis of *acanthamoeba polyphaga* surface carbohydrate exposure by FITC-lectin binding and fluorescence evaluation. *Journal of Application of Microbiology* 97(6):1319-1325.

Engel, A. 2000. The role of transparent exopolymer particles (TEP) in the increase in apparent particles stickiness (α) during the decline of a diatom bloom. *Journal of Plankton Research* 22:485-497.

Engel, A. & Passow, U. 2001. Carbon and nitrogen content of transparent exopolymer particles (TEP) in relation to their alcian blue adsorption. *Marine Ecology Progress Series* 219:1-10.

Engel, A., Goldthwait, S., Passow, U. & Alldredge, A. 2002.Temporal decoupling of carbon and nitrogen dynamics in a mesocosm diatom bloom. *Limnology of Oceanography* 47:753-761.

Engel, A. 2004. Distribution of transparent exopolymer particles (TEP) in the northeast Atlantic Ocean and their potential significance for aggregation processes. *Deep-Sea Research Part I* 51:83-92.

Engel, A. 2009. Determination of marine gel particles. *Practical Guidelines for the Analysis of Seawater*, edited by Oliver, W., pp 57-71. CRC Press, Taylor & Francis Group, Boca Raton, Florida.

Engel, A., Händel, N., Wohlers, J., Lunau, M., Petergrossart, H., Sommer, U. & Riebesell, U. 2011. Effects of sea surface warming on the production and composition of dissolved organic matter during phytoplankton blooms, results from a mesocosm study. *Journal of Plankton Research* 33:357-372.

Falkowski, P. G. 1997. Evolution of the nitrogen cycle and its influence on the biological sequestration of CO_2 in the ocean. *Nature* 387(6630): 272-275.

Falkowski, P. G., Barber, R. T. & Smetacek, V. 1998. Biogeochemical controls and feedbacks on ocean primary production. *Science* 281:200-206.

Falkowski, P., Scholes, R. J., Boyle, E., Canadell, J., Canfield, D., Elser, J., Gruber, N., Hibbard, K., Hogberg, P., Linder, S., Mackenzie, F. T., Moore, B., Pedersen, T., Rosenthal, Y., Seitzinger, S., Smetacek, V. & Steffen, W. 2000. The global carbon cycle: a test of our knowledge of earth as a system. *Science* 290(5490):291-296.

Falkowski, P. G. & Oliver, M. J. 2007. Mix and match: how climate selects phytoplankton. *Nature Reviews Microbiology* 5(10):813-819.

Falkowski, P. G. & Raven, J. A. 2007. *Aquatic Photosynthesis* (second edition), pp 200-484. Princeton University Press, Princeton, New Jersey.

Field, C. B., Behrenfeld, M. J., Randerson, J. T. & Falkowski, P. 1998. Primary production of the biosphere: integrating terrestrial and oceanic components. *Science* 281:237-240.

Fogg, G. E. 1983. The ecological significance of extracellular products of phytoplankton photosynthesis. *Botanica Marina* 26:3-14.

Fogg, G. E. & Thake, B. 1987. Algal culture and phytoplankton ecology. *Algal Culture Techniques*, edited by Andersen, R. A., pp 59-129. Elsevier Academic Press, San Diego, California.

Franklin, D. J. & Berges, J. A. 2004. Mortality in cultures of dino-flagellate *Amphidinium carterae* during senescence and darkness. *Proceeding of Royal Society B* 271:2099-2107.

Franklin, D. J., Brussaard, C.P.D. & Berges, J. A. 2006. What is the role and nature of programmed cell death in phytoplankton ecology? *European Journal of Phycology* 41:1-14.

Franklin, D. J., Choi, C. J., Hughes, C., Malin, G. & Berges, J. A. 2009. Effect of dead phytoplankton cells on the apparent efficiency of photosystem II. *Marine Ecological Progress Series* 382:35-40.

Franklin, D. J., Airs, R. L., Fernandes, M., Bell, T. G., Bongaerts, R. J., Berges, J. A. & Malin, G. 2012. Identification of senescence and death in *Emiliania huxleyi* and *Thalassiosira pseudonana*: cell staining, chlorophyll alterations, and dimethylsulfoniopropionate (DMSP) metabolism. *Limnology and Oceanography* 57:305-317.

Fukao, T., Kimoto, K., Yamatogi, T., Yamamoto, K., Yoshida, Y. & Kotani, Y. 2009. Marine mucilage in Ariake Sound, Japan, is composed of transparent exopolymer particles produced by the diatom *Coscinodiscus granii*. *Fish Science* 75:1007-1014.

Fukao, T., Kimoto, K. & Kotani, Y. 2010. Production of transparent exopolymer particles by four diatom species. *Fish Science* 76:755-760.

Fukao, T., Kimoto, K. & Kotani, Y. 2012. Effect of temperature on cell growth and production of transparent exopolymer particles by the diatom *Coscinodiscus granii* isolated from marine mucilage. *Journal of Applied Phycology* 24:181-186.

Fukuda, R., Ogawa, H., Nagata, T. & Koike, I. 1998. Direct determination of carbon and nitrogen contents of natural bacterial assemblages in marine environments. *Application of Environmental Microbiology* 64(9):3352-3358.

Gärdes, A., Kaeppel, E., Shehzad, A., Seebah, S., Teeling, H., Yarza, P., Glöckner, F. O., Grossart, H. P. & Ullrich, M. S. 2010. Complete genome sequence of *Marinobacter adhaerens* type strain (HP15), a diatom-interacting marine microorganism. *Standards in Genomic Sciences* 3:97-107.

Gärdes, A., Iversen, M. H., Grossart, H. P., Passow, U. & Ullrich, M. S. 2011. Diatom associated bacteria are required for aggregation of *Thalassiosira weissflogii*. *The International Society for Microbial Ecology Journal* 5:436-445.

Gärdes, A., Ramaye, Y., Grossart, H. P., Passow, U. & Ullrich, M. S. 2012. Effects of *Marinobacter adhaerens* HP15 on polymer exudation by *Thalassiosira weissflogii* at different N: P ratios. *Marine Ecological Progress Series* 461:1-14.

Gasch, A., Spellman, P., Kao, C., Harel, O. & Eisen, M. 2000. Genomic expression programs in the response of yeast cells to environmental changes. *Molecular Biology of the Cell* 11:4241-4257.

Geider, R.J. & La Roche, J. 2002. Redfield revisited: variability of C: N: P in marine microalgae and its biochemical basis. *European Journal of Phycology* 37:1-17.

Genty, B., Briantas, J. M. & Baker, N. R. 1989. The relationship between the quantum yield of photosynthetic electron transport and quenching of chlorophyll fluorescence. *Biochimica et Biophysica Acta* 990:87-92.

Giordano, M., Norici, A., Forssen, M., Eriksson, M. & Raven, J. A. 2003. An anaplerotic role for mitochondrial carbonic anhydrase in *Chlamydomonas reinhardtii*. *Plant Physiology* 132:2126-2134.

Giordano, M., Beardall, J. & Raven, J. A. 2005. CO_2 concentrating mechanisms in algae: mechanisms, environmental modulation, and evolution. *Annual Review Plant Biology* 56:99-131.

Goldman, J. C., Mccarthy, J. J. & Peavey, D. G. 1979. Growth-rate influence on the chemical composition of phytoplankton in oceanic water. *Nature* 279(5710):210-215.

Grossart, H. P. & Simon, M. 1993. Limnetic macroscopic organic aggregates (lake snow), occurrence, characteristics, and microbial dynamics in Lake Constance. *Limnology and Oceanography* 38:532-546.

Grossart, H. P., Simon, M. & Logan, B. E. 1997. Formation of macroscopic organic aggregates (lake snow) in a large lake, the significance of transparent exopolymer particles (TEP), phyto- and zooplankton. *Limnology Oceanography* 42:1651-1659.

Grossart, H. P., & Simon, M. 1998. Bacterial colonization and microbial decomposition of limnetic organic aggregates (lake snow). *Aquatic Microbial Ecology* 15:127-140.

Guillard, R. R. L. & Hargraves, P. E. 1993. *Stichocrysis immobilis* is a diatom not a chrysophyte. *Phycologia* 32:234-236.

Guillard, R. R. L. & Sieracki, M. S. 2005. Chapter 16. Counting cells in cultures with the light microscope. *Algal Culturing Techniques*, edited by Andersen R. A., pp 251-289. Academic Press, Boston, Massachusetts.

Gustin, M. C., Albertyn, J., Alexander, M. & Davenport, K. 1998. MAP kinase pathways in the yeast *Saccharomycescerevisiae*. *Microbiological Molecular Biology Reviews* 62:1264-1300.

Hanisch, K., Scweitzer, B. & Simon, M. 1996. Use of dissolved carbohydrates by planktonic bacteria in a mesotrophic lake. *Microbial Ecology* 31:41-55.

Hoagland, K. D., Rosowski, J. R., Gretz, M. R. & Roemer, S. C. 1993. Diatom extracellular polymeric substances, function, fine-structure, chemistry, and physiology. *Journal of Phycology* 29:537-566.

Hobbie, J. E., Daley, R. & Jasper, S. 1977. Use of uuclepore filters for counting bacteria by fluorescence microscopy. *Applied and Environmental Microbiology* 33(5):948-951.

Honjo, S.1982. Seasonality and interaction of biogenic and lithogenic particulate flux at the Panama Basin. *Science* 218:883-884.

Huang, C. C. & Santschi, P. H. 2001. Spectrophotometric determination of total uronic acids in seawater using cation exchange separation and pre-concentration lyophilization. *Analytical Chimica Acta* 427:111-117.

Hunter, P. 2008. Not so simple after all. A renaissance of research into prokaryotic evolution and cell structure. *EMBO Report* 9 (3):224-226.

IPCC 2013. Climate change: the physical science basis. Summary for policy makers. contribution of working group I to the fourth assessment report of the intergovernmental panel for climate change. *IPCC Secretariat*. Geneva 21.

Jackson, G. A. 1990. A model of the formation of marine algal flocs by physical coagulation processes. *Deep-Sea Research Oceanography Part A* 37(8):1197-1211.

Jackson, G. A. 1995. Coagulation of marine algae. *Advances in Chemistry Series* 244:203-217.

Jackson, G. A. & Burd, A. B. 1998. Aggregation in the marine environment. *Environmental Science and Technology* 32:2805-2814.

James, T. W. 1961. Continuous culture of microorganisms. *Annual Review of Microbiology* 15:27-46.

Jiménez, C., Capasso, J. M., Edelstein, C. L., Rivard, C. J., Lucia, S., Breusegem, S., Berl, T. & Segovia, M. 2009. Different ways to die: cell death modes of the unicellular chlorophyte *Dunaliella viridis* exposed to various environmental stresses

are mediated by the caspase-like activity DEVDase. *Journal of Experimental Botany* 60:815-828.

Kaeriyama, H., Katsuki. E., Otsubo, M., Yamada, M., Ichimi, K., Tada, K. & Harrison, J. P. 2011. Effects of temperature and irradiance on growth of strains belonging to seven *Skeletonema* species isolated from Dokai Bay, southern Japan. *European Journal of Phycology* 46(2):113-124.

Kahl, L. A., Vardi, A. & Schofield, O. 2008. Effects of phytoplankton physiology on export flux. *Marine Ecological Progress Series* 354:1-16.

Kay, S. H., Quimby, P. C. & Ouzts, J. D. 1982. H_2O_2: a potential algicide for aquaculture. *In Proceedings of the 35th Annual Meeting of the Southern Weed Science Society*, pp 275-289. Atlanta, Georgia.

Kent, M. L., Whyte, J. N. C. & Latrace, C. 1995. Gill lesions and mortality in seawater pen-reared Atlantic salmon *Salmo salar* associated with a dense bloom of *Skeletonema costatum* and *Thalassiosira* species. *Diseases of Aquatic Organisms* 22:77-81.

Kepkay, P. 2000. Colloids and the ocean carbon cycle. *The Handbook of Environmental Chemistry*, edited by Wangersky P., pp 536-560. Springer Verlag, Berlin, Germany.

Khandeparker, R. D. S. & Bhosle, N. B. 2001. Extracellular polymeric substances of the marine fouling diatom *amphora rostrata*, biofouling. *Journal of Bioadhesion and Biofilm Research* 17(2):117-127.

Kiørboe, T. & Hansen, J. L. S. 1993. Phytoplankton aggregate formation, observations of patterns and mechanisms of cell sticking and the significance of exopolymeric material. *Journal of Plankton Research* 15:993-1018.

Kiørboe, T., Tiselius, P., Mitchell-Innes, B., Hansen, J. L. S., Visser, A. W. & Mari, X. 1998. Intensive aggregate formation with low vertical flux during an upwelling-induced diatom bloom. *Limnology Oceanography* 43(1):104-116.

Kirby, R. R., Beaugrand, G., Lindley, J. A., Richardson, A. J., Edwards, M. & Reid, P. 2007. Climate effects and benthic-pelagic coupling in the North Sea. *Marine Ecology Progress Series* 330:31-38.

Klessig, D. F., Durner, J., Noad, R. & Navarre, D. A. 2000. Nitric oxide and salicylic acid signaling in plant defense. *PNAS* 97:8849-8855.

Kranck, K. & Milligan, T. G. 1988. Macroflocks from diatoms in situ photography of particles in Bedford Basin, Nova Scotia. *Marine Ecology Progress Series* 44:183-189.

Lancelot, C. & Mathot, S. 1985. Biochemical fractionation of primary production in Belgian coastal waters during short and long term incubations with ^{14}C bicarbonate: mixed diatom population. *Marine Biology* 86:219-226.

Lassen, M. K., Nielsen, K. D., Richardson, K., Garde, K. & Schluter, L. 2010. The effects of temperature increases on a temperate phytoplankton community-A

mesocosm climate change scenario. *Journal of Experimental Marine Biology and Ecology* 383(1):79-88.

Latifi, A., Ruiz, M. & Zhang, C. 2009. Oxidative stress in cyanobacteria. *FEMS Microbiology Reviews* 33:258-278.

Leonardos, N. & Geider, R. J. 2004. Responses of elemental and biochemical composition of *Chaetoceros muelleri* to growth under varying light and nitrate: phosphate supply ratios and their influence on critical N: P. *Limnology Oceanography* 49(6):2105-2114.

Lewandowska, A. & Sommer, U. 2010. Climate change and the spring bloom: a mesocosm study on the influence of light and temperature on phytoplankton and mesozooplankton. *Marine Ecology Progress Series* 405:101-111.

Liu, D., Wong, P. T. S. & Dutka, B. J. 1973. Determination of carbohydrates in the lake sediment by a modified phenol sulfuric acid method. *Water Research* 7:741-746.

Logan, B. E., Grossart, H. P. & Simon, M. 1994. Direct observation of phytoplankton, TEP and aggregates on polycarbonate filters using brightfield microscopy. *Journal of Plankton Research* 16:1811-1815.

Logan, B. E., Passow, U., Alldredge, A. L., Grossart, H. P. & Simon, M. 1995. Rapid formation and sedimentation of large aggregates is predictable from coagulation rates (half-lives) of transparent exopolymer particles (TEP). *Deep-Sea Research II* 42:203-214.

Long, R. A. & Azam, F. 1996. Abundant protein-containing particles in the sea. *Aquatic Microbial Ecology* 1:213-221.

Malej, A. & Harris, R. P. 1993. Inhibition of copepod grazing by diatom exudates: a factor in the development of mucus aggregates? *Marine Ecology Progress Series* 96:33-42.

Mari, X. & Adrian, B. 1998. Seasonal size spectra of transparent exopolymeric particles (TEP) in a coastal sea and comparison with those predicted using coagulation theory. *Marine Ecology Progress Series* 163:63-76.

Mari, X. 1999. Carbon content and C: N ratio of transparent exopolymeric particles (TEP) produced by bubbling exudates of diatoms. *Marine Ecology Progress Series* 183:59-71.

Martens, D. E., de Gooijer, C. D., van der Velden-de Groot, C. A. M., Beuvery, E. C. & Trampe, J. 1993. Effect of dilution rate on growth, productivity, cell cycle and size, and shear sensitivity of a hybridoma cell in a continuous culture. *Biotechnology and Bioengineering* 41:429-439.

Mccracken, I. R. 1989. Purifying algal cultures. A review of chemical methods. *Proceedings of the Nova Scotian Institute of Science* 38:146-168.

McGinn, P. J. & Morel, F. M. M. 2008. Expression and inhibition of the carboxylating and decarboxylating enzymes in the photosynthetic C_4 pathway of marine diatoms. *Plant Physiology* 146:300-309.

Menden-Deuer, S. & Lessard, E. J. 2000. Carbon to volume relationships for dinoflagellates, diatoms, and other protist plankton. *Limnology and Oceanography* 45(3):569-579.

Miller, W. M., Blanch, H. W. & Wilke, C. R. 1988. A kinetic analysis of hybridoma growth and metabolism in batch and continuous suspension culture: effect of nutrient concentration, dilution rate, and pH. *Biotechnology and Bioengineering* 32(8):947-965.

Miller, G. W., Morgan, C. A., Kieber, D. J., King, D. W., Snow, J. A., Heikes, B. G., Mopper, K. & Kiddle, J. J. 2005. Hydrogen peroxide method intercomparison study in seawater. *Marine Chemistry* 97:4-13.

Møller, E.F. 2007. Production of dissolved organic carbon by sloppy feeding in the copepods *Acartia tonsa*, *Centropages typicus*, and *Temora longicornis*. *Limnology and Oceanography* 52:79-84.

Mopper, K. 1977. Sugars and uronic acids in sediment and water from the Black Sea and North Sea with emphasis on analytical techniques. *Marine Chemistry* 5:585-603.

Myklestad, S. & Haug, A. 1972. Production of carbohydrates by the marine diatom *Chaetoceros affinis Var. willei (Gran) Hustedt*. I. Effect of the concentration of nutrients in the culture medium. *Journal of Experimental Marine Biology and Ecology* 9:125-136.

Myklestad, S. 1974. Production of carbohydrates by marine planktonic diatoms. I. Comparison of nine different species in culture. *Journal of Experimental Marine Biology and Ecology* 15:261-274.

Myklestad, S. M. 1995. Release of extracellular products by phytoplankton with special emphasis on polysaccharides. *The Science of the Total Environment* 165:155-164.

Myklestad, S. M. 2000. Dissolved organic carbon from phytoplankton. *The Handbook of Environmental Chemistry*, edited by Wangersky, P., pp 111-148. Springer Verlag, Berlin, Germany.

Myklestad, S. V., Skanoy, E. & Hestmann, S. 1997. A sensitive method for analysis of dissolved mono- and polysaccharides in seawater. *Marine Chemistry* 56:279-286.

Neill, N., Desikan, R. & Hancock, J. 2002. Hydrogen peroxide signaling. *Current Opinion in Plant Biology* 5:388-395.

Ogawa, H., Amagai, Y., Koike, I., Kaiser, K. & Benner, R. 2001. Production of refractory dissolved organic matter by bacteria. *Science* 292:917-920.

Paerl, H. W. & Huisman, J. 2008. Blooms like it hot. *Science* 320:57-58.

Pakulski, J. & Benner, R. 1992. An improved method for the hydrolysis and MBTH analysis of dissolved and particulate carbohydrates in seawater. *Marine Chemistry* 40:143-160.

Panagiotopoulos, C. & Sempéré, R. 2005. The molecular distribution of combined aldoses in sinking particles in various oceanic conditions. *Marine Chemistry* 95:31-49.

Pandolfil, P. P., Sonati, F., Rivi, R., Mason, P., Grosveld, F. & Luzzatto, L. 1995. Targeted disruption of the housekeeping gene encoding glucose 6-phosphate dehydrogenase (G6PD): G6PD is dispensable for pentose synthesis but essential for defense against oxidative stress. *The EMBO Journal* 14 (21):5209-5215.

Parsons, T. R., Maita, Y. & Lalli, C. M. 1984. *A Manual of Chemical and Biological Methods for Seawater Analysis*, pp 173. Pergamon Press, Oxford, UK.

Passow, U. & Alldredge, A. L. 1994. Distribution, size and bacterial colonization of transparent exopolymer particles (TEP) in the ocean. *Marine Ecology Progress Series* 113:185-198.

Passow, U. & Alldredge, A. L. 1995. Aggregation of a diatom bloom in a mesocosm: the role of transparent exopolymer particles (TEP). *Deep-Sea Research Part II* 42:99-109.

Passow, U. 2002a. Transparent exopolymer particles (TEP) in aquatic environments. *Progress in Oceanography* 55:287-333.

Passow, U. 2002b. Production of transparent exopolymer particles (TEP) by phyto- and bacterioplankton. *Marine Ecology Progress Series* 236:1-12.

Passow, U. 2002c. Formation of transparent exopolymer particles, TEP from dissolved precursor material. *Marine Ecology Progress Series* 192:1-11.

Passow, U. & Carlson, C. A. 2012. The biological pump in a high CO_2 world. *Marine Ecology Progress Series* 470:249-271.

Pereira, S., Micheletti, E., Zille, A., Santos, A., Moradas-Ferreira, P., Tamagnini, P. & De -Philippis, R. 2011. Using extracellular polymeric substances (EPS)-producing cyanobacteria for the bioremediation of heavy metals: do cations compete for the EPS functional groups and also accumulate inside the cell? *Microbiology* 157:451-458.

Ploug, H., Iversen, M. H. & Fischer, G. 2008. Ballast, sinking velocity, and apparent diffusivity within marine snow and zooplankton fecal pellets: implications for substrate turnover by attached bacteria. *Limnology Oceanography* 53(5):1878-1886.

Porter, K. G. & Feig, Y. S. 1980. The use of DAPI for identifying and counting aquatic microflora. *Limnology and Oceanography* 25:943-948.

Price, G. D., Badger, M. R., Woodger, F. J. & Long, B. M. 2007. Review advances in understanding the cyanobacterial CO_2-concentrating-mechanism (CCM): functional components, Ci transporters, diversity, genetic regulation and prospects for engineering into plants. *Journal of Experiment Botany* 59(7):1441-1461.

Qian, H., Yu, S., Sun, Z. Xie, X., Liu, W. & Fu, Z. 2010. Effect of copper sulfate, hydrogen peroxide and N- phenyl-2-naphthylamine on oxidative stress and the

expression of genes in volved photosynthesis and microcystin disposition in Microcystis aeruginosa. *Aquatic Toxicology* 99:405-412.

Quigg, A., Finkel, Z. V., Irwin, A. J., Rosenthal, Y., Ho, T.Y., Reinfelder, J. R., Schofield, O., Morel, F. M. M. & Falkowski, P. G. 2003. The evolutionary inheritance of elemental stoichiometry in marine phytoplankton. *Nature* 425(6955):291-294.

Ramaiah, N., Yoshikawa, T. & Furuya, K. 2001.Temporal variations in transparent exopolymer particles (TEP) associated with a diatom spring bloom in a subarctic ria in Japan. *Marine Ecology Progress Series* 212:79-88.

Raven, J. A., Ball, L. A., Beardall, J., Giordano, M. & Maberly, S. C. 2005. Algae lacking carbon concentrating mechanisms. *Canadian Journal of Botany* 83:879-890.

Raven, J. A. & Larkum, A. W. 2007. Are there ecological implications for the proposed energetic restrictions on photosynthetic oxygen evolution at high oxygen concentrations? *Photosynthesis Research* 94(1):31-42.

Raven, J. A., Cockell, C. S. & De La-Rocha, C. L. 2008. The evolution of inorganic carbon concentrating mechanisms in photosynthesis. *Philosphical Transactions of the Royal Society B Biological Sciences* 27(1504):2641-2650.

Raven, J. A. 2010. Inorganic carbon acquisition by eukaryotic algae: four current questions. *Photosynthesis Research* 106:123-134.

Redfield, A. C., Ketchum, B. H. & Richards, F. A. 1963. The influence of organisms on the composition of sea-water. *The Sea* 2:554-546.

Riebesell, U. 1991. Particle aggregation during a diatom bloom. II. Biological aspects. *Marine Ecology Progress Series* 69:281-291.

Rijstenbil, J. W. 2002. Assessment of oxidative stress in the planktonic diatom *Thalassiosira pseudonana* in response to UVA and UVB radiation. *Journal of Plankton Research* 24:1277-1288.

Roberts, K., Granum, E., Leegood, R. C. & Raven, J. A. 2007a. Review carbon acquisition by diatoms. *Photosynthesis Research* 93(13):79-88.

Roberts, K., Granum, E., Leegood, R. C. & Raven, J. A. 2007b. C_3 and C_4 pathways of photosynthetic carbon assimilation in marine diatoms are under genetic, not environmental, control. *Plant Physiology* 145(1):230-235.

Rzadkowolski, C. E. & Thornton, D. C. O. 2012. Using laser scattering to identify diatoms and conduct aggregation experiments. *European Journal of Phycology* 47:30-41.

Sarmento, H., Montoya, J. M., Vázquez-Domínguez, E., Vaqué, D. & Gasol, J. M. 2010. Warming effects on marine microbial food web processes: how far can we go when it comes to predictions? *Philosophical Transactions of the Royal Society* 365:2137-2149.

Sarno, D., Kooistra, W. H. C. F., Medlin, L. K., Percopo, I. & Zingone, A. 2005. Diversity in the genus *Skeletonema* (*Bacillariophyceae*). II. An assessment of the taxonomy of *S. costatum*-like species with the description of four new species. *Journal of Phycology* 41:151-176.

Serra, T., Colomer, J., Cristina, X. P., Vila, X., Arellano, J. B. & Casamitjana, X. 2001. Evaluation of laser in situ scattering instrument for measuring concentration of phytoplankton, purple sulfur bacteria, and suspended inorganic sediments in lakes. *Journal of Environmental Engineer* 127(11):1023-1030.

Shimeta, J. 1993. Diffusion encounter of submicrometer particles and small cells by suspension feeders. *Limnology and Oceanography* 38:456-465.

Smetacek, V. 1985. Role of sinking in diatom life history cycles: ecological, evolutionary, and geological significance. *Marine Biology* 84:239-251.

Smith, D. C., Simon, M., Alldredge, A. L. & Azam, F. 1992. Intense hydrolytic enzyme activity on marine aggregates and implications for rapid particle dissolution. *Nature* 359:139-141.

Smith, D. J. & Underwood, G. J. C. 1998. Exopolymer production by intertidal epipelic diatoms. *Limnology Oceanography* 43(7):1578-1591.

Snoeijs, P., Busse, S. & Potapova, M. 2002. The importance of diatom cell size in community analysis. *Journal of Phycology* 38:265-272.

Sorhannus, U., Ortiz, J. D., Wolf, M. & Fox, M. G. 2010. Microevolution and speciation in *Thalassiosira weissflogii* (*Bacillariophyta*). *Protist* 161:237-249.

Staats, N., Stal, L. J. & Mur, L. R. 2000. Exopolysaccharide production by the epipelic diatom *Cylindrotheca closterium*: effects of nutrient conditions. *Journal of Experimental Marine Biology and Ecology* 249:13-27.

Stal, L. J. 2003. Microphytobenthos, their extracellular polymeric substances, and the morphogenesis of intertidal sediments. *Journal of Geomicrobiology* 20:463-478.

Stoderegger, K. & Herndl, G. J. 1998. Production and release of bacterial capsular material and its subsequent utilization by marine bacterioplankton. *Limnology and Oceanography* 43:877-884.

Thornton, D. C. O. & Thake, B. 1998. Effect of temperature on the aggregation of *Skeletonema costatum* (*Bacillariophyceae*) and the implication for carbon flux in coastal waters. *Marine Ecology Progress Series* 174:223-231.

Thornton, D. C. O. 2002. Diatom aggregation in the sea: mechanisms and ecological implications. *European Journal of Phycology* 37:149-161.

Thornton, D. C. O. 2012. Primary production in the ocean. *Advances in Photosynthesis-Fundamental Aspects*, edited by Najafpour, M. M., pp 563-588. Intech, Croatia.

Thornton, D. C. O. 2013 (accepted). Dissolved organic matter (DOM) release by phytoplankton in the contemporary and future ocean. *European Journal of Phycology.*

Tranvik, L. J., Sherr, E. B. & Sherr, B. F. 1993. Uptake and utilization of colloidal DOM by heterotrophic flagellates in seawater. *Marine Ecology Progress Series* 92:301-309.

Underwood, G. J. C., Paterson, D. M. & Parkes, R. J. 1995. The measurement of microbial carbohydrate exopolymers from intertidal sediments. *Limnology Oceanography* 40:1243-1253.

Underwood, G. J. C. & Paterson, D. M. 2003. The importance of extracellular carbohydrate production by marine epipelic diatoms. *Advances in Botanical Research* 40:183-240.

Underwood, G. J. C., Boulcott, M., Raines, C. A. & Waldron, K. 2004. Environmental effects on exopolymer production by marine benthic diatoms: dynamics, changes in composition, and pathways of production. *Journal of Phycology* 40:293-304.

van Montfort, R. L., Congreve, M., Tisi, D., Carr, R. & Jhoti, H. 2003. Oxidation state of the active-site cysteine in protein tyrosine phosphatase 1B. *Nature* 423:773-777.

Vardi, A., Haramaty, L., Mooy, B. A. S., van Fredricks, H. F., Kimmance, S. A., Larsen, A. & Bidle, K. D. 2012. Host–virus dynamics and subcellular controls of cell fate in a natural coccolithophore population. *PNAS* 109:19327-19332.

Veldhuis, M. J. W., Kraay, G. W. & Timmermans, K. R. 2001. Cell death in phytoplankton: correlation between changes in membrane permeability, photosynthetic activity, pigmentation and growth. *European Journal of Phycology* 36:167-177.

Verardo, D. J., Froelich, P. N. & McIntyre, A. 1990. Determination of organic carbon and nitrogen in marine sediments using the Carlo Erba NA-1500 analyzer. *Deep-Sea Research Part A* 37:157-165.

Verdugo, P., Alldredge, A. L., Azam, F., Kirchman, D., Passow, U. & Santschi, P. 2004. The oceanic gel phase: a bridge in the DOM-POM continuum. *Marine Chemistry* 92:67-85.

Verdugo, P. & Santichi, P. H. 2010. Polymer dynamics of DOC networks and gel formation in seawater. *Deep Sea Research Part II* 57:1486-1493.

Vrede, T., Persson, J. & Aronsen, G. 2002. The influence of food quality (P: C ratio) on RNA: DNA ratio and somatic growth rate of *Daphnia. Limnology and Oceanography* 47(2):487-494.

Wetz, M. S. & Wheeler, P. A. 2007. Release of dissolved organic matter by coastal diatoms. *Limnology and Oceanography* 52(2):798-807.

Wigglesworth-Cooksey, B. & Cooksey, K. E. 2005. Use of fluorophore-conjugated lectins to study cell-cell interactions in model marine biofilms. *Application Environmental Microbiology* 71(1):428-435.

Witter, A. E. & Luther, G. W. III. 2002. Spectrophotometric measurement of seawater carbohydrate concentrations in neritic and oceanic waters from the U. S. middle Atlantic Bight and the Delaware estuary. *Marine Chemistry* 77:143-156.

Wolfstein, K. L. & Stal, J. 2002. Production of extracellular polymeric substances (EPS) by benthic diatoms: effect of irradiance and temperature. *Marine Ecology Progress Series* 236:13-22.

Wu, Z., Song, L. & Li, R. 2008. Differential tolerances and responses to low temperature and darkness between water bloom forming cyanobacterium *Microcystis* and a green alga Scenedesmus. *Hydrobiologia* 596:47-55.

Young, E. B. & Beardall, J. 2005. Modulation of photosynthesis and inorganic acquisition in a marine microalga by nitrogen, iron and light availability. *Canadian Journal of Botany* 83:917-928.

Zack, G. W., Rogers, W. E. & Latt, S. A. 1977. Automatic measurement of sister chromatid exchange frequency. *Journal of Histochemistry & Cytochemistry* 25:741-753.

Zhou, J., Mopper, K. & Passow, U. 1998. The role of surface active carbohydrate in the formation of transparent exopolymer particles (TEP) by bubble adsorption of seawater. *Limnology and Oceanography* 43:1860-1871.

Zlotnik, I. & Dubinsky, Z. 1989. The effect of light and temperature on DOC excretion by phytoplankton. *Limnology and Oceanography* 34:831-839.

APPENDIX

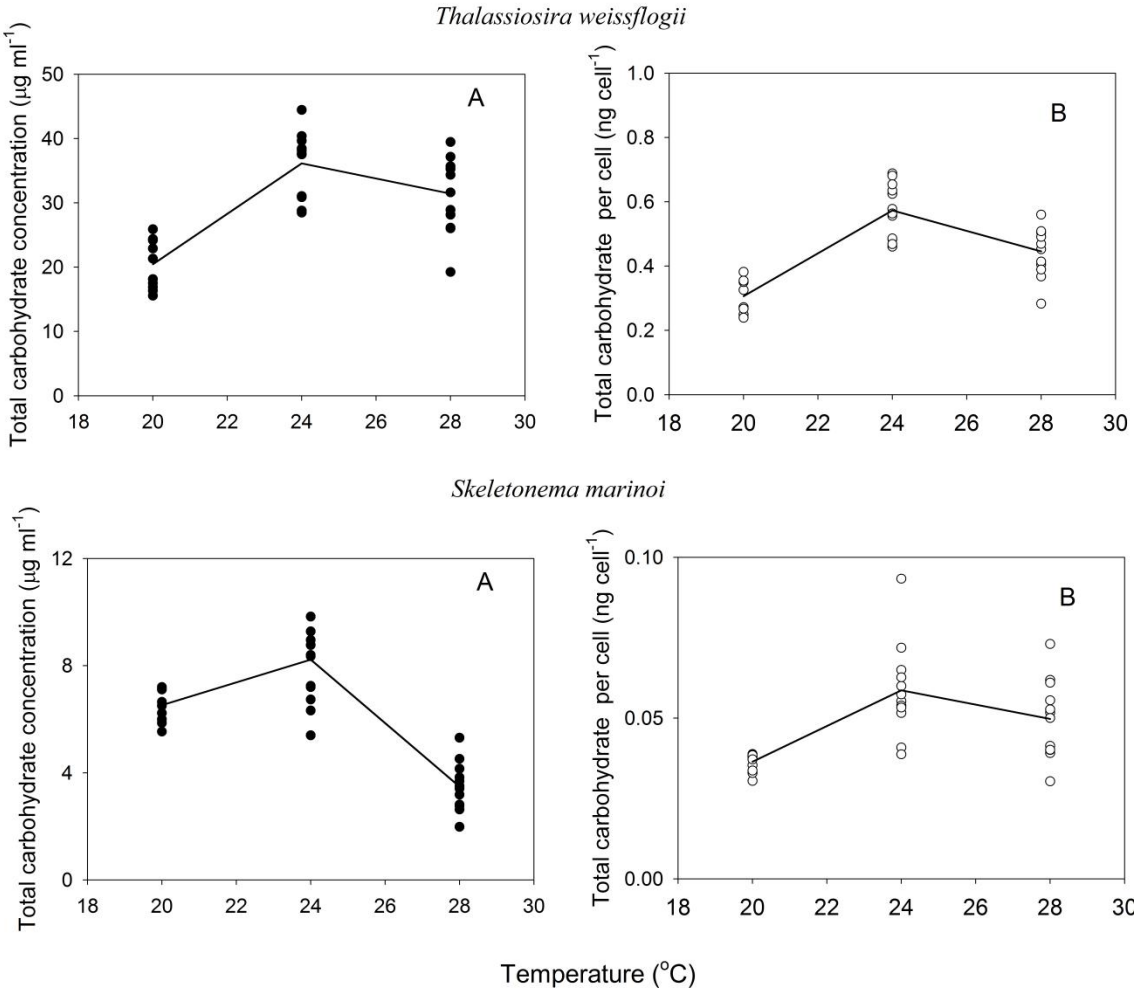

Figure A-1.Total carbohydrate concentration and total carbohydrate concentration per cell in semi-continuous cultures of *Thalassiosira weissflogii* and *Skeletonema marinoi* when they grown at 20°C, 24°C and 28°C. A) Total carbohydrate concentration. B) Total carbohydrate concentration per cell. Solid cycles represent the total carbohydrate concentration in cultures at each sampling time (n = 12). Open cycles represent the total carbohydrate per cell in cultures at each sampling time (n = 12). Solid lines represent the mean value of total carbohydrate content in the cultures at 20°C, 24°C and 28°C (n = 36).

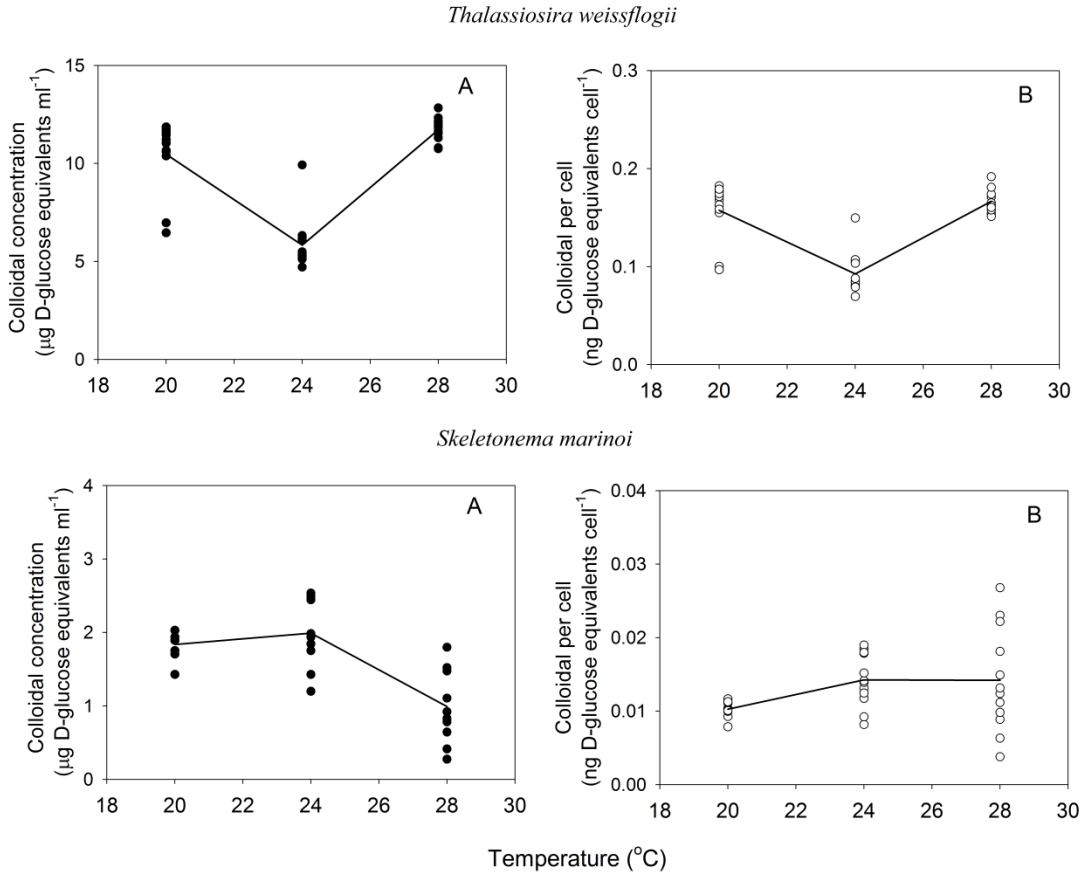

Figure A-2. Colloidal concentration and colloidal concentration per cell in semi-continuous cultures of *Thalassiosira weissflogii* and *Skeletonema marinoi* when they grown at 20, 24 and 28 °C. A) Colloidal concentration. B) Colloidal concentration per cell. Solid cycles represent the colloidal concentrations in cultures at each sampling time (n = 12). Open cycles represent the colloidal per cell in cultures at each sampling time (n = 12). Solid lines represent the mean value of colloidal content in cultures at 20, 24 and 28°C (n = 36).

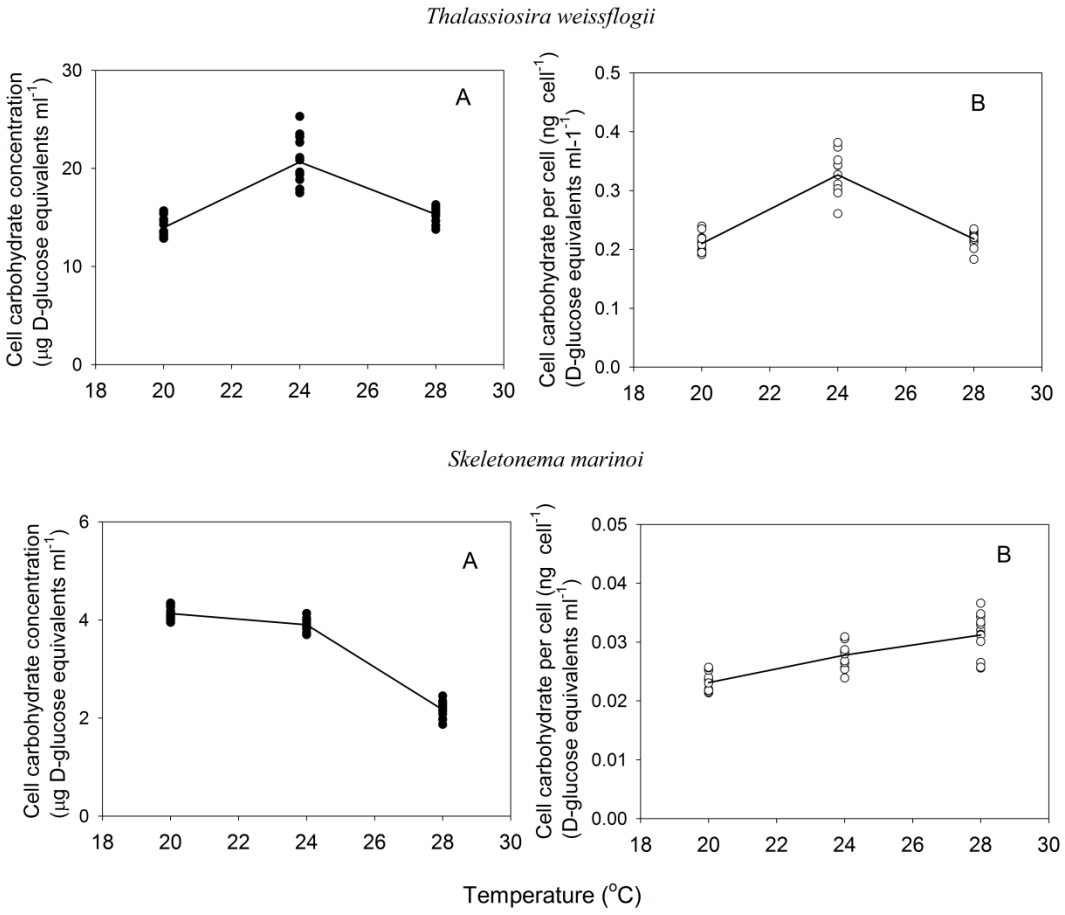

Figure A-3. Cell pellet concentration and cell pellet concentration per cell in semi-continuous cultures of *Thalassiosira weissflogii* and *Skeletonema marinoi* when they grown at 20, 24 and 28 °C. A) Cell pellet concentration. B) Cell pellet concentration per cell. Solid cycles represent the mean value of cell pellet concentration in cultures at each sampling time (n = 12). Open cycles represent the mean value of cell pellet per cell in cultures at each sampling time (n = 12). Solid lines represent the mean value of cell pellet content in cultures at 20, 24 and 28 °C (n = 36).

Table A-1. Carbohydrate fractions concentration in *Thalassiosira weissflogii* grown at different temperatures.

Temperature (°C)	TOC (µg ml^{-1})		TOC per cell (ng cell^{-1})		CL (µg ml^{-1})		CL per cell (ng cell^{-1})		EPS (µg ml^{-1})		EPS per cell(ng cell^{-1})		Cell associated carbohydrate (µg ml^{-1})		Cell associated carbohydrate per cell(ng cell^{-1})	
	Mean	DEV	Mean	DEV	Mean	DEV	Mean	DEV	Mean	DEV	Mean	DEV	Mean	DEV	Mean	DEV
20	21.276	4.429	0.317	0.059	11.364	0.290	3.007	5.572	2.821	0.162	0.042	0.004	13.287	0.298	0.199	0.006
20	18.599	3.996	0.278	0.050	9.183	2.864	3.094	4.255	3.193	0.340	0.048	0.005	13.951	0.924	0.209	0.010
20	21.495	2.929	0.324	0.040	10.845	0.597	2.952	5.267	3.707	0.794	0.056	0.011	14.674	1.068	0.222	0.020
24	38.088	0.323	0.580	0.031	5.179	0.342	1.533	2.441	4.947	0.562	0.076	0.012	23.670	1.142	0.360	0.020
24	40.500	2.897	0.665	0.025	5.687	0.655	1.758	2.636	4.110	0.323	0.068	0.006	19.680	1.560	0.323	0.022
24	29.803	1.354	0.474	0.012	6.633	2.227	2.337	3.019	2.738	0.404	0.044	0.007	18.585	1.073	0.297	0.027
28	27.911	6.621	0.401	0.091	11.618	0.584	3.174	5.633	6.427	0.718	0.093	0.009	15.747	0.371	0.227	0.004
28	29.526	4.136	0.428	0.062	11.860	0.910	3.315	5.707	6.892	0.713	0.100	0.012	15.218	0.785	0.221	0.011
28	36.888	1.898	0.507	0.039	11.675	0.322	3.136	5.696	6.624	0.990	0.091	0.012	14.963	0.946	0.206	0.017

Table A-2. Carbohydrate fractions concentration in *Skeletonema marinoi* grown at different temperatures.

Temperature (°C)	TOC (µg ml^{-1})		TOC per cell (ng cell^{-1})		CL (µg ml^{-1})		CL per cell (ng cell^{-1})		EPS (µg ml^{-1})		EPS per cell (ng cell^{-1})		Cell associated carbohydrate (µg ml^{-1})		Cell associated carbohydrate per cell(ng cell^{-1})	
	Mean	DEV	Mean	DEV	Mean	DEV	Mean	DEV	Mean	DEV	Mean	DEV	Mean	DEV	Mean	DEV
20	7.164	0.044	0.038	0.000	1.879	0.087	0.010	0.001	0.919	0.021	0.005	0.000	4.061	0.031	0.022	0.000
20	6.264	0.523	0.035	0.004	1.752	0.229	0.010	0.001	0.904	0.029	0.005	0.000	4.098	0.102	0.023	0.001
20	6.148	0.283	0.036	0.002	1.879	0.133	0.011	0.001	0.907	0.061	0.005	0.000	4.234	0.152	0.025	0.001
24	8.006	1.156	0.053	0.009	1.590	0.346	0.011	0.002	1.055	0.061	0.007	0.001	3.809	0.078	0.025	0.001
24	8.317	1.994	0.060	0.014	2.179	0.336	0.016	0.003	1.086	0.061	0.008	0.001	3.983	0.114	0.029	0.002
24	8.341	2.572	0.063	0.020	2.202	0.340	0.017	0.002	1.150	0.161	0.009	0.001	3.915	0.129	0.030	0.001
28	3.183	0.901	0.046	0.014	1.302	0.609	0.019	0.009	0.673	0.068	0.010	0.002	2.163	0.067	0.031	0.004
28	3.887	0.443	0.055	0.005	0.909	0.509	0.013	0.008	0.547	0.093	0.008	0.002	2.185	0.155	0.031	0.003
28	3.379	1.287	0.049	0.016	0.759	0.138	0.011	0.002	0.630	0.038	0.009	0.000	2.158	0.279	0.031	0.005